Synthesis and Characterization of Un-Doped/Doped TiO_2 by Sol-Gel and Sol-Hydrothermal Routes to Improve Photo-Catalytic Properties

By:

Muhammad Imran

(2010MSPhD-EM-E 08)

This work is submitted as a MS thesis in partial fulfillment of the requirement for the degree of

(MS in Energetic Materials Engineering)

Supervisor Name: Dr. Amir Habib

School of Chemical and Materials Engineering (SCME)

National University of Sciences and Technology (NUST), H-12

Islamabad, Pakistan

Aug, 2012

In The Name of Allah
The most Beneficient,
The most Merciful

DECLARATION

This is to certify that this dissertation submitted by **Muhammad Imran** is accepted in its present form by the School of Chemical and Materials Engineering, NUST, Islamabad, Pakistan, as satisfying the dissertation requirements for the degree of **Master of Science** in **Energetic Materials Engineering.**

1. **Dr. Amir Habib**

   _____

   School of Chemical and Materials Engineering (Supervisor)
   NUST, Islamabad.

2. **Dr. Habib Nasir**

   _____

   School of Chemical and Materials Engineering (Co-Supervisor)
   NUST, Islamabad.

3. **Dr. Mohsin Raza**

   _____ (External Examiner)

Dedicated to

My **parents** and **palvasha Ijaz** who have supported me all the way.

ACKNOWLEDGEMENTS

All praise and glory is to **"ALMIGHTY ALLAH"** the ultimate creator of this universe: from particles to the stars, who blessed us with the ability to think and an eager to explore this whole universe. Countless salutations upon the **"HOLY PROPHET HAZRAT MUHAMMAD (P.B.U.H)"**: the source of knowledge and blessings for entire mankind. I am thankful to almighty **"ALLAH"** who has provided me health and energies to pursue and fulfill my highest academic achievement. I am thankful to the NUST that provide me opportunity to achieve my objective.

I owe my deep gratitude to my respected supervisor **Dr. Amir Habib** Assistant Professor SCME, NUST for his valuable guidance, philanthropic attitude and encouragement throughout my research work. He always answered in yes whenever I asked for new experimentation. He played vital role in the development of thinking and patience in me. I am thankful to the Co-supervisor **Dr. Habib Nasir**, Foreign Professor at SCME, NUST for their valuable guidance and **Prof. Dr. M. Mujahid** Dean of SCME and **Prof. Dr. Asghari Maqsud** for providing necessary research facilities.

I have no words to acknowledge the sacrifices, efforts, lot of prayers, guidance, support, encouragement and firm dedication of especially my loving parents, brothers Irfan, Behram and sisters and my fiancé Palvasha Ijaz. I am also thankful to Ahsan bhai for supporting me all the way. Their endless prayers contributed to the successful completion of this research project. Words become meaningless when I look at them as icons of strength for being what i am today. In the end I want to present my unbending thanks to all those hands that prayed for my betterment and serenity.

(Muahammad Imran)

ABSTRACT

Un-doped and doped TiO_2 nanoparticles in the range 10-30 nm are synthesized via Sol-Gel and Sol- hydrothermal routes. The obtained powders are characterized for their elemental phase analysis, particle size, structural morphology, and band gap studies by X-Ray Diffraction, Scanning Electron Microscopy and UV VIS spectroscopy. Addition of silver (Ag), zinc (Zn) and Ag-Zn impurities via in situ doping process is done to reduce the band gap of TiO_2. The applications and unique properties of TiO_2 depend upon the method of synthesis. Un-doped TiO_2 nanoparticles were synthesized via Sol-Gel and Sol-hydrothermal routes by the reaction of titanium tetra chloride in acidic solution. HCl and $NaOH/NH_4OH$ are used as catalyst in the pH range of 2-13. In case of doped TiO_2, the metallic solution of Ag or Zn or Ag-Zn was used in hydrolysis process with Ti-precursor. The XRD data shows that average crystallite size for hydrothermally treated doped/un-doped Titania samples remain in the range 10-12.9 nm while 20-30 nm for the samples via Sol-Gel route. It is observed via XRD results that we get mixed phases of anatase and rutile are obtained by Sol-Gel synthesized samples while only anatase phase stabilized in case of Sol-hydrothermal process. The EDX results indicated presence of titanium, oxygen and dopants in stoichiometric ratios. Due to small crystallite size the surface area of hydrothermally synthesized samples was high as compared to Sol-Gel. The SEM and showed that the particles have spherical morphology for sample obtained via Sol-hydrothermal route. UV-Vis measurements confirm the decrease in band gap of synthesized samples that is also higher in hydrothermally synthesized samples as compared to Sol-Gel.

Table of Contents

List of Figures

List of Tables

CHAPTER 1

Introduction

TiO_2 occurs in three crystalline phases' i.e. rutile, anatase and brookite. The brookite, anatase and rutile are metastable, stable and most stable phases respectively. Anatase phase is most difficult to synthesize. The purposes of the particular study is to develop innovative synthetic route that permit to get mono stable phases of TiO_2, high surface area, higher crystallinity, specific morphological features, small crystallite size and reduced band gap resulting an increase in the photo catalytic efficiency of the synthesized material. The band gap of TiO_2 can be reduced by introducing metal or nonmetals impurities into the pure TiO_2. This Thesis was performed in the context of these studies. The TiO_2 nanoparticles synthesized via most of the traditional routes are amorphous. Consequently, additional calcinations are generally required to induce crystallization, which frequently leads to the particle growth and agglomeration. Earlier researchers mostly focused to study the effects of temperature, solvent/precursor ratios, and effects of concentrations of reagents, gaseous atmosphere and varying calcinations temperatures and in a few cases aging period and drying conditions. Many researchers focused to study and enhance the photo-catalytic activity of TiO_2. The preparation of TiO_2 nanoparticles in solution phase would be one of the best synthetic routes. The main aim of the work is to synthesize pure and doped nano-crystalline Titanium Dioxide at different pH ranges by using sol–gel and sol-hydrothermal techniques with controlled properties by using low cost materials and simple experimental setup. We have focused on the preparation of nano-crystalline TiO_2 under milder conditions. In the present study we made an attempt to synthesize nano-crystals of pure 100% anatase TiO_2 by Sol-Gel method and sol-hydrothermal methods at low temperature while others reported mixed phases. The prime importance of study is to decrease band gap by controlling all basic features and introducing impurity atoms of metals. The attention was paid on the effect of different synthesis routes on the crystallinity and obtained phases of pure/doped TiO_2 powders. The size, shape, and crystal structure of nanoparticles are important parameters that control their chemical, optical, and electrical properties and catalytic activity. Solution

pH alters such properties at the nano scale. The effort has been dedicated to the synthesis of TiO_2 with a controllable crystal structure and morphology. Characterizations of the samples were performed through different analytical techniques including XRD, SEM, EDX and UV-Vis spectrophotometer. It was hoped that the final outcome of the thesis would have been the best way to synthesize TiO_2 nanoparticles in anatase phases. In this we have succeeded to find a future path to be followed to get the desired phase. Process simplification can lead to lower production costs and makes continuous process possible. In addition, low treatment temperature makes it possible to produce highly crystalline powders in desired phase with higher specific surface area and soft particle agglomeration, which will strongly affect the resulting physico-chemical behaviors.

1.1 Energy Needs and the Environment

Economic prosperity, global stability and the quality of human life mainly depends on a ready and reliable supply of energy. The global current rate of energy consumption is approximately 4.1×10^{20}J/yr, that's equivalent to 13 trillion watts per annum. According to World Bank prediction the demand of energy will be double (about to 30 trillion watts) by 2050 with an increase of the world's population to 9 billion people accompanied by a rapid technological development and economic growth [1]. U.S. Department of Energy reported in 2006 that fossil fuels presently deliver about 80% of the worldwide energy demand [2]. The resources of fossil fuels will run out during this century and renewable energy sources will need to be harnessed to satisfy this enormous energy demand. Furthermore, environmental pollution is rising continuously and threatens climate change due to the rising levels of greenhouse gases and pollutants produced by the combustion of fossil fuels, which has also increased public concern. Therefore, finding and utilizing renewable energy resources like neutral carbon source to meet the world's energy challenges and resolve the pollution problem which are world community's major challenge in coming years [3,4].

In this regard, solar energy is considered to be the most promising and long lasting source in order to meet this growing energy demand with minimal associated environmental pollution. The annual total energy coming to the earth from the sun is approximately 3×10^{24} joules, which is about 10^4 times more than the worlds current energy demand.

Therefore, by utilizing solar energy, it is possible to satisfy the enormous energy demand as well as to solve the environmental pollution problem.

1.2 Solar Energy

The energy from the sun arrives on earth as a radiation distributed across the electromagnetic spectrum ranging from infrared to ultra-violet wavelengths. 1000 W/m^2 amount of solar energy is available at Earth's crust in sun's direction. In 21^{st} century, scientists are expecting significant rise in use of solar energy to achieve required energy demands due to its subsequent advantages compared to conventional energy [5] i.e.

- Solar energy is almost free after recovery of its initial cost. Therefore, payback time is short compared to cost of current carbon based energy resources.
- Solar energy systems generated energy individually that's why they don't need any power or natural fuel source.
- Exponential reduction in environmental pollution by use of solar energy.

Solar energy can be used successfully in many ways. However, major applications of using solar energy are combined in three primary classes:

i. Heating or solar thermal
ii. Electricity production
iii. Chemical processes.

1.2.1 Heating

Utility costs are reduced by use of solar heating systems. Efficiency and dependability makes the solar heating systems really attractive for domestic and commercial use. The mainly used applications of solar energy are for water and space heating. Commercially, solar energy is applied as crop drying, outdoor and indoor pools, preheating boiler feed water etc. In active solar-heating systems, solar collectors are the key component that collects energy directly from sun, convert it into heat and then to water, air or solar fluid. Several types of solar collectors are available such as:

- flat-plate collectors
- evacuated-tube collectors
- integral collector-storage systems

Usually, copper pipes are main part of solar energy collection system. However, there is a tremendous energy loss due to thermal radiation, which can be reduced by using an optically selective absorber surface. Parameters such as high absorbance in solar regions and low emittance in thermal regions are ideal behaviors of an optical absorber surface. No perfect optical selective material has been discovered till now. There are two schemes followed to achieve desired optical selectivity [6]:

- A mirror is placed for maximum reflection of infrared rays and transmission of solar rays opposite to black absorber.
- Thin films which absorbs the radiation but only transmits the infrared rays.

1.2.2 Electricity

Photovoltaic (PV) devices based on multi thin films of semiconducting materials that directly converts the solar energy into electricity. Photovoltaic cell generates electric current proportional to quantity of solar rays it receives. PV cells can help to reduce the widespread dependence on dwindling oil reserves and mitigate adverse effects on the environment. Currently, crystalline silica-based solar cells are the most popular form of PV device, given their high solar conversion efficiencies, ease of manufacture, resistance to degradation, and the abundance of siliceous starting materials [8]. However, for PV to be a competitive energy alternative, their cost needs to be reduced to at least 20% of their current market value [9]. Hence, there is a need to investigate new highly efficient PV materials. According to the recent literature reports, TiO_2 nano-structured materials offer tremendous opportunities to enhance the efficiency of capturing solar energy, thereby reducing the overall cost [10-12].

1.2.3 Chemical Processes

In chemical processes, solar energy can be used in two ways:

- solar detoxification technologies for cleaning of water and air
- Producing fuel such as H_2 and CH_3OH by photo-electrolysis of water and reducing CO_2 [13].

In the presence of a suitable catalyst such as TiO_2 or TiO_2 supported Pt, Cu. As figure (1.1) depicts the basic principle by which solar energy removes organics from polluted water or produces fuel.

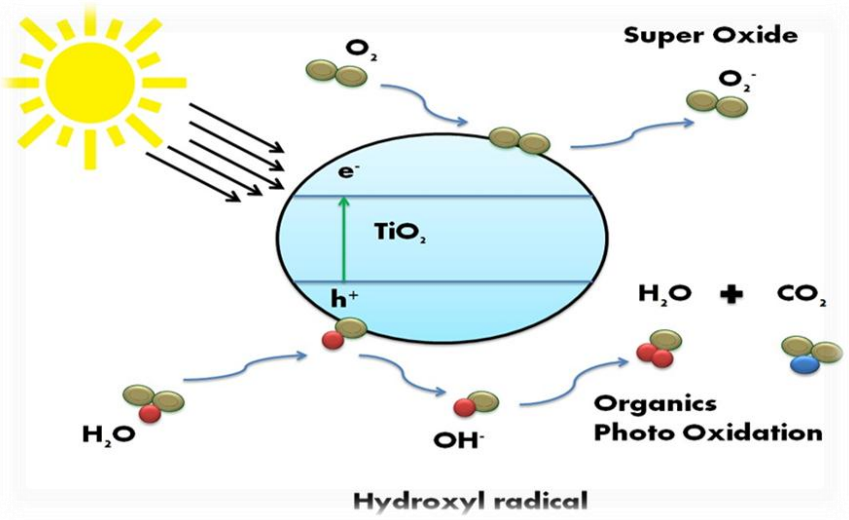

Figure 1.1 Mechanism of Semi-conductor Photo-catalysis

When TiO_2 (a semiconductor) absorbs ultraviolet radiation from sunlight, it produces pairs of electrons and holes. The energy available in excess promotes electron to conduction band by creating hole (h+) in valance band. The produced hole of TiO_2 converts the molecule water to hydrogen gas and a hydroxyl radical, which rapidly destroys the chemical bonds of the contaminant. Super oxide anion is formed by the reaction of negative electron with an oxygen molecule. This cycle continues as long as light is available [14].

Photo-catalysis process is initiated by the generation of electron hole pairs after the excitation of band gap. As the light strikes the semiconducting material surface with energy equal to or greater than the band-gap, photo-catalytic mechanism take place and the valence band electrons excited to the conduction band by creating a hole in the valence band.

$$Photo-catalyst(TiO_2) \xrightarrow{hv} e_{CB^-} + e_{VB^+}$$

The input energy releases as a heat on recombination of electron and hole pairs without any chemical effect. While if the electrons and holes move to the upper surface without recombination, these can participate in various oxidation and reduction reactions which adsorbed such organic or inorganic species, oxygen, water and several other. The positive holes have ability to oxidize pollutants directly by reacting with water to produce hydroxyl radical, these radicals have oxidizing potential of 2.8 V and act as a very strong Oxidant. Hydroxyl radicals rapidly attack the pollutants and mineralize them to carbon

dioxide, water etc. Titanium dioxide is the most popular photo-catalyst because of following characteristics,

- Its relatively high activity
- Chemical stability
- Non-toxicity
- Low production costs and availability
- Due to above mentioned reasons it's extensively studied and demonstrated potential to completely oxidize a wide variety of organic compounds [16].

1.3 TiO_2 and Solar Energy

TiO_2 nano-materials are one of the potential candidates for solar energy application due to TiO_2's unique optoelectronic and photochemical properties [17,18]. Especially, as a photo-catalyst to clean air/water and in electrolysis of water to produce hydrogen, TiO_2 nano-materials have been receiving a great deal of attention [14,17]. While it only absorbs 3% of the solar energy, due to this limiting factor output is very less. Therefore, a considerable portion of the available solar energy is not utilized [3,19]. Moreover, the low surface area and high electron-hole recombination rate of TiO_2 nano-materials are also considered as negative factors to wide-scale application. Bulk modification by cations and anion doping has been found very effective to improve the properties of TiO_2 [4,19-24]. So the significant progress in the research and development of nano TiO_2 is required to make sure that solar technology can achieve its full potential. Solar electricity from photo-voltaic is currently very costly with a limited production capacity. Solar thermal systems are economical but require large open area to collect sunlight. Hence, the practical utilization of solar energy is strongly limited due to the available low efficiency and high cost materials with ≤ 2 % of the available solar energy currently being used. Therefore, it is highly required to enhance the performance of solar energy systems by designing new materials as well as increasingly understanding the electronic and molecular basis of capture, conversion, and storage of this clean, abundant, and economic energy. One of the most important research areas towards this means is to synthesize new efficient nano-structured materials for solar energy applications with low cost using a green technology.

CHAPTER 2

Literature Review

2.1 Titanium dioxide (TiO_2)

Titanium is a transition metal with atomic number 22. It's a light weight, corrosion resistant, lustrous and strong. Titanium dioxide is its most frequently used compound. TiO_2 is n-type wide band gap semiconducting material with electron as a majority charge carriers [25]. Titanium dioxide (TiO_2) is naturally found in the mineral sources such as ilmenite, rutile, anatase and brookite. Ilmenite (FeTiO) or titanic iron ore is a grey mineral containing magnetic black iron. It was firstly discovered at Ural Ilmen Mountain (Russia) in 1827 by Kupffer who named it. Ilmenite mine is used as a raw material for pigment production, which is grounded into white titanium dioxide powder. It is used as base in the manufacturing of high quality paint, paper and plastic etc. most stable phase of titanium dioxide is rutile and it was found in 1803 by Werner in Spain. Naturally it contains 10% of Fe and other elements as an impurity. Generally its color is reddish brown while sometimes it may be violet, yellowish or bluish. It is used in the manufacturing of ceramics, as a pigments and production of titanium metal. Anatase is metastable phase of TiO_2, called as octahedrite in general and was named by Haüy in 1801. Last, brookite is a dark brown to greenish black mineral mainly consisting of titanium oxide. Naturally its occurrence is very rare as compared to the anatase and rutile forms of titanium dioxide. It was firstly found by A Levy in 1825 at Snowen, England.

2.2 Crystal structure and properties

There are three principal crystal structures, anatase and rutile has tetragonal geometry while brookite has orthorhombic geometry as shown in figure (2.1) [26]. The structures of anatase and rutile are based on octahedral geometry (TiO_6), but they differ from each other by the distortion and assembly patterns of the octahedral chains. Anatase is built up from vertices connected octahedral. In rutile octahedral are connected by their edges. In brookite both edge and vertices connections are present and its geometry is orthorhombic.

Anatase and rutile have the same tetragonal geometry, but the only difference is anatase has longer vertical axis of crystals than rutile.

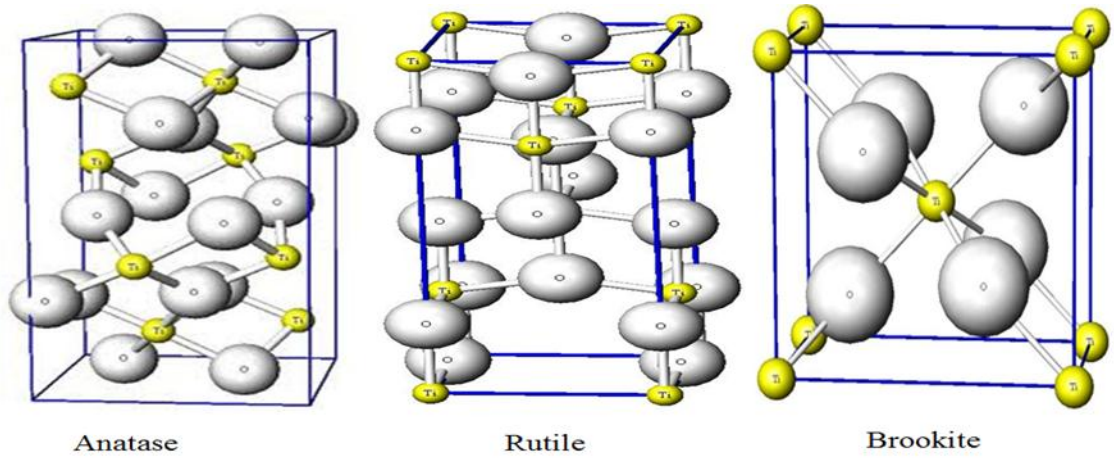

Figure 2.1 Phases of Titania

Rutile is the most stable phase of titanium dioxide while anatase and brookite are metastable phases. The metastable structures are almost as stable as rutile at ordinary temperature and pressure due to small difference in the Gibbs free energy (4 - 20 kJ/mol) between three phases [27]. In rutile, oxygen ions form a slightly distorted hexagonal compact lattice the three Ti-O-Ti angles are roughly equal to 120°. In anatase, the oxygen forms an face centered cubic (FCC) lattice and one Ti-O-Ti angle is about 180° while the two others are close to 90° [28]. Regarding the band gap energy, 3.26 eV (~380 nm) is the band gap energy of anatase and in rutile 3.05 eV (~406 nm) is its energy. Other crystal properties of all three forms of TiO_2 are shown in Table (2.1).

Table 2.1 Properties of TiO_2

Crystal structure	System	Space group	Lattice constants (nm)			Density (kg/m^3)	Band gap (eV)
			a	b	c		
Brookite	Orthorhombic	Pbca	0.5436	0.9166	0.5134	4170	3.05
Anatase	Tetragonal	I41 /amd	0.3733	0.3733	0.937	3830	3.26
Rutile	Tetragonal	P42 /mmm	0.4584	0.4584	0.2953	4240	3.05

Titanium dioxide is wide band gap semiconducting material used in solar and chemical processes that emerged as a tremendous substantial for environmental refinement [30].

Titanium dioxide is an n-type semiconductor with electrons as the majority carriers with three phases as discussed above. It is non-toxic, chemically stable and low cost material that has a positive impact on the environment

2.3 Application of Titanium dioxide

Titanium dioxide is a multidimensional composite material that has a high number of industrial applications. Titanium dioxide is nontoxic, chemical stable and low cost semiconducting material these properties make it an ideal choice for several applications. Titanium dioxide is used to synthesize many environmental friendly products such as, solar cells, fabrics, self-cleaning surfaces, cosmetic, ceramic tiles, electric devices (varistors & MSFETS), hydrogen and electric energy production and due to its non-toxicity it plays an imperative role in the biocompatibility of bone implants [31]. Some of these are discussed in this chapter.

2.3.1 Photo-catalytic Applications

A catalyst is a substance that increases the rate of reaction of a chemical process while the term photo-catalysis is used when photons are involved in the reaction mechanism to accelerate the catalyst. Photo-catalysis is defined as the reaction where the catalyst in the presence of sunlight are used to influence a reaction in the reactants by keeping the catalyst unaltered and chemical structures of the reactants are modified [32].

Since last three decades photo-catalytic semiconducting materials becomes a promising way out to meet energy challenges and environmental issues. TiO_2, especially anatase TiO_2, is the most active photo-catalyst. Semiconductors with photo-catalytic activity show specific electronic, structural, surface and morphologic features.

$$TiO_2 + h\nu \rightarrow e^-_{CB} + h^+_{VB}$$
$$h^+_{VB} + H_2O \rightarrow OH + H^+$$
$$e^-_{CB} + O_2 \rightarrow O_2^-$$
$$2O_2^- + 2H_2O \rightarrow H_2O_2 + 2OH^- + O_2$$
$$H_2O_2 + e^-_{CB} \rightarrow OH + OH$$

The photo-catalysis is basically the acceleration of a photoreaction in the presence of catalyst. In photo-catalysis no energy is stored [33]. Ultra violet (UV) photo-excitation process requires photons of wavelength lower than 390 nm. The photo-catalytic

properties of TiO_2 were discovered by Akira Fujishima in 1967 and published in 1972. Thephoto-catalytic process on the surface of the TiO_2 is known Honda-Fujishima effect. TiO_2 have a forbidden gap i.e. band gap, a region that devoid the energy levels, between the valence and the conduction band. Photo-catalysis process is initiated by the absorption of a photon with energy equal to or greater than its band gap. As a result electrons (e^-) jump from valence band (VB) to the conduction band (CB) producing a charge carrier pair i.e. electron-hole (e^-/h^+) pair as shown in the figure (2.2). Hydroxide (-OH), or other radicals formed from available holes and free electrons, which act as oxidant (oxidize organic chemicals, or reduce metal species). The positive holes are created in the valence band and electrons in valance band, act as oxidizing and reducing agent simultaneously. The photo-generated electrons and holes migrate to the nano-crystal surface, where they act as redox sources. The primary photo-catalytic mechanism is believed to proceed as follows. The photo-generated holes have strong oxidizing power with very good redox efficiency [34-40].

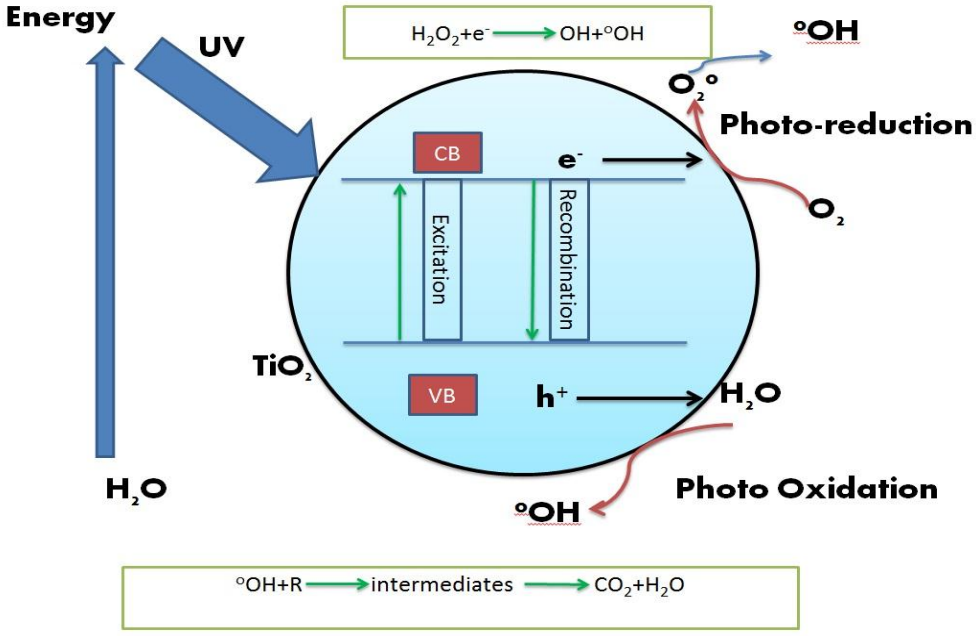

Figure 2.2 Titania Photo-catalysis process

Photo-catalytic property of TiO_2 depends on heat treatment during synthesis. Crystallinity of Titania nanoparticles increases at high temperature treatment and it demonstrate superior photo-catalytic activity while surface area decreased [41].

Photo-catalytic performance of TiO_2 depends on following factors:

- Synthesis method
- Particle size
- Crystal structure
- Surface area
- Porosity

To achieve high photo-catalytic activity impurity atom in the form of metal / nonmetal dopant are added. We will discuss this in detailed later. A good photo catalyst possesses the following characteristics, it should be:

- Able to absorb visible and/or UV light.
- Chemically and biologically inert and photo stable.
- Inexpensive and Nontoxic.
- Photoactive.

TiO_2 is the most used photo-catalytic material and fulfills all of these requirements [42].

2.3.2 Photo induced super-hydrophilic applications

In 1997, Wang et al. reported the phenomenon of super-hydrophilicity was reported in 1997 [43]. When titanium dioxide thin films are exposed to ultraviolet light, the continuous decrease in contact angle of the water was observed and finally it approaches almost zero. Numerous commercial products on the basis of this concept have been designed and named as self-cleaning materials. Transparent super-hydrophilic self-cleaning TiO_2 coating films are applied on glass substrates such as mirrors, window glasses, windshields of automobiles and so on. TiO_2-coated glass is antifogging and self-cleaning. The super-hydrophilic property of the surface allows water to spread completely across the surface rather than remain as droplets thus making the surface anti-fogging and easy to wash. In the case of a film, which consists of only TiO_2 the contact angle of water almost becomes about zero during UV irradiation and it was also found that the contact angle increases faster comparatively in a dark place, i.e. the film loses its hydrophilicity quickly after removing UV irradiation. It is desirable that the contact angle

rises slow in a dark place and maintains hydrophilicity for a long time. By adding SiO_2 the contact angle of water was low and the maintenance of hydrophilicity in a dark place was also good [44, 45].

2.3.3 Photovoltaic Applications

TiO_2 Nano crystalline electrodes are contributing efficiently as a photovoltaic. Monolayer thin film of TiO_2 nano-crystalline materials capable of charge transfer dye adsorbed at the surface and act as a major part of the solar cell. The film is placed in contact with a redox electrolyte.

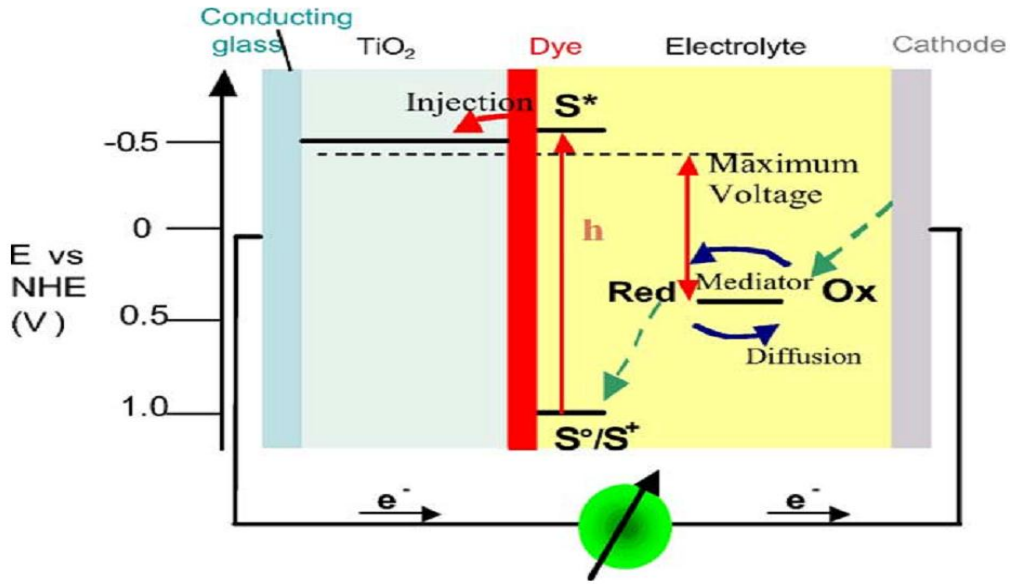

Figure 2.3 Principle of operation and energy level scheme of the dye-sensitized nano-crystalline TiO_2solar cell

The dye provides an electron upon photo-excitation which is introduced into the conduction band of TiO_2, these electrons conducted to external circuit that generate electric power and via electrolyte the original state of dye is restored. Organic solvent such as iodide/triiodide couple containing redox system is used as electrolyte. Electron captured by oxidized dye is prevented by regeneration of sensitizer. By the reduction of triiodide at the counter electrode the iodide is regenerated. Beneath illumination, the generated voltage is the difference between the Fermi level of TiO_2 and the redox potential of corresponding electrolyte. In general, there are no permanent chemical transformations when DSSC generates electric power from light. The nano-crystallinity

and mesoporosity of TiO_2 are imperative parameters to obtained high surface area that ultimately leads to higher adsorption of dies. Furthermore, upon insertion of small particles in electrolyte they almost get depleted and transport of electron due to proximity of the electrolyte to all particles is relatively easy [17].

2.3.4 Electronic Properties

Electronic structure is responsible for optical properties of material. The electronic structure is mainly dependent on physical dimension, arrangement and chemical composition. Electronic states of TiO_2 are mainly divided into three parts:

i. valence band
ii. lower conduction band
iii. upper conduction band [48]

TiO_2 has excellent electron transfer properties with n-type semiconducting property. TiO_2 has large band gap (3.0 eV for rutile and 3.2 eV for anatase). Based on the energy band structure, density of states, electrical conduction properties, materials are classified into Insulator, conductors and semiconductors. The electrical conductivity of a semiconductor lies in between those of insulators and conductors and typically has resistivity of the order of 10-8 Ω-m. The semiconductors nearly conduct electricity. The semiconductor may be in the form of a powder suspended in the water or fixed on a support. In terms of energy bands, semiconductors can be defined as those materials, which at room temperature have:

- Partially-filled conduction band
- Partially-filled valence band, and
- A very narrow energy gap (of the order of 1eV) between them [49-51].

By changing the structure or composition of semiconductors, we can make and design them either conduct electricity, or not conduct electricity. In addition, they interact significantly with light, which strongly depends on their band structure that in turn depends on the composition.

The band gap is the energy separation between the top filled energy level of the valence band and the nearest unfilled level in the conduction band above it as shown in figure (2.4). In order for an electron to jump from a valence band to a conduction band, it

requires a specific minimum amount of energy i.e. the band gap energy for the transition. The band gap energy of insulators is large (> 4 eV) but lower for semiconductors (< 3 eV).

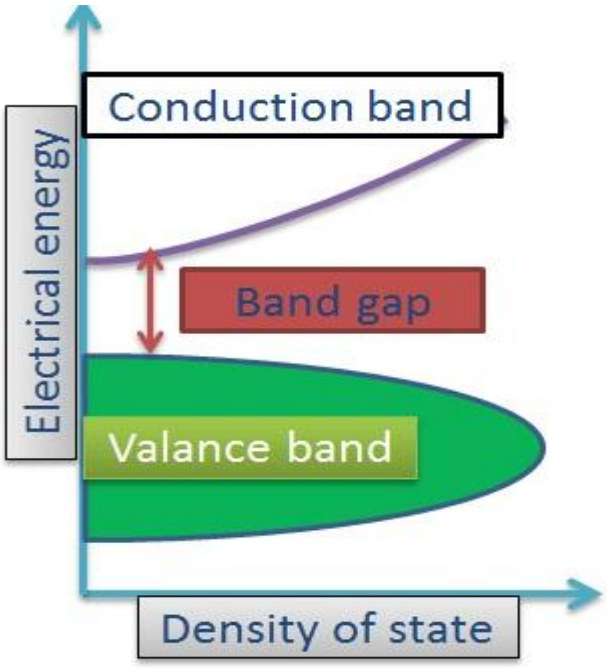

Figure 2.4 Band energies of different materials in terms of conduction and valence bands[52]

In semiconductors the highest occupied band is completely full of electrons and the next band up is close by. Although there is no space for the electrons to move around on the band, it is not too hard for an electron to gain the extra energy required to leap up into the nearby higher band, where it can move freely carrying an electric current. This leaves a gap or hole in the lower band, which can also move. Since we can easily supply the extra energy from outside, or by intuitive design we can control the way the semiconductor conducts electric current. The electric current is carried by both 'electrons' and 'holes' in semiconductors. Movement of Electric charge carrier through semiconductors depends on its compositions, so we can make different sorts of semiconductor structure. There are two types of semiconducting materials:

i. Direct band gap semiconductors
ii. Indirect band gap semiconductors

The TiO_2 is an indirect band gap semiconductor. As the crystal size decreases below a certain limiting size, associated with its exciton Bohr diameter, the spacing between

levels in the bands becomes larger (the energy structure changes from a quasi-continuum (band) to discrete, quantized levels) and the band gap increases [53-54]. In a bulk semiconductor a bound electron-hole pair, called an **exciton,** can be produced by a photon having energy greater than that of the band gap of the material. The photon excites an electron from the filled band to the unfilled band above. The result is a hole in the otherwise filled valence band, which corresponds to an electron with an effective positive charge. Because of the Coulomb attraction between the positive hole and the negative electron, a bound pair, called an **exciton,** is formed that can move through the lattice. The electrons and holes have opposite electric charges they can attract each other and form 'excitons'. However their motion is affected by imperfections in the lattice, as well as by the phonons. The separation between the hole and the electron is lattice parameter [59]. The existence of the exciton has a strong influence on the electronic properties of the semiconductor and its optical absorption. The larger band gap of TiO_2 can be deceased by using suitable dopants in order to improve the photo catalytic efficiency. In any material e.g. TiO_2, ZnO [60] etc. there will be a size below which one observes a fundamental shift in electronic and optical properties as a function of size [55-56].

2.3.5 Surface and adsorption properties

The surface chemistry is of vital importance in numerous processes, including corrosion, adsorption, oxidation, reduction, and catalysis. The adsorption of oxygen affects the photo activity. High specific surface area enhances photo catalytic activity. The chemical property of the surfaces is important factor which affects the hydrophilic property. With the increase of chemically absorbed –OH on the surface, the hydrophilic property will be enhanced. TiO_2 is transparent to visible light having high brightness and very high refractive index (n = (n ≈2.4 to 2.7) but low absorption coefficient. It has excellent textural, structural, optical light-scattering, light-reflecting and antireflective properties and its high surface area improves surface sensitive reactions [57-61].

CHAPTER 3

Synthesis Routes & Characterization Techniques

3.1 Industrial Production of TiO_2

Titanium dioxide is not available in pure form and it is synthesized from ilmenite or leucoxene ores on bulk scale by three main processes:

3.1.1 Chloride Process

This process was developed during the 1960's involves vapor phase generation of Titania. The crude ore (70% TiO_2 minimum) is reduced using carbon and then oxidized with chlorine produces titanium tetrachloride in this process. Titanium tetrachloride is further distilled and then re-oxidized in pure oxygen flame at 1500–2000 K and pressures (~300 kPa) to give pure TiO_2 while also regenerating chlorine. The overall reaction of oxidation process is given below [62]:

$$TiCl_4 + O_2 \longrightarrow TiO_2 + 2Cl_2$$

Frequently aluminium chloride is also added in this process as a rutile promoter. Product produced without mixing of aluminium chloride mostly exists in anatase phase.

3.1.2 Sulphate process

The sulphate process developed during 1940s. This process deals with liquid phase synthesis of titania, developed during the 1940's. This process utilizes ilmenite as TiO_2source, which is digested in sulfuric acid [63].

3.1.3 Becher Process

Major content of ilmeniteis titanium as TiO_2 i.e. 55-65% and remaining is iron oxide. This process is used for removal of iron oxide leaving residue of synthetic rutile. Major content of residue is mainly 90% TiO_2. In recent days, a rising curiosity in hydrolysis based aerosol synthesis because of much lower temperature requirements and the absence highly pure oxygen [63-64].

3.2 Methods for the Synthesis of Crystalline TiO_2 Nanoparticles

The TiO_2 nanoparticles synthesis with precise size, morphology, phase and composition is of scientific interest. Different fabrication processes have been developed to produce TiO_2 nanoparticles (4.4-2300 nm), with various morphologies such as nanorods, nanotubes, nanowires, and nano-spheres. Using this process highly crystallized TiO_2 spherical particles are produced. Few works have focused on the preparation of shape controlled Titania nanoparticles [65, 66].

Different synthesis methods for TiO_2 nanoparticles are listed below. We can classify these methods into two main types i.e. the methods in which TiO_2 nanoparticles are synthesized below 250^{o}C are called *"low temperature methods"* and the methods in which synthesis is done above 250^{o}C are called *"high temperature synthesis methods"*.

3.2.1 High Temperature Synthesis Routes

The high temperature synthesis routes are

i. Aerosol Processes (gas or vapor phase) [67-70].
ii. High Temperature Thermal Hydrolysis Reactions [71].
iii. Hydrothermal Processes [72].
iv. Flame Synthesis [74].
v. No hydrolytic Solution-Based Reactions [75].
vi. Hydrazine Method [76].
vii. Thermal Plasma Treatment [77].
viii. Template Based Synthesis of TiO_2 Nanoparticles [78].

In all these methods different chemical precursors are used and the TiO_2 nanoparticles can be synthesized either by oxidation, thermal decomposition or hydrolysis.

Merits

(i) These methods produce good-quality crystals with control over their composition and morphology.

(ii) The aerosol reactor offers several advantages such as product purity, ease of collection, energy efficiency and absence of unit operations of filtration, washing and drying involving large liquid volumes.

(iii) For commercial applications, aerosol processes with low cost precursors and uninterrupted processing at lower temperature are favored.

(iv) Mostly rutile phase is obtained in large amounts.

(v) In these methods the crystalline perfection was high.

(vi) Rod like rutile TiO_2 nanocrystals have been observed in acidic media upon hydrothermal treatments along with coexistence of anatase and/or brookite traces in some cases.

(vii) Anatase TiO_2 nano fibers are also formed.

(viii) Vapor phase hydrolysis of Titanium tetrachloride yields low cost anatase at temperature (<387 K) and rutile phase TiO_2 at temperature of <673 K).

(ix) The solution combustion method gives highly crystalline fine TiO_2 particles.

(x) By Diffusion flame method well-dispersed TiO_2 nanoparticles with controlled crystal structures and particles size are obtained.

(xi) In case of Thermal plasma method, there are several advantages:

- the availability of extremely high temperature reaction zone
- high enthalpies
- sharp heating/cooling rates
- compact reactor
- high throughputs
- non-equilibrium phases
- extremely fine crystallinity
- rapid one-step synthesis process

It is continuous process. TiO_2 nanoparticles, anatase coatings and TiO_2 composites can be synthesized by this method.

(xii) In case of Template based synthesis the mesoporous silica SBA-15 is most suitable host material for synthesis of highly dispersed TiO_2 nanoparticles.

Demerits

(i) High price of alkoxide precursors.

(ii) Hydrothermal syntheses are directly carried out at high temperatures.

(iii) Expensive aerosol reactor and autoclaves.

(iv) The resulting nanocrystals are rather agglomerating.

(v) Titanate nanotubes and Nano whiskers produce by hydrothermal method instead of nanoparticles.

(vi) Chemical impurities are present in final synthesized products in flame synthesis method. The presence of such impurities badly affects the application of TiO_2 in Photocatalytic reactions and also in other chemical processes.

(vii) The yields are usually low.

(viii) Many particles exhibited irregular shapes.

(ix) Wide size distribution of the particles is present in case of thermal plasma, which arise due to uncontrolled quenching and coagulation process in a thermal plasma environment.

(x) In case of template based method the preparation of hard template and the removal of the organic template by thermal treatments in presence of air at 550^{o} C for continuous 7 h make this process expensive and complex. Also limited pore voids limited growth of TiO_2 nanoparticles during heat-treatments process.

3.2.2 Low Temperature Synthesis Routes

Recently, considerable interest has been directed towards the synthesis of Titania by solution based, low temperature processes. Several low temperature methods available for TiO_2 nanoparticles synthesis:

(i) Low Temperature Thermal Hydrolysis Reactions.

(ii) Microwave-Hydrothermal Process [78].

(iii) Alcohothermal Method [79].

(iv) Solvothermal Synthesis:

  a. Aqueous Based Solvothermal Route [80].

  b. Non-Aqueous Solvothermal Route [81].

(v) By aging at low temperature [82].

(vi) Synthesis of TiO_2 nano powders from per oxo titanium solutions [83].

(vii) By Pyrolysis at 70 ^{o}C [84].

(viii) Low temperature dissolution re-precipitation process (LTDRP) in liquid media [85].

(ix) Solvent evaporation-induced crystallization.

(x) Low temperature Vapor Phase processes.

(xi) The Sol-Gel method [86].

(xii) Sol-Gel Synthesis by Ultrasound-irradiation [86].

(xiii) Micro emulsion-based Synthesis of TiO_2 [86].

Merits

(i) The absence of amorphous Titania indicates the unusual high crystallinity.

(ii) Ti and O elements in the product with an approximate molar ratio of 1:2 are present.

(iii) Spherical TiO_2 nanoparticle with narrow and pore size distribution and large surface area are produced.

(iv) Mostly TiO_2 anatase nanoparticles are obtained.

(v) Microwave Hydrothermal process involves rapid heating treatment, exceptionally rapid kinetics of crystallization and there is molecular homogeneity.

(vi) Titanium halides are cheaper than their alkoxides.

(vii) Better control over morphology and size distribution of the nanocrystals is achieved in non-aqueous synthesis.

(viii) Synthesis is achieved at low temperatures and less time.

(ix) The TiO_2 powder, prepared by LTDRP method, has very high specific surface area than the sample prepared by hydrothermal method.

(x) Sol-Gel method yields high surface area TiO_2 [87].

Demerits

(i) The high price of alkoxide precursors imposes commercial limits.

(ii) Sol-Gel process yields usually amorphous or poorly crystalline TiO_2 because low processing temperature in this wet chemistry route.

(iii) Irregular shaped TiO_2 nanoparticles are observed in some cases.

(iv) In some cases the nanoparticles are linked one by one to form a scaffold.

(v) Presence of spherical aggregates of TiO_2 nanoparticles is observed.

(vi) In some cases bi-phase TiO_2 is obtained.

(vii) In Sol-Gel synthesis the amorphous precipitates need subsequent thermal processing to get crystalline nanoparticles, which induce significant sintering of the nanocrystals, particle size increases.

(viii) pH values variation in the reaction solution or suspension changed during the progress of the synthesis process.

(ix) In some cases gases are evolved during the synthesis process.

(x) Unfortunately, most synthetic anatase crystals are dominated by the less-reactive (101) surface.

3.2.3 Others Methods

(i) Electrochemical Synthesis of TiO_2 nanoparticles [88].

(ii) Selective Synthesis of TiO_2 nano powders (detonation method) [89].

These methods are used not only for TiO_2 nano particles synthesis but can also be used for the synthesis of various TiO_2 nano composites with other materials and TiO_2 thin films. During synthesis various metals can also be doped in TiO_2 nanoparticles.

3.3 Synthesis of TiO_2 by Sol-Gel Method

The Sol-Gel process is a wet chemical technique. This process is widely used in materials science field and was discovered in 1846 by Ebelmann [90]. Research on Sol-Gel method grew to be so important and from 1990s more than 35,000 papers have been published worldwide. Sol-Gel chemistry provides a convenient route for the synthesis of 3-dimensionalmetal oxides [91]. This process occurs at room temperature. Nano materials can be synthesized using this method in different forms like thin films, fibers, fine powders and even monoliths [49]. Materials derived from this technique have various applications in energy, optics, electronics, sensors, space, separation technology, and medicine [92]. By Sol-Gel chemistry doped and un-doped TiO_2 nanoparticles can be synthesized with well-controlled morphological and structural features. This method provides control over reaction parameters, compositional homogeneity, grain size, particle morphology and porosity. We get mono-disperse spherical Nano crystalline TiO_2 powders with high chemical purity, high surface areas, small crystallite size, by hydrolysis process and

condensation of Titanium precursors in liquid phase or non-aqueous medium at ambient temperature and atmospheric pressure. Physio-chemical and electrochemical properties of TiO_2 can be improved to make it efficient through this synthesis method [87, 93].

Materials synthesis (typically metal oxides) started from solution (sol) that acts as a precursor for integrated network (gel) of detached particles or network (polymers). There are four stages of Sol-Gel formation [94].

(i) Hydrolysis

(ii) Condensation and polymerization of monomers to form particles.

(iii) Growth of particles.

(iv) Gel is formed as the agglomeration of particles leads to networks that extend throughout the liquid medium as well as increasing the thickness.

The process involves processes such as hydrolysis and polymerization of metal precursors (alkoxide or halides). The solutions of precursors are reacted and forms irreversible gels which shrink to rigid oxide forms after drying [96,97]. The metal oxides are synthesized by the hydrolysis of reactive metal precursors, usually alkoxides in an alcoholic solution, resulting in the corresponding hydroxide. The titanium precursor in appropriate concentration is added to the selected solvent. The contents are stirred vigorously for various times. The precursors for TiO_2 are mostly titanium alkoxides and titanium chlorides they undergo hydrolysis and poly-condensation reactions. On reaction they form either a network "elastic solid" or a colloidal suspension that is a system of distinct sub micrometer particles spread to great extinct in host fluid. Formation of a titanium oxide contains metal origin with oxo (Ti-O-Ti) or hydroxo (Ti-OH-Ti) bridges at controlled reaction pH, consequently making metal-oxo or metal-hydroxo polymers in solution. Elimination of water leads to the formation of a network of metal hydroxide by condensing the hydroxide molecules. By linking all hydroxide species in one network like structure, gelation is attained and a dense porous gel is achieved. Gel is polymer of a three dimensional frame surrounding interrelated pores. Therefore, the sol develops towards the development of inorganic network called gel, is diphasic system containing both a liquid phase and solid phase. The condensation liberates small molecules such as water or alcohol.

The precipitate obtained as a result of hydrolysis is then filtered (or centrifuge). In gel the phase separation can be accomplished in number of ways. The advancement in technical

developments of solvent removal and drying process as simplified the fabrication process at nano scale with unique properties. The simplest method to produce such nano particles is to allow time for sedimentation and then pour off residual liquid. Also Centrifugation can be used to accelerate the separation process. The remaining liquid is removed by drying process. Shrinkage and densification of gel is due to drying process. Solvent removal rate can be measured by distribution of porosity in gel. The microstructure of final specie will obviously be strongly inclined by the changes applied during processing phase. Then the precipitate is washed with deionized water or some weak electrolyte to remove the impurities. Further heat treatment of the hydroxide forms ultrafine powder of the metal oxide. The precursor solution can be placed on a substrate for the formation film via dip coating or spin coating technique or it may be used to synthesize powders. Since the process starts with a nano sized unit and experiences reactions on the nanometer scale, it results in nanometer [37].

3.3.1 Hydrolysis Reactions

Hydrolysis and condensation rates are significant constraints that contribute toward mainly the chemical and physical properties of the final product. More controlled and slower hydrolysis leads to smaller particle sizes and more exclusive properties. Hydrolysis and condensation rates depend on the electro negativity of the metal atom, the alkoxy group, solvent system, and molecular structure. The hydrolysis and condensation reaction depends upon [34,63,99]:

(i) pH of solution.
(ii) Temperature
(iii) Reaction Time.
(iv) Concentrations of reagent.
(v) Nature of catalyst.
(vi) H_2O: M (Metal) molar ratio.

3.3.2 Hydrolysis of Metal Alkoxides

Metal alkoxides (organometallic compounds) contains one or more than one metallic atoms in their molecule. Metal alkoxides (R-O-M) are like alcohols (R-OH) with a metal atom, M, substituting hydrogen “H” in hydroxyl group. They are mostly used for many metallic

oxides and metal nanoparticles in Sol-Gel synthesis as chemical precursors. In hydrolysis the reaction occurs by addition of water, resulting in replacement of alkoxide groups (OR) with hydroxyl groups (OH). Following condensation reactions involving the Metal-OH groups yield M-O-M plus by products water. Hydrolysis follows until all -OR (alkoxy) groups are swapped by -OH (hydroxyl) [100]. Hydrolysis of metal alkoxides (M (OR) z) includes nucleophilic reactions with water as follows:

$$M(OR)_y + xH_2O \leftrightarrow M(OR)_{y-x}(OH) + xROH$$

$$TTIP + 2H_2O \rightarrow TiO_2 + 4C_3H_7OH$$

The above reaction is hydrolysis reaction because hydroxyl ions are attached to the metal atom. This reaction involves the addition of OH^- group to positively charged metal center (M^+). The H^+ ion is transferred to an alkoxy group followed by the removal of R-OH. Condensation takes place when the hydroxide molecules, relief water molecules and a gel of the hydroxide are attained [96].

3.3.3 Hydrolysis of Metal Halides

Similarly metal chlorides undergo hydrolysis as follows:

$$MX_4(y) + H_2O(l) \rightarrow M(OH)_4(s) + 4HX(g)$$

$$TiCl_4(g) + 4H_2O(g) \rightarrow Ti(OH)_4(s) + 4HCl(g)$$

3.3.4 Reaction Mechanism

The mechanism of nuclear reaction for producing TiO_2 at low temperature by the hydrolysis of $TiCl_4$ is:

$$TiCl_4(g) + 4H_2O(g) \rightarrow Ti(OH)_4(s) + 4HCl(g)$$

$$Ti(OH)_4.H_2O \rightarrow TiO_2 + H_2O$$

The reaction of $TiCl_4$ with H_2O upon mixing, yields hydro chloric acid gas and $Ti(OH)_4$ nuclei, that grow by the formation of oxo and hydroxyl bridges. These particles grow further by coagulation or condensation.

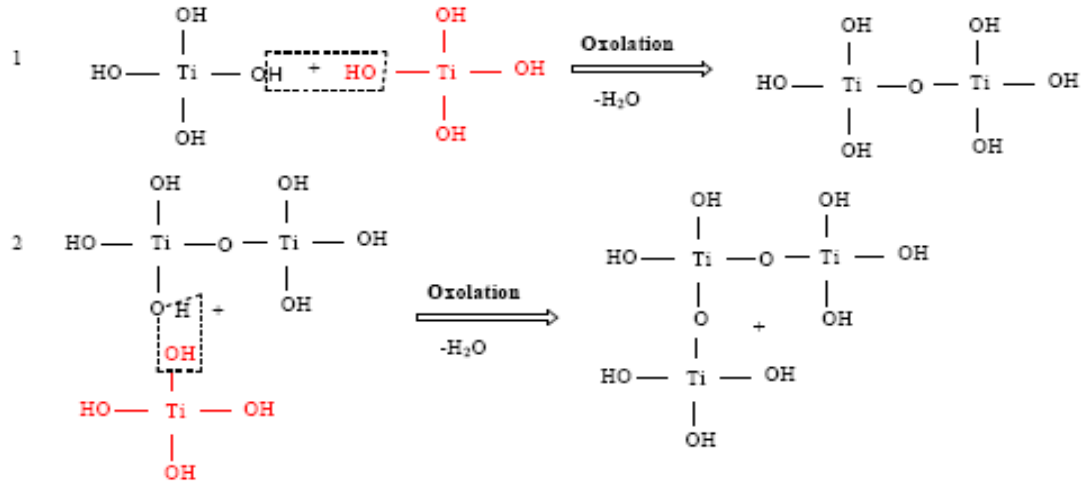

Figure 3.1 Growth Mechanism of TiO_2 by the Bridging molecule $Ti(OH)_4$ [101]

Through Sol-Gel process anatase content is high. Pure anatase crystals are more difficult to obtain than their rutile counterparts. The mixture of anatase and rutile particles can be converted to pure rutile by heating at temperatures greater than 400°C [102].

3.3.5 Heat of Formation

The "heat of formation" (ΔH^o_f), of a compound is the amount of heat given off or absorbed when one mole of that compound is prepared from its constituent elements [59].

$$\Delta H_{reaction} = \sum_{products} \Delta H^o_f - \sum_{reactanats} \Delta H^o_f$$

We calculate ΔH for the reaction below, using heats of formation."

$$TiCl_4\ (l) + 2\ H_2O\ (l) \rightarrow TiO_2(s) + 4\ HCl\ (g)$$

Table 3.1 Heats of formation of different compounds

Compound	Heat of formation
$TiCl_4$(l)	-763 kJ/mol
H_2O(l)	-286 kJ/mol
TiO_2(s)	-945 kJ/mol
HCl(g)	-92 kJ/mol

The ΔH_f^o values of the products are;

1 mol TiO_2 (s) × -945 kJ/mol = -945 kJ

4 mol × -92 kJ/mol = -368 kJ

Sum = -1313 kJ

The ΔH_f^o values of the reactants are;

1 mol $TiCl_4$ (I) × -763 kJ/mol = -763 kJ

2 mol H_2O (I) × -286 kJ/mol = -572 kJ

Sum = -1335 kJ/mol

For the overall reaction:

ΔH = (-1313 kJ) – (-1335 kJ) = 22 kJ

3.4 Applications of Sol-Gel Method

(i) Sol-Gel is very useful technique that can be applied for coating on various substrates via spin coating or dip coating method. It is used to get protective and optical coating like thin films.

(ii) Optical and Refectory ceramic fiber can be synthesized by controlling the solution viscosity that find their potential application in optic sensors and thermal insulation respectively

(iii) Via precipitation method Very-fine and uniform ceramic powders can be synthesized. This powder may contain the composition of more than one element. These compositions can be made in sub-micrometer particle size for dental and biomedical applications.

(iv) Metal oxides, zeolites, ceramic membranes for microfiltration, nano-filtration, pre evaporation and reverse osmosis can be synthesized by this technique.

(v) Highly porous and extremely low density material called aerogel is obtained if the liquid in a wet gel is removed under a supercritical condition.

(vi) Drying the gel at low temperature from 25 to 100 °C may leads to porous solid matrices called aerogel.

Merits

(i) It does not need complicated set-up.

(ii) This particular method has several advantages over other techniques in terms of purity, homogeneity, ease of introducing dopants in higher concentrations, stoichiometric control, ease of processing and composition control.

(iii) At lower temperature densification is often achieved.

(iv) By this method small quantity of dopants, such as metals, metal oxides, organic dyes and rare earth metals can be introduced in the sol and uniformly dispersed in the final product.

(v) Production of homogeneous product is achieved by this method.

(vi) Nanoparticles with size ranging from 1 to 10 nm along with steady crystal structure, unique morphological features and a high degree of mono-dispersity have been processed by this technique.

(vii) Less expensive precursors are used.

(viii) Low temperature processing.

(ix) The procedure initiates with homogeneous mixture and the resulting product is a uniform ultra-fine porous powder.

(x) Sol-Gel process can also be scaled up to industrial-scale production.

(xi) Simple chemistry and precise stoichiometry.

(xii) TiO_2 nanoparticles, nano sheets, nano fibers and nano rods can be synthesized.

(xiii) At very low temperatures brookite phase is obtained, at relatively higher temperature anatase is obtained and at further higher temperatures the gel is dehydrated to yield rutile [34, 42,103].

Demerits

(i) Sol-Gel preparations (based on both hydrolytic and non-hydrolytic reaction pathways) provide amorphous Titanium dioxide. Calcination of gels or thermal annealing of micro emulsions are therefore required to induce crystallization of the nanoparticles, although leading to phase transformation, sintering, grain growth, and loss of surface area in many cases.

(ii) Titanium alkoxides are expensive and toxic.

(iii) Poorly crystalline product due to the low processing temperature in this wet-chemistry route [93,105].

3.5 Reaction Parameters and Effect of Processing Conditions

The important parameters in any type of synthesis method are precursors, additives, catalysts, pH, solvent and temperature that affect the degree of crystallization, particle size, phase composition and morphologies [106]. The important reaction parameters are:

3.5.1 Nature of the Catalyst

The catalysts used are acids such as HCl, H_2SO_4, HF, HNO_3 and CH_3COOH, and bases like NaOH, NH_4OH, Tertiary amines or Quaternary ammonium hydroxide/ammonia solution that affect the rate of hydrolysis and condensation of metal precursors. They also control the rate of protonation and deprotonation of metal hydroxides formed after hydrolysis. For hydrolysis bases provide better nucleophile (OH^-) but condensation rate is enhanced by deprotonation of metal hydroxide groups. The rate of reaction is dependent on the strength and concentration of acid base catalyst. Acid work as a chemical catalyst during crystal growth process and become a cause of change in crystallization mechanism that reduces the activation energy brookite and rutile formation [42,106].

3.5.2 Nature of the Leaving Group

Usually alkoxides (-OR) and halides are the leaving groups. Moreover acid catalyst such as NHR or NH_2may is used as well. As the size of –OR groups increases the sensitivity of metal oxide toward hydrolysis decreases which means smaller is –OR group resulting in higher reactivity of corresponding alkoxide. In order to avoid from hydrolysis and uncontrolled precipitation careful handling in dry atmospheres is required because metal alkoxides are highly reactive toward water. The chloride ion accelerates the nucleation of anatase [63].

3.5.3 Nature of the Solvent

The solvents used are alchols (ethanol, isopropanol), deionized water, mixed solvent of water and n-propanol, aqueous NaCl, aq.CH_3COOH, HCl solution, Ionic liquid such as 1-butyl-3-methylimidazoliumtetrafluoroborate, THF, dioxane, DMF etc. Frequently the

alcohol which is the conjugated acid of the leaving group (EtOH, MeOH) is used for metal alkoxides. Deionized water is used for metal halides precursors. However if organic solvent is used then after hydrolysis reactions the remaining organic molecules may contribute toward incomplete crystallization if the calcination is not being done at temperature [107,108].

3.5.4 Nature and Concentration of the Reagents

Growth behavior of TiO_2 particles influence their crystallinity, surface area, particle size and morphology and all these parameters depend upon the choice of precursor, acidic/basic conditions, processing temperate etc. The concentration and nature of the precursors, H_2O, catalysts and precursor/ substrate ratio are important parameters. The concentration of the aqueous $TiCl_4$ solution influences the phase formation, morphology and grain size of the products. The rate of condensation and hydrolysis depends on the alkoxy group, electronegativity (metal atom), solvent nature and finally the molecular structure of the metal alkoxides. Hydrolysis phenomenon is slower in metals with higher electro negativities as compared to those having lower electro negativities. Very acidic (high valent) cations will readily hydrolyze in aqueous solution, often even at low pH. These cations tend to form the polymeric metal oxide chains. This hydrolysis can be controlled by addition of acids [109]. The most common precursors used for synthesis of TiO_2 are:

(i) Titanium tetra iso-propoxide (TTIP, Ti-$(OC_3H_7)_4$, di iso-propoxititanate is (acetylacetonate) (DIPBAT).

(ii) Titanium tetra chloride ($TiCl_4$).

(iii) Amorphous TiO_2

(iv) Titanium iso-propoxide ($C_{12}H_{28}O_4Ti$)

3.5.5 Temperature

Temperature has significant effect in the poly-condensation phase as well as in the growth of the solid phase. The crystallinity, surface area, particle size and morphology depend upon the processing and calcination temperatures. The change in physico-chemical properties of Titania significantly depend on condition of heat treatment conditions.

3.5.6 Geometry of the Molecular Entity

It is flexible, rigid linear, planar, tetrahedral, etc. are important reaction parameters.

3.5.7 Morphology Controllers / Surfactants

The morphology and size can be controlled by:

(i) By the addition of auxiliary agents like surfactants or compounds with distinct structures e.g. sodium dodecyl benzene sulfonate (DBS), sodium dodecyl sulfate (SDS), oleic acid, hydroxyl propyl cellulose (HPC), Pluronic P-123 triblock copolymer and carboxylic acid group-containing organics.

(ii) By controlling the reaction conditions in order to control size and morphology.

In many cases organic shape-controllers in aqueous media are used to control the morphology. Stabilizing agents have been used to prevent agglomeration, but, with a few exceptions, particles are crystalline after a long (3 days) or short (from 5 min to a few hours) aging at moderate (140°C) or high temperatures (250-300°C), respectively. Recently, the growth of nearly spherical anatase TiO_2 nanoparticles has been demonstrated even at 40°C by means of a time-consuming (7-14 days) nonaqueous procedure [110, 111].

3.6 Effect of pH

The effects of pH value on morphology, phase composition, agglomerate, microstructure and specific surface area of titanium dioxide significantly, while type of solvent and coexisting ion, etc. in the solution may also affect. By adjusting pH value in Sol-Gel process we can control particle size, shape, phase and agglomeration. It is reported that larger surface area is obtained at smaller pH values (pH-3) and it is also reported that anatase TiO_2 can be synthesized at pH-3 by controlling several parameters. Synthesis of TiO_2 under basic conditions results in small cubic like nano crystals, hexagonal nano crystals, or short rod-like nano crystals while in acidic condition results in in truncated tetragonal bi-pyramidal nano crystals. Growth rate of anatase depends on pH and surplus dilution during synthesis may leads to partial dissolution of TiO_2 nanocrystals, possibly resulting in spherical nanoparticles. Final nano morphology depends upon the value of the pH. Very acidic (high value) cations will readily hydrolyze in aqueous solution, even at low pH. These cations tend to form the polymeric metal oxide chains. This hydrolysis can be

controlled by addition of acids. Point of zero charge can be defined by pH. The pH values for which surface charge is equal to zero at specified temperature, pressure and aqueous solution composition is known as point zero charge.

Table 3.2 Point zero Charge of TiO_2

Oxidation State	Material	PZC
+IV	TiO_2	5.2 --- 7

Following types of point zero charge are acknowledged [34]:

(i) The pH value at which the net proton surface charge is zero is known as point of zero net proton charge.

(ii) The pH at which the net intrinsic surface charge is zero is known as point of zero net charge.

(iii) The pH value at which the net total particle charge is equal to zero is known as point zero charge. No additional surface charge is required to be neutralized by ions.

Varying pH not only shifts the band energies of the metal oxide semiconductor, but also varies the surface charge [113-116].

3.7 Characterization of TiO_2 Nanoparticles

A variety of modern techniques are used to characterize nanoparticles for their phase identification, structure, shape, surface morphology, band gape studies and size of the particles. The techniques employed in this project include:

- XRD (X-ray Diffraction)
- SEM (Scanning Electron Microscopy)
- EDX (Energy Dispersive X-ray Analysis)
- UV-Vis Spectroscopy

3.7.1 XRD (X-Ray Diffraction) Technique

By XRD we determine the crystallinity and crystallite size of the sample under study. Particle size is measured by x-ray diffraction line broadening. The simplest method to evaluate XRD profile is the application of the Scherer equation to obtain average crystallite size [17,243,244]. The Debye–Scherer equation is given below

$$D = K\lambda/\beta \cos\theta$$

Where,

D is the crystal size of the sample,

K = 0.9 is a coefficient,

λ = (CuKa = 1.5406 A°) is the X-Ray wavelength,

β is the full width at half maximum (FWHM) of the catalyst,

θ is the diffracting angle.

Surface area of the sample is calculated by using the given formula:

$$S = 6 \times 10^3/\rho L$$

Where,

S is the specific surface area ($m^2\ g^{-1}$),

L is the average crystallite size,

and ρ is the density of the Titania (3.9 g/cm3).

Anatase and rutile phases proportion in given sample can be calculated from the relative intensities of the primary peaks corresponding to the different phases as described by (Spurr and Myers, 1957). The fraction of rutile in the sample can be estimated using the equation:

$$x_R = \frac{1}{(1+0.8I_A / I_R)}$$

Where x_R is the weight fraction of rutile, I_A and I_R are relative intensities of the primary peaks corresponding to anatase (101) peak at $2\theta = 25.4^0$ and rutile (110) peak at $2\theta = 27.5^0$ respectively [117-119].

3.7.2 Scanning Electron Microscopy (SEM)

Microscope is used to study morphology and structure of the corresponding samples and this phenomenon is known as microscopy. In SEM electron beam is responsible for the formation of sequential images that are focused by lenses as the scanning probe. Electrons upto 30 keV energy are focused at surface of specimen in the microscope and scanned across it as a pattern of parallel lines. Several phenomenon take place at the surface, most important that is responsible for scanning purpose is emission of secondary electrons with energies of few tons of eV and reemission of high energy back scattered electrons from the

primary beam. The intensity of emission of both the beams depend the angle at which these beams strikes the surface of the sample. Electronic current of the emitted beam is collected by amplifier as the electron probe is scanned across the specimen variation in the resolution signal strength occur that are used to vary the brightness of the trace cathode ray tube being scanned in the synchronism with the probe, So there is a direct positional correspondence between the electron beam scanning across the specimen and the fluorescent image on the cathode ray tube. Produced magnification is the ratio of the dimensions of final image display and the field scans on the specimen. The magnification of the image can be altered by varying the extent of scan on the specimen and keeping the size of the display constant [63,104].

3.7.3 Energy Dispersive X-ray Analysis (EDX)

A focused electron beam is used to interact with the atoms of the sample by electron microscope. As the electron displaces into sample, detection equipment converts the scattered electron into a microscopic image. One more phenomenon occurs in this interaction, which is the generation of characteristic x-rays. An electron from an outer atomic shell “drops” into the vacancy of the inner shell In order to return the atom to its normal state and this result as the loss in specific amount of energy that is difference of energy between the vacant and contributing electron shell. This energy is supplied in the form of electromagnetic radiation. Energy levels in all elements correspond to different energies, so the characteristic x-rays is generated that belongs to specific element. The energy of the generated ray is measured by detection equipment. X-ray energy is converted into an electronic “count” by using semiconducting material in order to detect multichannel analyzer and x-rays. These energy counts accumulate and create a spectrum that shows the chemical analysis of the sample. By an electron microscopy we can observe the surface morphology of the sample’s while energy dispersive x-ray microanalysis gives us the information that what elements are present in the sample and their composition. When modern EDX is coupled with Transmission electron microscope (TEM) or Scanning electron microscope (SEM) than it is capable of detecting the X-rays counts of all the elements existing in sample which have higher atomic number than sodium [63,104].

3.7.4 UV-Vis Spectroscopy

Most of the molecules absorb light within the visible or ultraviolet (UV) spectrum range. This absorption of visible or ultra violet light is due to the excitation of outer electrons from their ground state to an excited state. The absorption of light is measured by using Bouguer Lambert Beer law. According to this law, absorbance is directly proportional to the path length, l, and the concentration of the absorbing substance, c, and can be expressed as $A = \alpha lc$, where α is a constant of proportionality, called the absorbtivity. In addition, absorption strongly depends on the types of samples, and the environment of the sample. For instance, molecules absorb radiation of various wavelengths depending on the structural groups present within the molecules, and show a number of absorption bands in the absorption spectrum. The solvent in which the absorbing species is dissolved also has an effect on the spectrum of the species. Moreover, the size of the particle is also important. If the size of the particle $d \gg \lambda$, light interacts with the samples instead of absorption, with parts of the light scattered and reflected.

CHAPTER 4

Experimental Procedure

4.1 Synthesis of pure TiO_2 Nano particles

4.1.1 Chemicals Used

Titanium tetrachloride (98% $TiCl_4$), Sodium Hydroxide (NaOH), Hydrochloric acid (37% HCl), Ammonium hydroxide/ ammonia solution were used in the synthesis. All chemicals used in the synthesis were pure and analytical grade reagents of noted firms such as Merck, Fluka and Aldrich and were used without any further purification. Titanium tetrachloride is used as precursor for Titanium. $TiCl_4$ is a chemical product widely used in the chemical industry. Accidental releases of $TiCl_4$ are known to be harmful due to its hydrolysis by the atmospheric humidity that produces HCl which is a toxic gas. To avoid rapid hydrolysis and uncontrolled precipitation cautious supervision in dry atmospheres is required because metal halides are extremely reactive toward water. So during experiment dry conditions were applied to avoid reaction of $TiCl_4$ with air and humidity. The simple laboratory glassware were used such as volumetric and titration flasks, condenser, three-neck round bottom flask, beakers, thermometer and pH meter etc.

4.1.2 Synthesis Procedure

0.5M acidic solution was prepared by adding 10 ml of HCl to 250 ml of deionized water. Then 0.5M stock solution for Ti^{+4} was prepared by adding 14.06 ml of $TiCl_4$ in the 235 ml of acidic solution (HCl + deionized H_2O) in 3-neck round bottom flask. The solution is made acidic to avoid the explosive generation of orthotitanic acid $Ti(OH)_4$ formed when $TiCl_4$ is added to this solution. The acidic solution hinder the rapid condensation reaction that could leads to the formation of a dense inorganic network, uncontrolled size and phase composition yielding poorly structured materials. Using these dry conditions and acidic solution the hydrolysis and condensation speed of the metal ion precursor becomes quite low. The pH of the stock solution is reduced due to liberation of HCl gas produced as a result of reaction of $TiCl_4$ with water. Condenser was fitted in

middle neck to condense any vapors produced during the course of reaction, also to avoid the bursting of three neck flask, due to liberation of HCl gas.

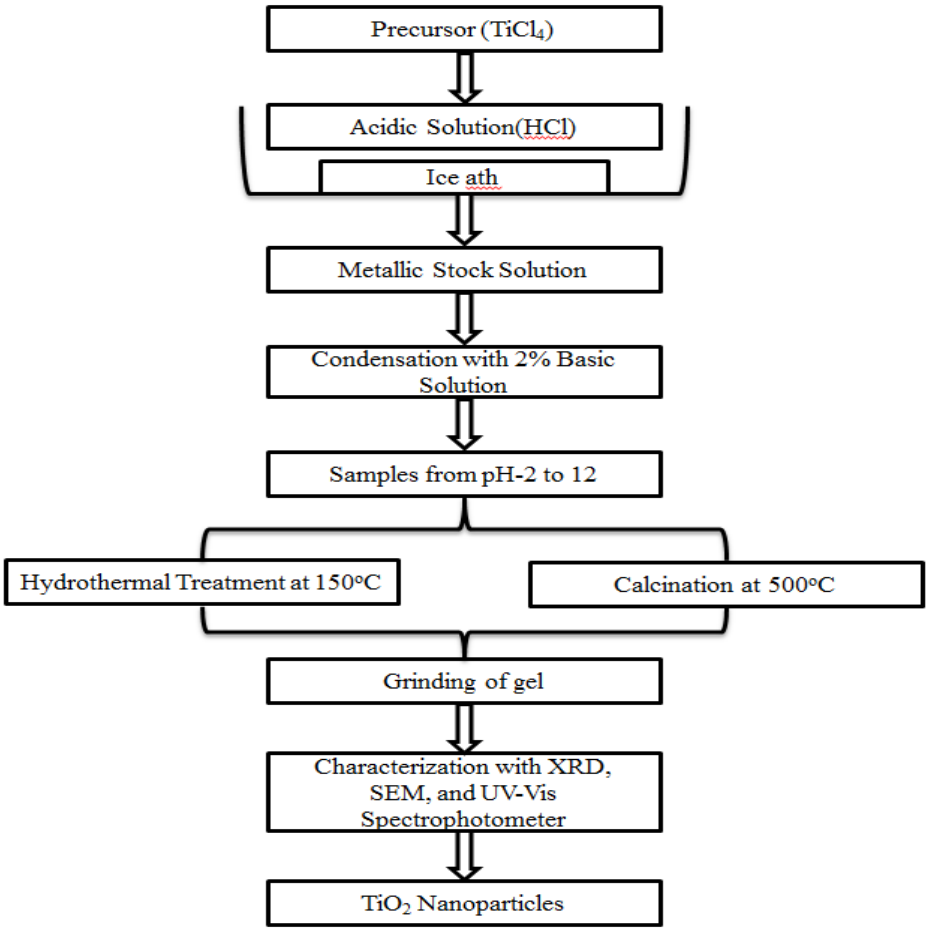

Figure 4.1 Flow sheet for Sol-Gel and sol hydrothermal synthesis of TiO_2 nano-particles

The $TiCl_4$ was added drop by drop from the dropping funnel fitted in neck of three necks round bottom flask. And in third neck of round bottom flask quick fit thermometer was inserted to trace the temperature. The three necks round bottom flask was keep in water bath containing ice to compensate heat generated during the hydrolysis reaction. The assembly was placed in Fume Hood. The solution was stirred to avoid formation of any precipitate. While dropping $TiCl_4$ drop by drop the color of the solution turns yellowish. But after dropping all the $TiCl_4$, the solution becomes colorless after sometime. The stock solution was prepared at room temperature. Then 30 ml from the stock solution was taken in a titration flask and is neutralized with 0.5M solution of Sodium Hydroxide till the pH reached to the desired value i.e. from pH=2 to pH=14 followed by

continuous stirring and the pH was monitored by Martini pH meter. During condensation process $Ti(OH)_4$ joined together to form a three dimensional lattice network forming the gel. The base provides the OH ions to the Ti+4cations to form $Ti(OH)_4$ network.. Each time 30 ml of stock solution was taken and neutralized with NaOH at desired pH value to get different samples. Heat treatment of obtained TiO_2 gel was done in two different ways i) Hydrothermal treatment by using auto clave ii) water was evaporated from gel at 100^oC, dry gel were grounded with mortar and pestle and calcination of dry powder was done in furnace at different temperature ranging from 250^o to 500^o C. The powder samples obtained were then saved in sample vials for characterization. The Sol-Gel-derived nano crystals were then characterized by XRD, SEM, EDX and XRF.

4.2 Synthesis of silver doped TiO_2 Nano particles

4.2.1 Chemicals Used

Titanium tetrachloride (98% $TiCl_4$), Sodium Hydroxide (NaOH), Hydrochloric acid (37% HCl), Ammonium hydroxide/ ammonia solution, ethanol, Nitric acid (HNO_3), Silver nitrate ($NaNO_3$) were used in the synthesis. All chemicals used in the synthesis were pure and analytical grade reagents of noted firms such as Merck, Fluka and Aldrich and were used without any further purification. Titanium tetrachloride is used as precursor for Titanium. $TiCl_4$ is a chemical product widely used in the chemical industry. Accidental releases of $TiCl_4$ are known to be harmful due to its hydrolysis by the atmospheric humidity that produces HCl which is a toxic gas. To avoid rapid hydrolysis and uncontrolled precipitation cautious supervision in dry atmospheres is required because metal halides are extremely reactive toward water. So during experiment dry conditions were applied to avoid reaction of $TiCl_4$ with air and humidity. The simple laboratory glassware's were used such as volumetric and titration flasks, condenser, three-neck round bottom flask, beakers, thermometer and pH meter etc.

4.2.2 Synthesis Procedure

0.5 M acidic solution was prepared by adding 10 ml of HCl to 250 ml of deionized water. Then 0.5 M stock solution for Ti^{+4} was prepared by adding 14.06 ml of $TiCl_4$ in the 235 ml

of acidic solution (HCl + deionized H_2O) in 3-neck round bottom flask. The solution is made acidic to avoid the explosive generation of orthotitanic acid $Ti(OH)_4$ formed when $TiCl_4$ is added to this solution. The acidic solution hinder the rapid condensation reaction that could leads to the formation of a dense inorganic network, uncontrolled size and phase composition yielding poorly structured materials. Using these dry conditions and acidic solution the hydrolysis and condensation speed of the metal ion precursor becomes quite low. The pH of the stock solution is reduced due to liberation of HCl gas produced as a result of reaction of $TiCl_4$ with water. Condenser was fitted in central neck to condense any vapors produced during the course of reaction, also to avoid the bursting of three neck flask, due to liberation of HCl gas. The $TiCl_4$ was added drop by drop from the dropping funnel fitted in neck of three necks round bottom flask. And in third neck of round bottom flask silver nitrate solution was added drop by drop. The three necks round bottom flask was keep in water bath containing ice to compensate heat generated during the hydrolysis reaction. The assembly was placed in Fume Hood. The solution was stirred to avoid formation of any precipitate. While dropping $TiCl_4$ drop by drop the color of the solution turns yellowish gray. But after dropping all the $TiCl_4$ and silver nitrate the solution becomes colorless. The stock solution was prepared at room temperature.

Then 30 ml from the stock solution was taken in a titration flask and is neutralized with 0.5M solution of Sodium Hydroxide till the pH reached to the desired value i.e. from pH=2 to pH=14 followed by continuous stirring and the pH was monitored by Martini pH meter. During condensation process $Ti(OH)_4$ joined together to form a three dimensional lattice network forming the gel. The base provides the OH ions to the Ti^{+4}cations to form $Ti(OH)_4$ network.. Each time 30 ml of stock solution was taken and neutralized with NaOH at desired pH value to get different samples. Heat treatment of obtained TiO_2 gel was done in two different ways

i) Hydrothermal treatment by using auto clave

ii) The water was evaporated from gel at 100^oC, dry gel were grounded with mortar and pestle and calcination of dry powder was done in furnace at different temperature ranging from 250^o to 500^o C.

The powder samples obtained were then saved in sample vials for characterization. The Sol-Gel-derived nano crystals were then characterized by XRD, SEM, EDX and XRF.

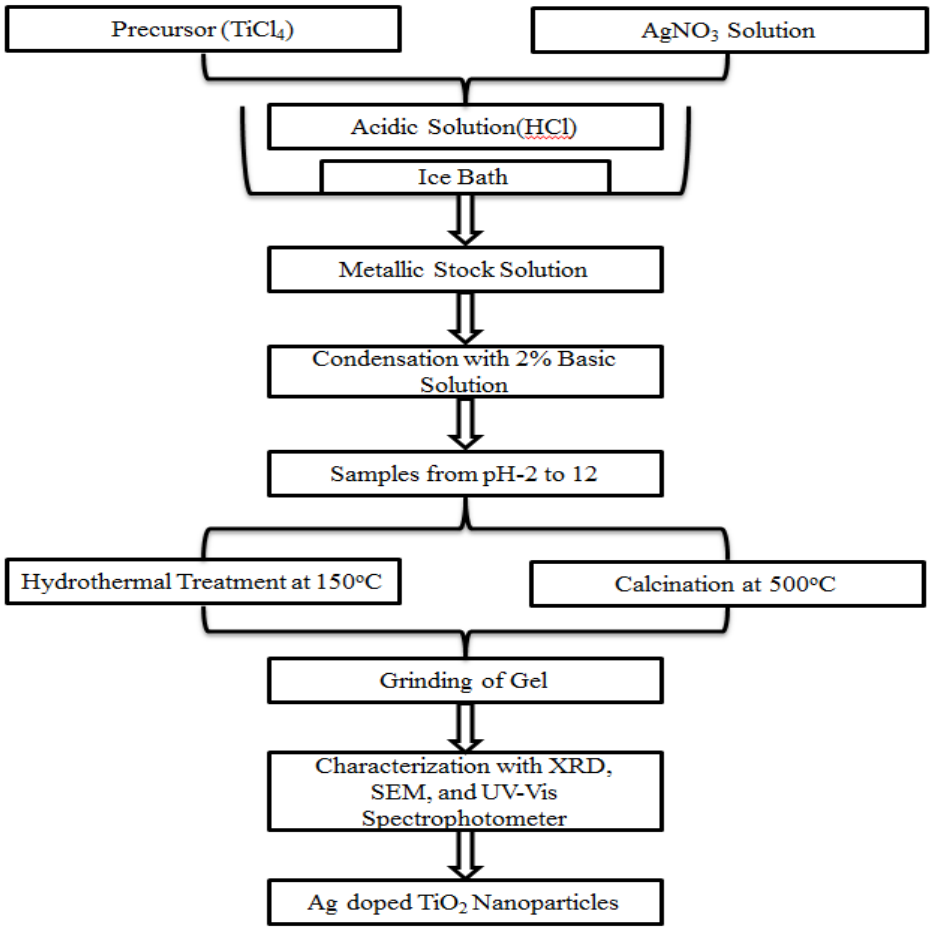

Figure 4.2 Flow sheet for Sol-Gel and sol hydrothermal synthesis of in situ silver doped TiO_2 nano-particles.

4.3 Synthesis of Zinc Doped TiO_2 Nano particles

4.3.1 Chemicals used

Titanium tetrachloride (98% $TiCl_4$), Sodium Hydroxide (NaOH), Hydrochloric acid (37% HCl), Ammonium hydroxide/ ammonia solution, ethanol, Nitric acid (HNO_3), zinc nitrate ($ZnNO_3$) were used in the synthesis. All chemicals used in the synthesis were pure and analytical grade reagents of noted firms such as Merck, Fluka and Aldrich and were used without any further purification.

4.3.2 Synthesis procedure

0.5M acidic solution was prepared by adding 10 ml of HCl to 250 ml of deionized water. Then 0.5M stock solution for Ti^{+4} was prepared by adding 14.06 ml of $TiCl_4$ in the 235 ml of acidic solution (HCl + deionized H_2O) in 3-neck round bottom flask. The solution is made acidic to avoid the explosive generation of orthotitanic acid $Ti(OH)_4$ formed when $TiCl_4$ is added to this solution. The acidic solution hinder the rapid condensation reaction that could leads to the formation of a dense inorganic network, uncontrolled size and phase composition yielding poorly structured materials. Using these dry conditions and acidic solution the hydrolysis and condensation speed of the metal ion precursor becomes quite low. The pH of the stock solution is reduced due to liberation of HCl gas produced as a result of reaction of $TiCl_4$ with water. Condenser was fitted in central neck to condense any vapors produced during the course of reaction, also to avoid the bursting of three neck flask, due to liberation of HCl gas. The $TiCl_4$ was added drop by drop from the dropping funnel fitted in neck of three necks round bottom flask. And in third neck of round bottom flask silver nitrate solution was added drop by drop. The three necks round bottom flask was keep in water bath containing ice to compensate heat generated during the hydrolysis reaction. The assembly was placed in Fume Hood. The solution was stirred to avoid formation of any precipitate. While dropping $TiCl_4$ drop by drop the color of the solution turns yellowish gray. But after dropping all the $TiCl_4$ and silver nitrate the solution becomes colorless. The stock solution was prepared at room temperature.

Then 30 ml from the metallic stock solution was taken in a titration flask and is neutralized with 0.5M solution of Sodium Hydroxide till the pH reached to the desired value i.e from pH=2 to pH=14 followed by continuous stirring and the pH was monitored by Martini pH meter. During condensation process $Ti(OH)_4$ joined together to form a three dimensional lattice network forming the gel. The base provides the OH ions to the Ti^{+4}cations to form $Ti(OH)_4$ network.

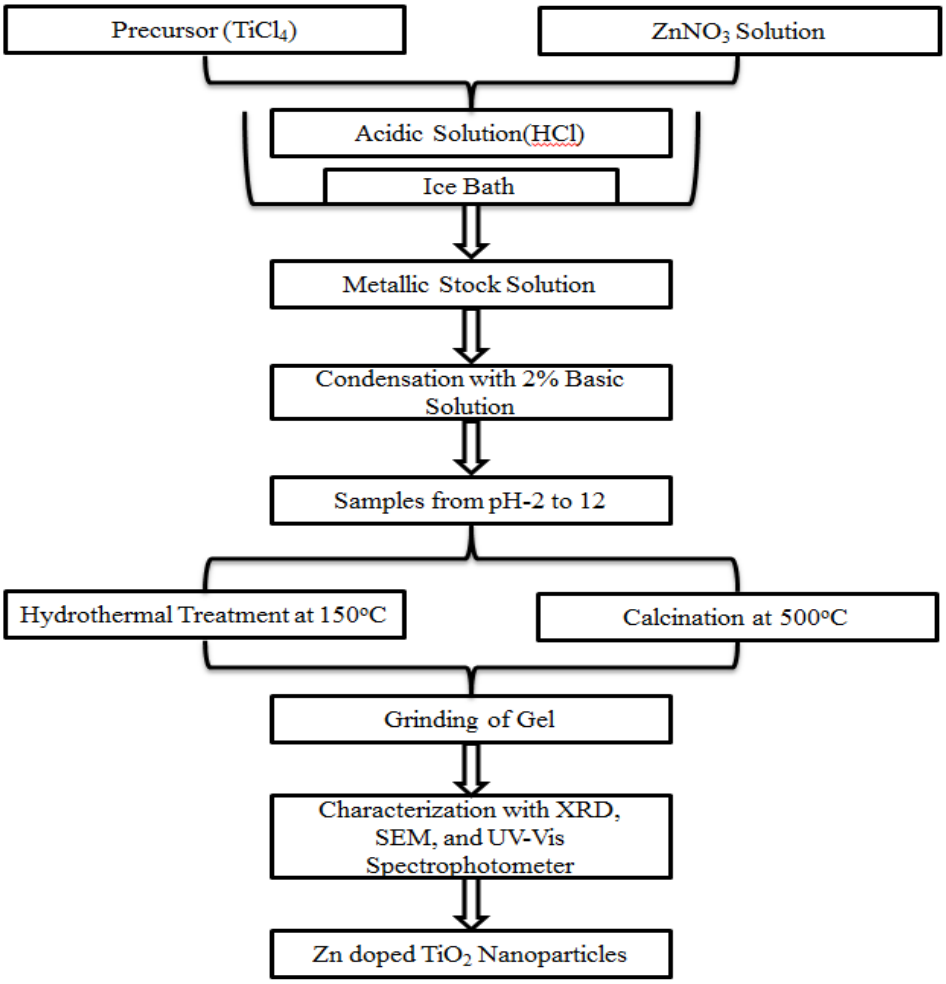

Figure 4.3 Flow sheet for Sol-Gel and sol hydrothermal synthesis of in situ zinc doped TiO_2 nano-particles

Each time 30 ml of metallic stock solution was taken and neutralized with NaOH and NH_4OH at desired pH value to get different samples. Heat treatment of obtained doped TiO_2 gel was done in two different ways

i) Hydrothermal treatment by using auto clave

ii) The water was evaporated from gel at 100^oC, dry gel were grounded with mortar and pestle and calcinations of dry powder was done in furnace at different temperature ranging from 250^o to 500^oC.

The powder samples obtained were then saved in sample vials for characterization. The Sol-Gel-derived nano crystals were then characterized by XRD, SEM, EDX.

4.4 Synthesis of co-doped TiO_2 Nano-particles

4.4.1 Chemicals used

Titanium tetrachloride (98% $TiCl_4$), Sodium Hydroxide (NaOH), Hydrochloric acid (37% HCl), Ammonium hydroxide/ ammonia solution, ethanol, Nitric acid (HNO_3), Silver nitrarte zinc nitrate ($ZnNO_3$) were used in the synthesis. All chemicals used in the synthesis were pure and analytical grade reagents of noted firms such as Merck, Fluka and Aldrich and were used without any further purification.

4.4.2 Synthesis procedure

0.5 M acidic solution was prepared by adding 10 ml of HCl to 250 ml of deionized water. Then 0.5 M stock solution for Ti^{+4} was prepared by adding 14.06 ml of $TiCl_4$ in the 235 ml of acidic solution (HCl + deionized H_2O) in 3-neck round bottom flask. The solution is made acidic to avoid the explosive generation of orthotitanic acid $Ti(OH)_4$ formed when $TiCl_4$ is added to this solution. The acidic solution hinder the rapid condensation reaction that could leads to the formation of a dense inorganic network, uncontrolled size and phase composition yielding poorly structured materials. Using these dry conditions and acidic solution the hydrolysis and condensation speed of the metal ion precursor becomes quite low. The pH of the stock solution is reduced due to liberation of HCl gas produced as a result of reaction of $TiCl_4$ with water. Condenser was fitted in central neck to condense any vapors produced during the course of reaction, also to avoid the bursting of three neck flask, due to liberation of HCl gas. The $TiCl_4$ was added drop by drop from the dropping funnel fitted in neck of three neck round bottom flask. And in third neck of round bottom flask silver nitrate solution was added drop by drop.when the silver nitrate solution finished ethanol 1/32 V/V ratio was addede drop by drop, after this 100 ml metallic solution of zinc nitrate was added via dropind funnel along with vigorous stirring. The three necks round bottom flask was keep in water bath containing ice to compensate heat generated during the hydrolysis reaction. The assembly was placed in Fume Hood. The solution was stirred to avoid formation of any precipitate. While dropping $TiCl_4$ drop by drop the color of the solution turns yellowish gray. But after dropping all the $TiCl_4$, Zinc Nitrate and silver nitrate the solution becomes colorless. The stock solution was prepared at room temperature.

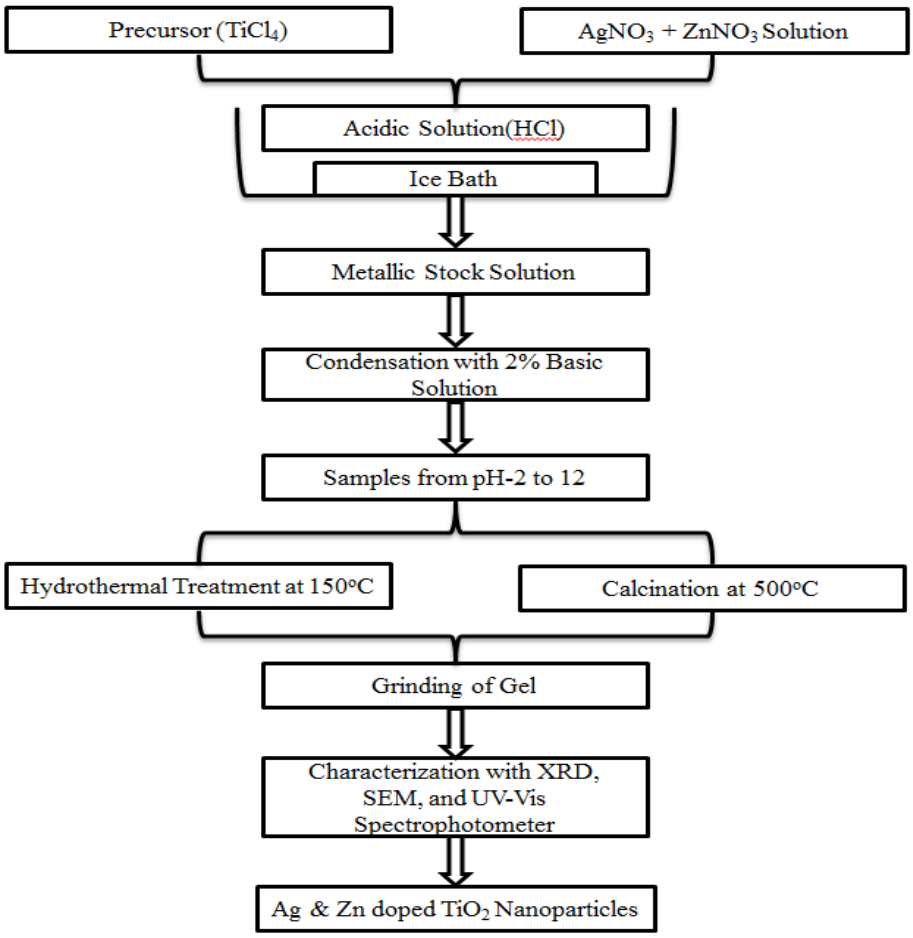

Figure 4.4 Flow sheet for Sol-Gel and sol hydrothermal synthesis of in situ co-doped TiO_2 nano-particles

Then 30 ml from the bi metallic stock solution was taken in a titration flask and is neutralized with 0.5 M solution of Sodium Hydroxide or Ammonium Hydro oxide till the pH reached to the desired value i.e from pH = 2 to pH = 12 followed by continuous stirring and the pH was monitored by Martini pH meter. During condensation process $Ti(OH)_4$ joined together to form a three dimensional lattice network forming the gel. The base provides the OH ions to the Ti^{+4}cations to form $Ti(OH)_4$ network.. Each time 30 ml of metallic stock solution was taken and neutralized with NaOH and NH_4OH at desired pH value to get different samples. Heat treatment of obtained doped TiO_2 gel was done in two different ways

i) Hydrothermal treatment by using auto clave

ii) The water was evaporated from gel at 100^{o}C, dry gel were grounded with mortar and pestle and calcinations of dry powder was done in furnace at different temperature ranging from 250^{o} to 500^{o} C.

The powder samples obtained were then saved in sample vials for characterization. The Sol-Gel-derived nano crystals were then characterized by XRD, SEM, EDX and XRF.

CHAPTER 5

Results

5.1 XRD Results

The crystal structure, phase composition and, crystallite size measurements for the sample powders were done using X-ray diffractometer using Cu Kα radiation with maximum output 60 kV and 60 mA. Absolute scan with step mode was used, the starting 2θ angle was 20° and end angle was 80° with step size = 0.025° and time per step was 2 s with incident beam width 15 mm at 40 KV and 45 mA. XRD results were analyzed with software package X´Pert High Score. The crystallite size was estimated by the line broadening using Scherer formula on the anatase (1 0 1) diffraction peaks (the highest intensity peak for each pure anatase.

5.1.1 Sol-Gel synthesis of Pure TiO_2

The samples were synthesized at room temperature and condensation was done with sodium hydroxide. Heat treatment was done in furnace at 500^{o} C for 5 hours.

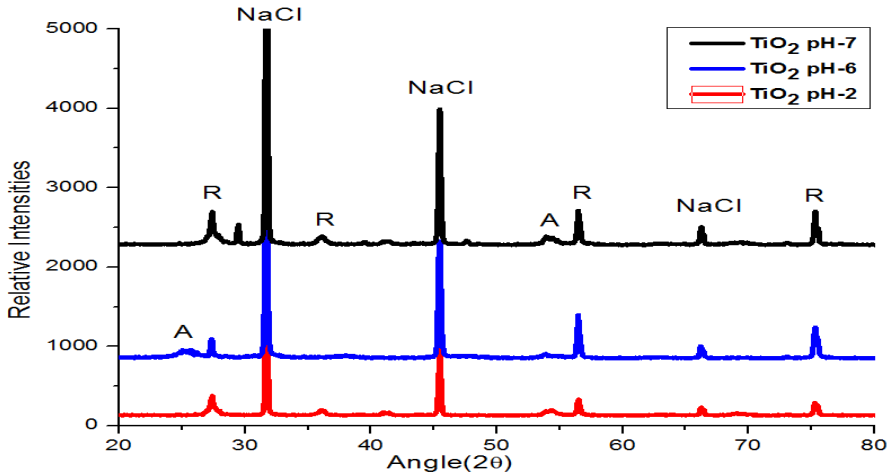

Figure 5.1 XRD results for Sol-Gel synthesis of TiO_2

Crystallite size is calculated by Scherer formula and its average is 45 nm.

The XRD result shows that at higher pH value rutile phase is stabilized while at smaller pH anatase phase is stabilized with NaCl as an impurity. The spectrums indicate that that all samples are crystalline no amorphous phase is observed. XRD cards verifying the result is 01-073-1764.

5.1.2 Sol Hydrothermal Synthesis of Un-doped TiO_2

The samples were synthesized via normal Sol-Gel process, condensation was done via ammonium hydro oxide and heat treatment was done in Autoclave at 150^{o}C for five hours and normal pressure. XRD result shows that anatase phase is stabilized at all pH values without any impurity.

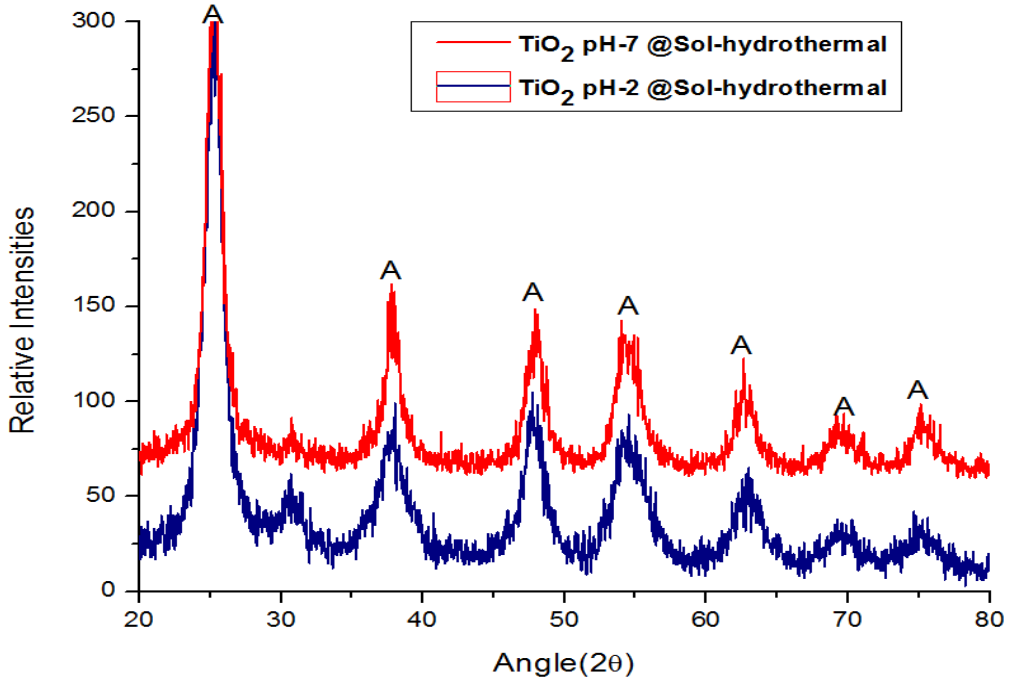

Figure 5.2 XRD results for sol hydrothermal synthesis of TiO_2

The spectrums indicate that that all samples are crystalline no amorphous phase is observed. The peaks indicate the presence of anatase phase with (101), planes respectively. XRD card verifying the result is 01-075-1537. The average crystallite calculated by Scherer formula is 12.9 nm.

5.1.3 Sol-Hydrothermal synthesis of Silver doped TiO_2

The samples were synthesized via normal Sol-Gel process, condensation was done via ammonium hydro oxide and heat treatment was done in Autoclave at 150 ^{o}C for five hours and normal pressure. XRD result shows that anatase phase is stabilized at all pH values along with dopants silver and silver oxide. The spectrums indicate that that all samples are crystalline no amorphous phase is observed. The peaks indicate the presence of anatase phase, with (101) planes along with silver and silver oxide.

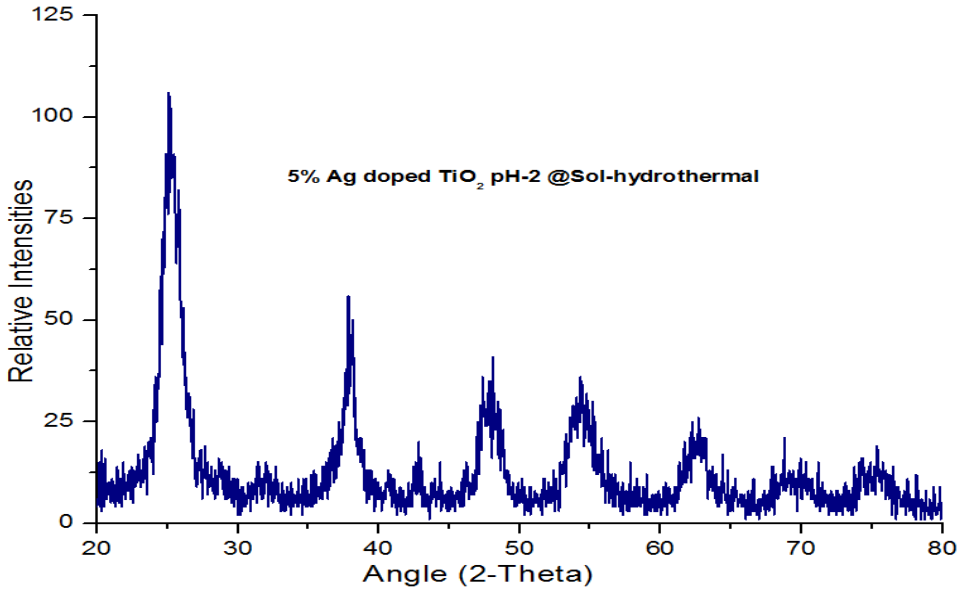

Figure 5.3 XRD results for sol hydrothermal synthesis of Ag doped TiO_2

Following phases shown in spectrum were observed and verified by XRD. XRD card verifying the result is 00-041-1104.

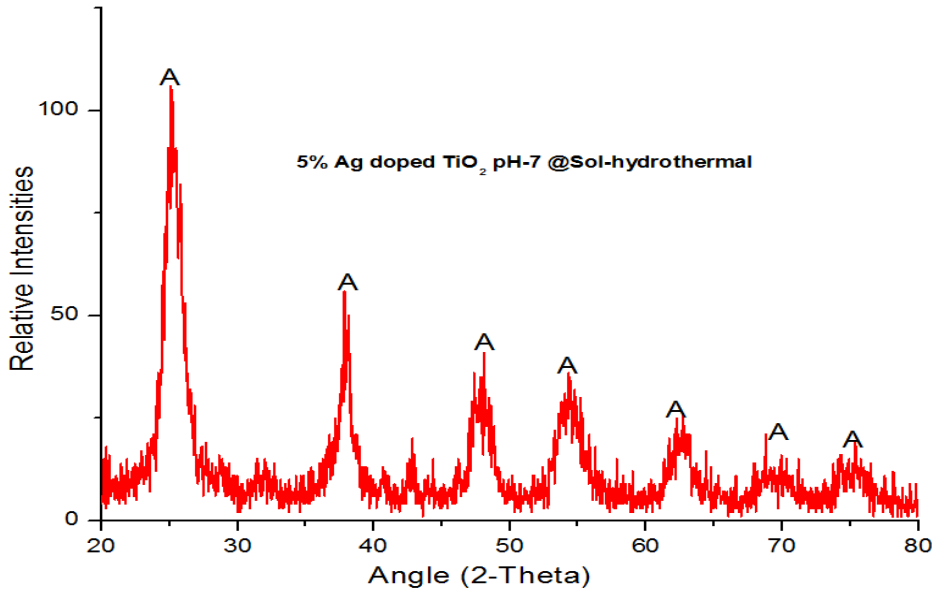

Figure 5.4 XRD results for sol hydrothermal synthesis of Ag doped TiO_2

5.1.4 Sol-Gel synthesis of Zinc doped TiO_2

The samples were synthesized via normal Sol-Gel process, condensation was done via ammonium hydro oxide and heat treatment was in furnace at 500^{o}C for five hours.

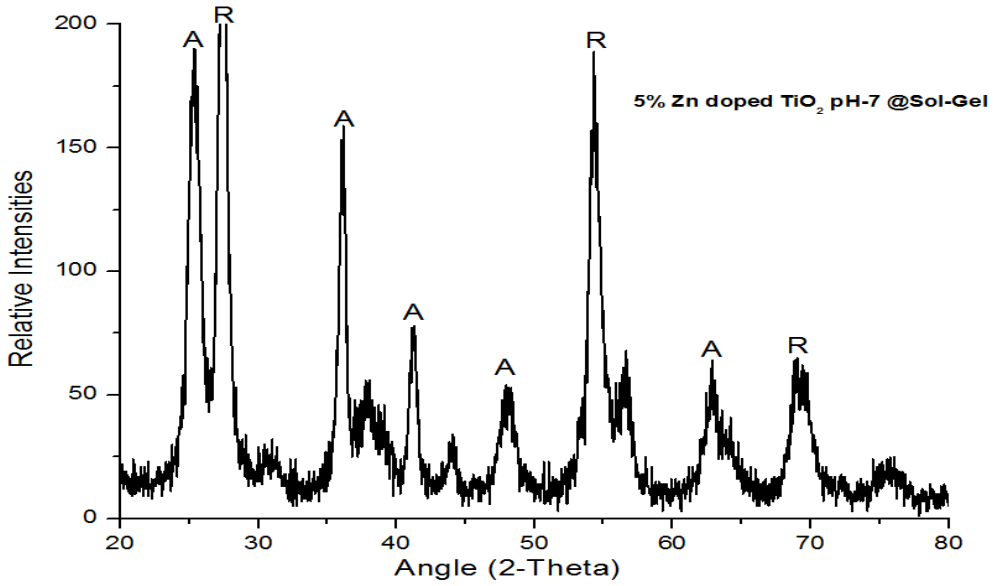

Figure 5.5 XRD results for Sol-Gel synthesize of zinc doped TiO_2

XRD result shows that anatase and rutile phases are stabilized along with dopants zinc and zinc oxide. The spectrums indicate that that all samples are crystalline no amorphous phase is observed. The peaks indicate the presence of anatase phase, with (101) planes along with zinc and zinc oxide. Following phases shown in spectrum were observed and verified by XRD. XRD card verifying the result is 03-065-2880.

5.1.5 Sol-Hydrothermal synthesis of Zinc doped TiO_2

The samples were synthesized via normal Sol-Gel process, condensation was done via sodium hydro oxide and heat treatment was in autoclave at 150^{o}C and normal pressure for five hours. XRD result shows that anatase phase is stabilized at all pH values along with dopants zinc and zinc oxide.

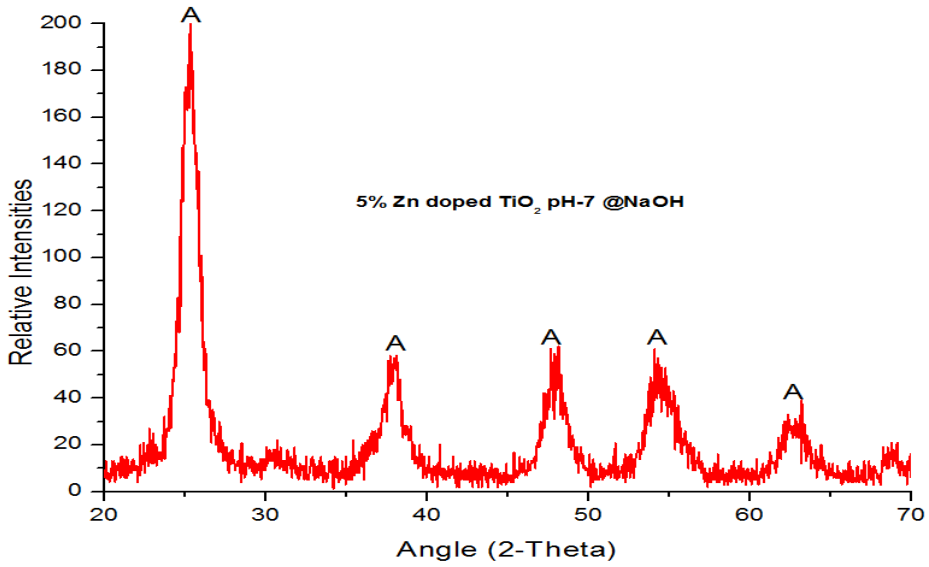

Figure 5.6 XRD results for sol-hydrothermally synthesized zinc doped TiO_2

The spectrums indicate that that all samples are crystalline no amorphous phase is observed. Following phases shown in spectrum were observed and verified by XRD. XRD card verifying the result is 03-065-2880.

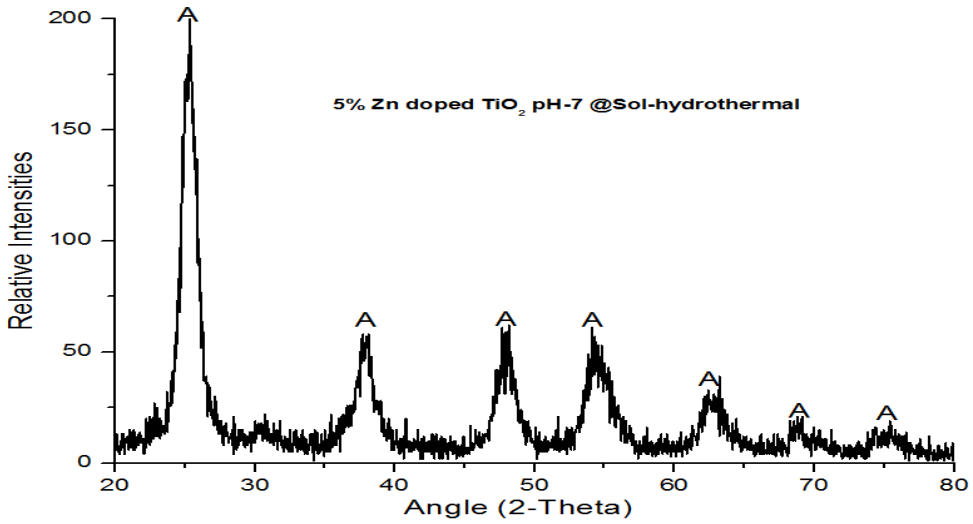

Figure 5.7 XRD results for sol-hydrothermally synthesized zinc doped TiO_2

5.1.6 Sol-Gel Synthesis of Co-doped TiO_2

The samples were synthesized via normal Sol-Gel process, condensation was done via ammonium hydro oxide and heat treatment was done in furnace at 500^{o}C for five hours.

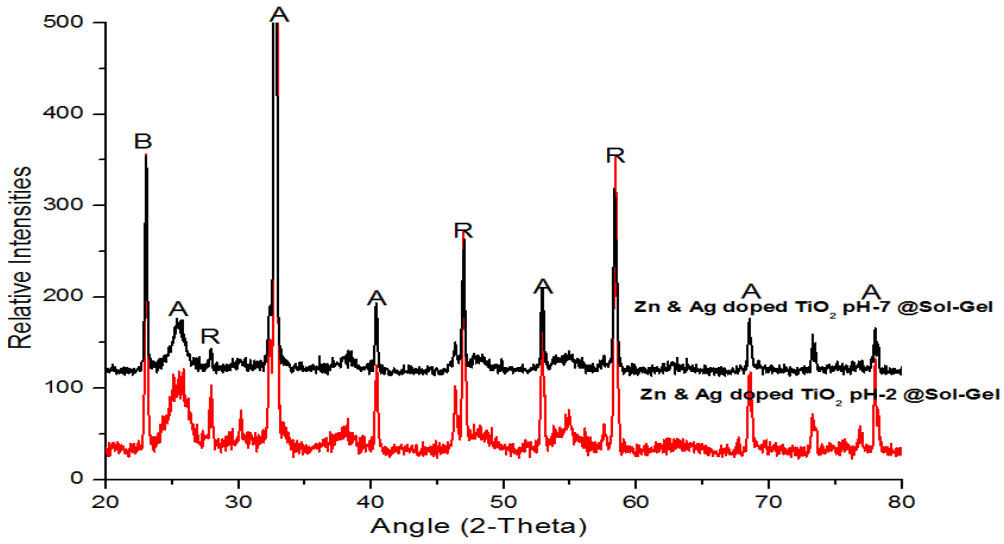

Figure 5.8 XRD results for Sol-Gel synthesized co-doped TiO_2

XRD result shows the presence of mixed phase i.e. anatase and rutile is stabilized along with zinc, zinc oxide, silver and silver oxide peaks of dopants. The spectrums indicate that that all samples are crystalline no amorphous phase is observed. Following phases

shown in spectrum were observed and verified by XRD. XRD card verifying the result is 01-071-1167.

5.1.7 Sol Hydrothermal synthesis of co-doped TiO_2

The samples were synthesized via normal wet chemical base route, condensation was done via sodium hydro oxide and heat treatment was in autoclave at 150^{o}C and normal pressure for five hours. XRD results shows that only anatase phase is stabilized along with zinc, zinc oxide, silver and silver oxide peaks of dopants. The spectrums indicate that that all samples are crystalline no amorphous phase is observed. Following phases shown in spectrum were observed and verified by XRD. XRD card verifying the result is 01-089-4921.

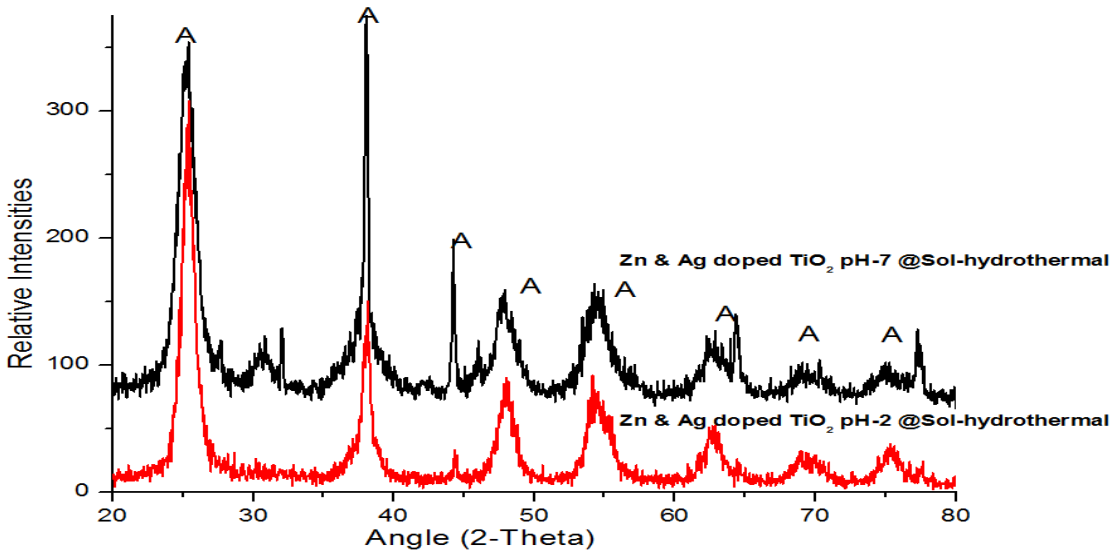

Figure 5.9 XRD results for Sol-Gel synthesized co-doped TiO_2

5.2 SEM Results

5.2.1 Pure TiO_2

A SEM result of un-doped TiO_2 synthesized via hydrothermal technique is shown in figure (5.10). The sample was dispersed in deionized water.

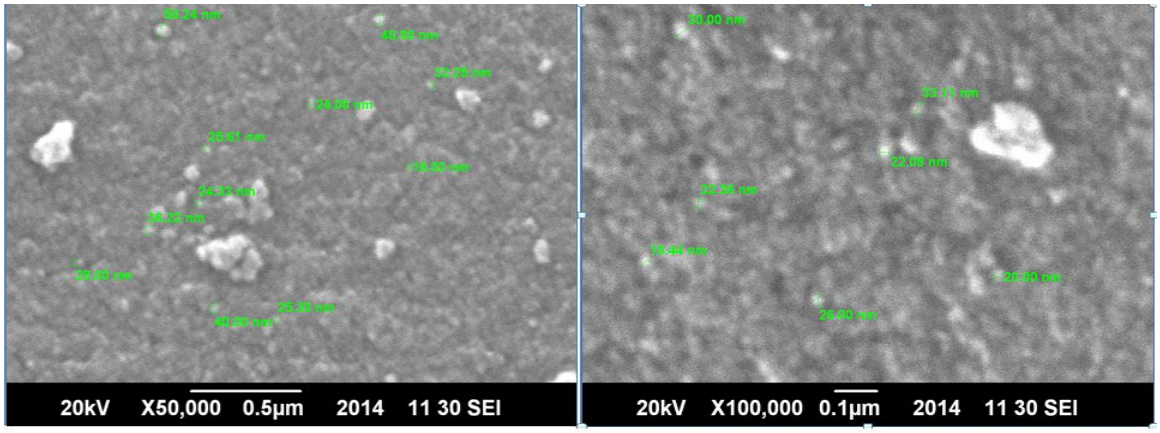

Figure 5.10 SEM results of un-doped TiO_2 synthesized via Sol-Gel process

SEM results of un-doped TiO_2 synthesized via hydrothermal technique shows the well dispersed with probably spherical morphology. The sample was dispersed in ethanol.

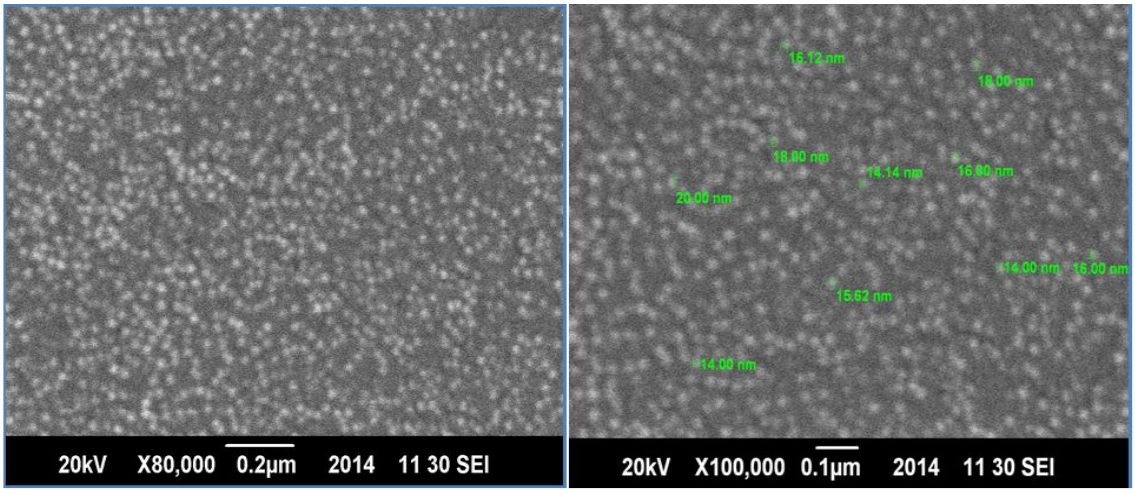

Figure 5.11 SEM results of un-doped TiO_2 synthesized via sol-hydrothermal process

5.2.2 Silver Doped TiO_2

Silver doped samples indicates that the crystallize size is in nano-domain, due to small size, even after sonication there are still agglomerates while the morphology was not much clear due to agglomerations.

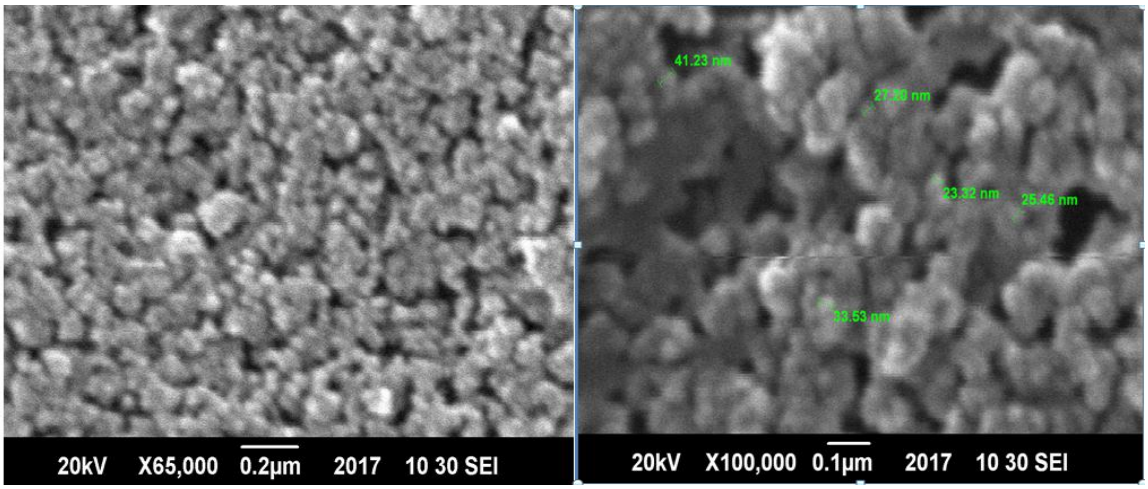

Figure 5.12 SEM results of silver doped TiO_2 synthesized via sol-hydrothermal process

5.2.3 Zinc doped TiO_2

Sol-Gel synthesized Zinc doped samples indicates that the crystallize size is in nano domain, with irregular morphology.

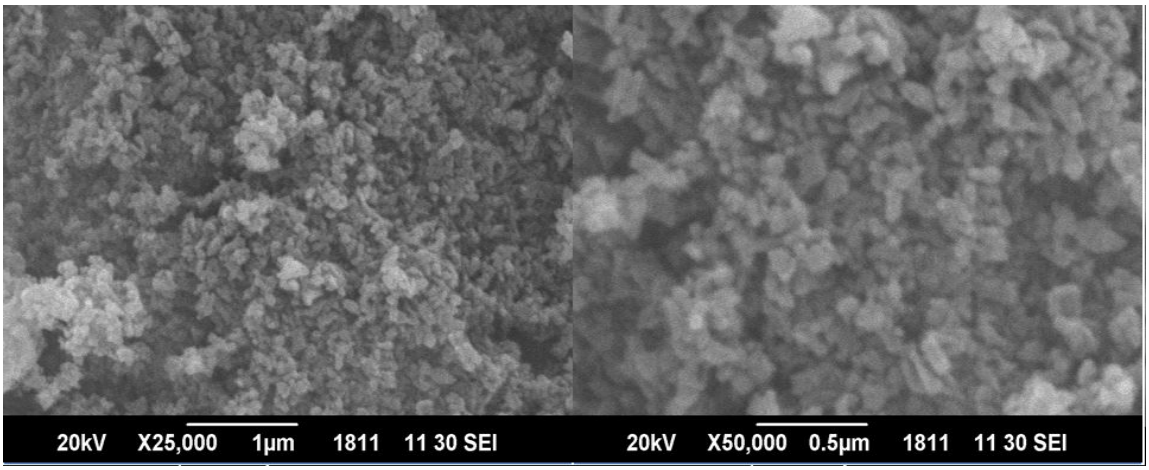

Figure 5.13 SEM results of zinc doped TiO_2 synthesized via Sol-Gel process

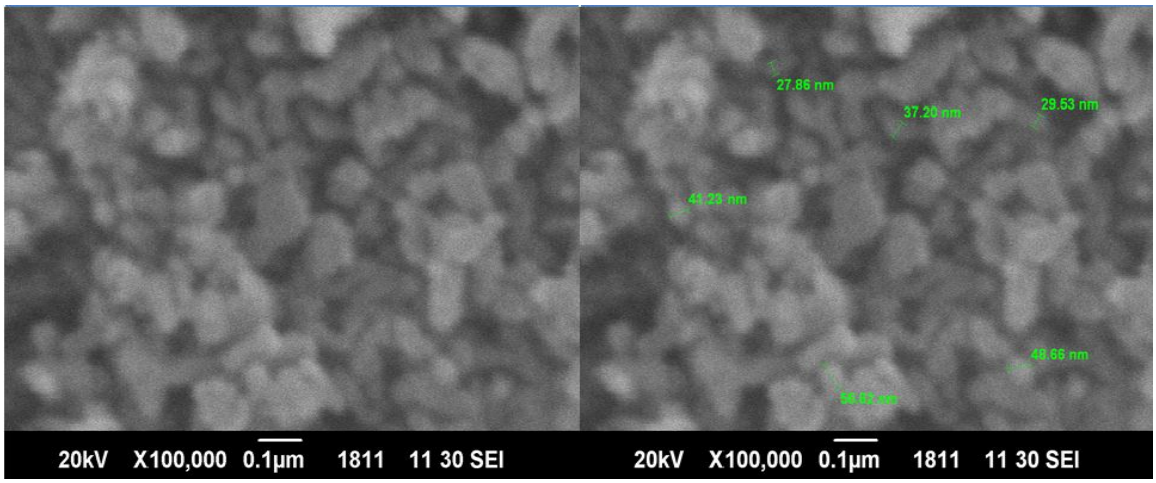

Figure 5.14 SEM results of zinc doped TiO_2 synthesized via Sol-Gel process

SEM results of hydrothermally synthesized zinc doped samples show the spherical morphology with average grain size up to 20 nm.

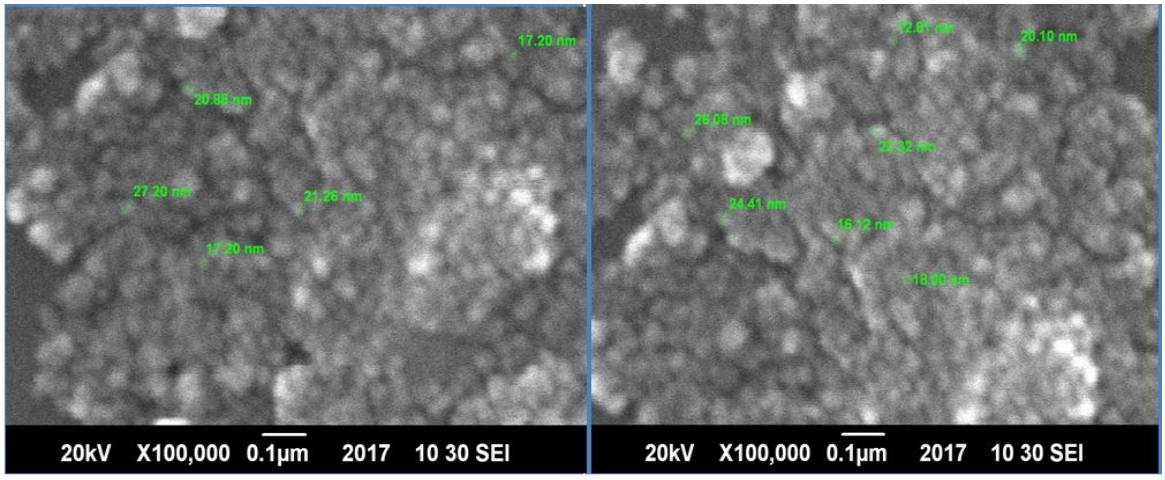

Figure 5.15 SEM results of zinc doped TiO_2 synthesized via sol-hydrothermal process

5.2.4 Co-doped TiO_2

Sol-Gel synthesized zinc and silver co-doped samples indicates that the crystallize size is in nano-domain, rod type morphology. SEM results show average grain size up to 40 nm.

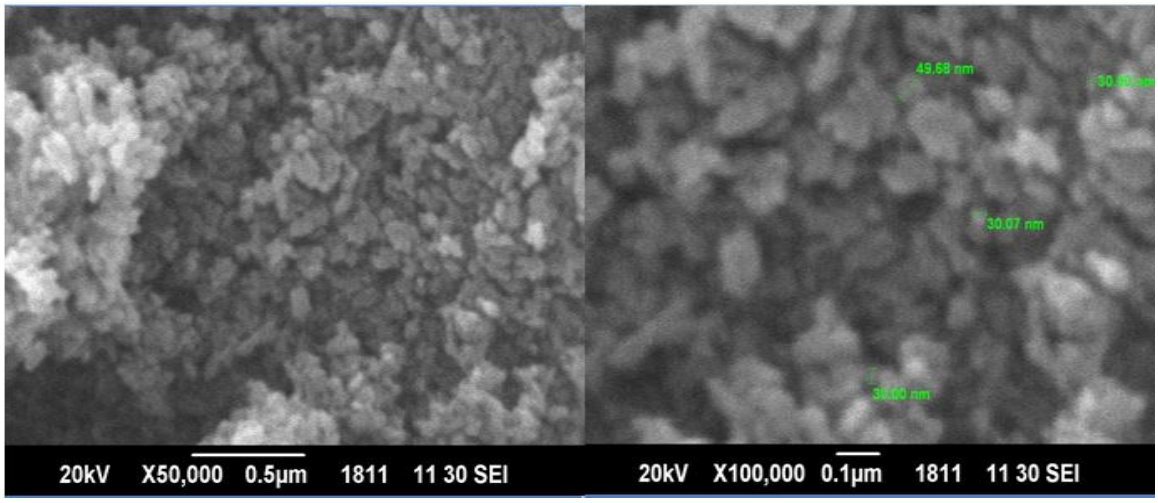

Figure 5.16 SEM results of co-doped TiO_2 synthesized via Sol-Gel process

Hydrothermally synthesized zinc and silver co-doped samples indicates that the grain size is in nano-domain, with spherical morphology. The average crystallite is same as calculated via Scherer formula by using peak position and full width half maxima.

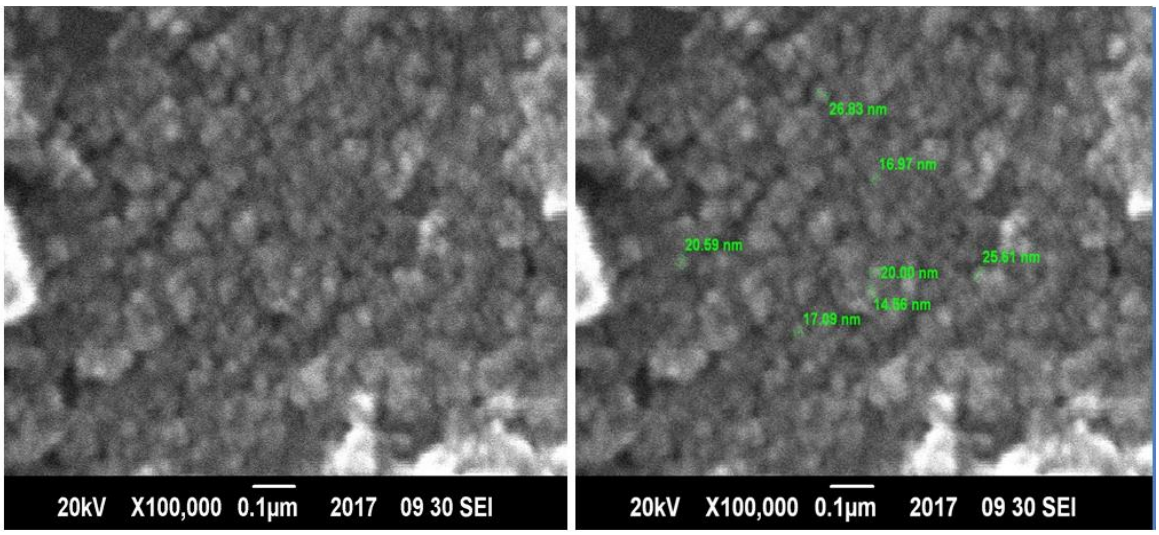

Figure 5.17 SEM results of co-doped TiO_2 synthesized via sol-hydrothermal process

5.3 EDX Results

The chemical composition of obtained samples was analysed with Energy Dispersive X-Ray (EDX) Analysis and XRF. EDX Spectroscopy is a chemical microanalysis technique used in conjunction with SEM. EDX analysis was performed to characterize the elemental

composition of the Sol-Gel and sol-hydrothermally derived un-doped and doped TiO_2 nano-particles. In addition to supplying micro analytical information, the EDX method can be used quantitatively to determine the fraction of substitutional impurity atoms which lie on particular sites in a crystal lattice. If characteristics X-rays from the trace elements of interest in crystalline region sample can be detected using the EDX system, then in most cases it is possible to determine the crystallographic site of the impurity. EDX analysis indicates that amount of Titanium and Oxygen present in the TiO_2samples.

5.3.1 Pure TiO_2

The EDX patterns of TiO_2 sample is given below that demonstrates the presence of Clas an impurity in the Sol-Gel-derived nano-crystalline Titania.

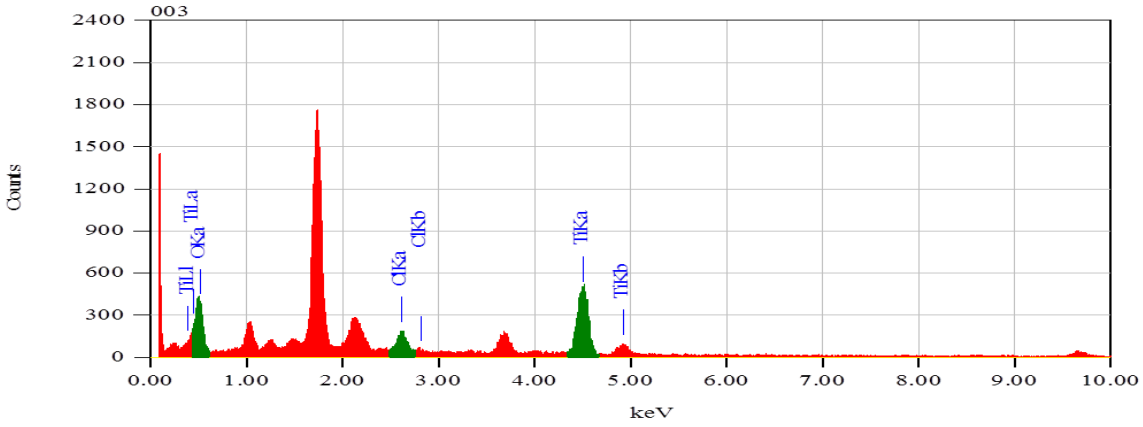

Figure 5.18 EDX results of un-doped TiO_2 synthesized via Sol-Gel process

The EDX patterns of TiO_2 sample is given below that demonstrates the absence of impurities in the sol-hydrothermally-derived nano-crystalline Titania.

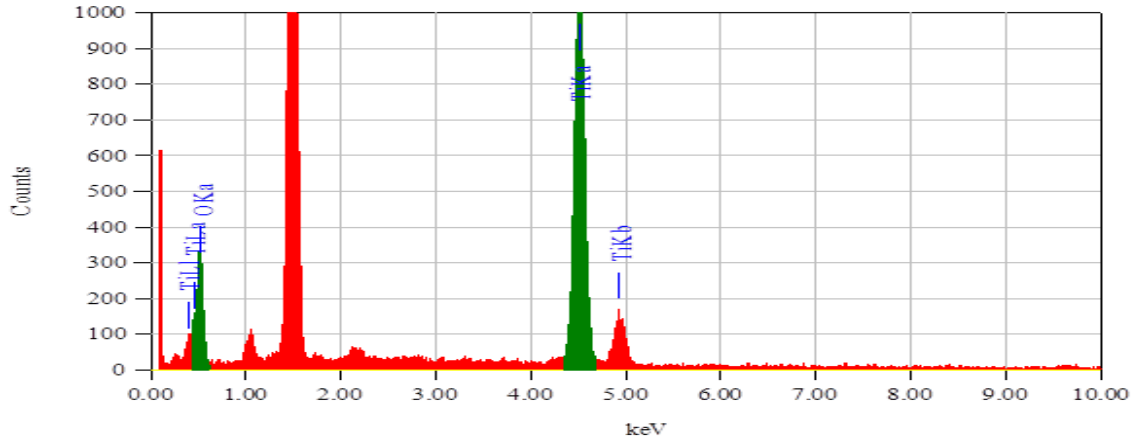

Figure 5.19 EDX results of un-doped TiO_2 synthesized via sol-hydrothermal process

5.3.2 Silver Doped TiO_2

The EDX patterns of silver doped TiO_2 sample is given below that shows the presence of zinc as doped impurities in the sol-hydrothermally-derived doped nano-crystalline Titania.

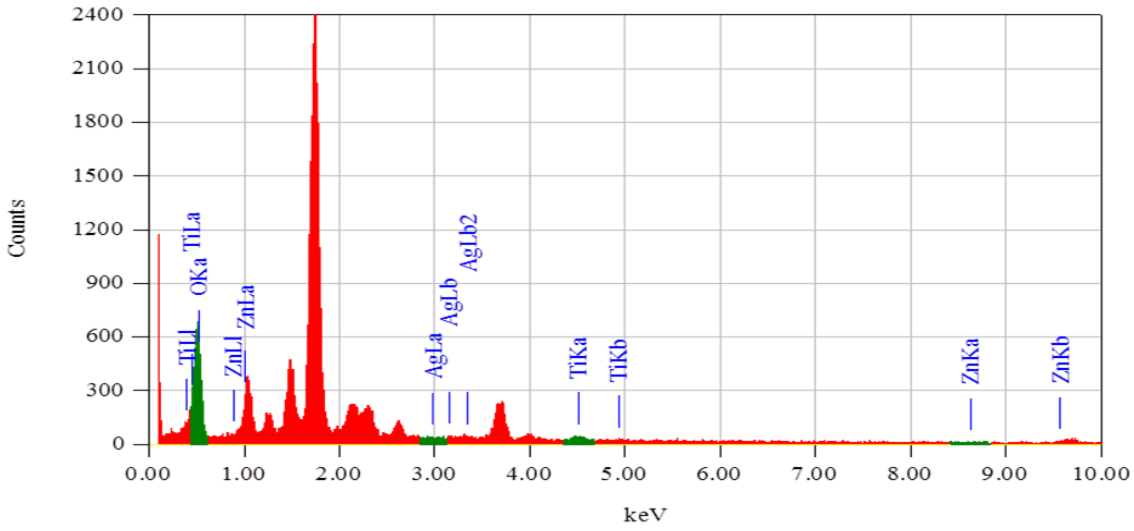

Figure 5.20 EDX results of silver doped TiO_2 synthesized via sol-hydrothermal process

5.3.3 Zinc Doped TiO_2

The EDX patterns of zinc doped TiO_2 sample is given below that demonstrates the absence of impurities in the Sol-Gel-derived nano-crystalline Titania.

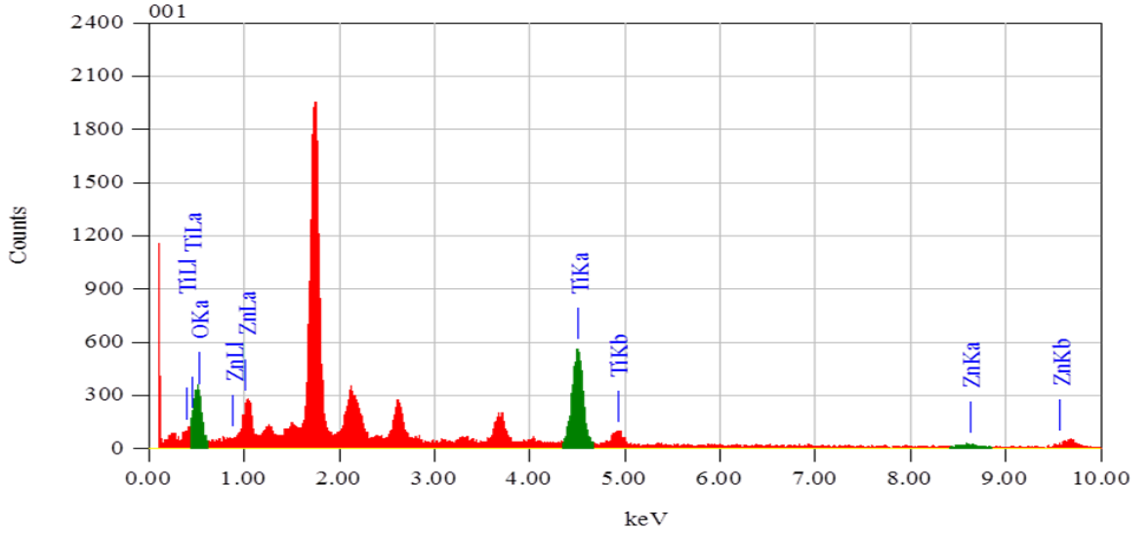

Figure 5.21 EDX results of zinc doped TiO_2 synthesized via sol-hydrothermal process

5.3.4 Co-doped TiO_2

The EDX patterns of zinc and silver co-doped TiO_2 sample is given below that demonstrates the absence of impurities in the sol-hydrothermally-derived nano-crystalline Titania.

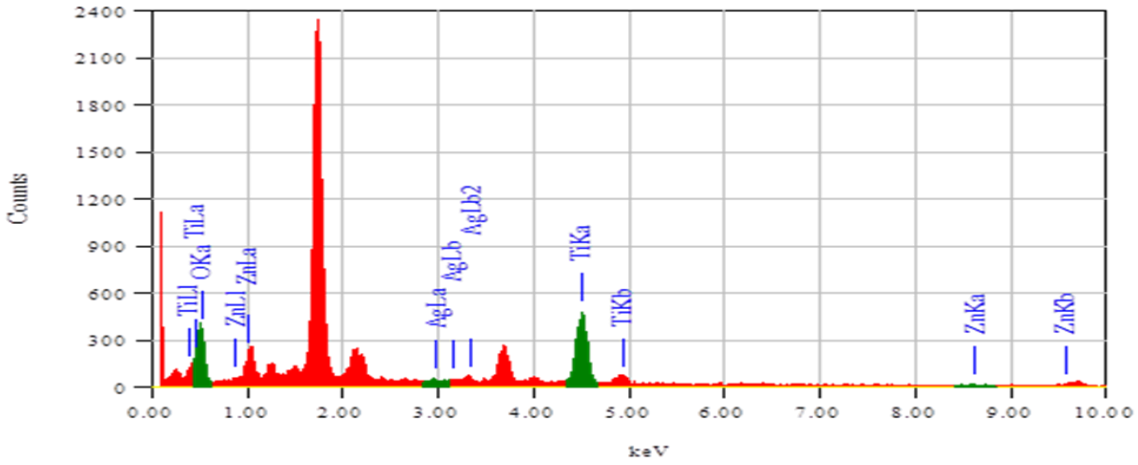

Figure 5.22 EDX results of co doped TiO_2 synthesized via sol-hydrothermal process

The EDX patterns of zinc and silver co-doped TiO_2 sample is given below that shows the presence of Cl as an impurity the Sol-Gel-derived doped nano-crystalline Titania.

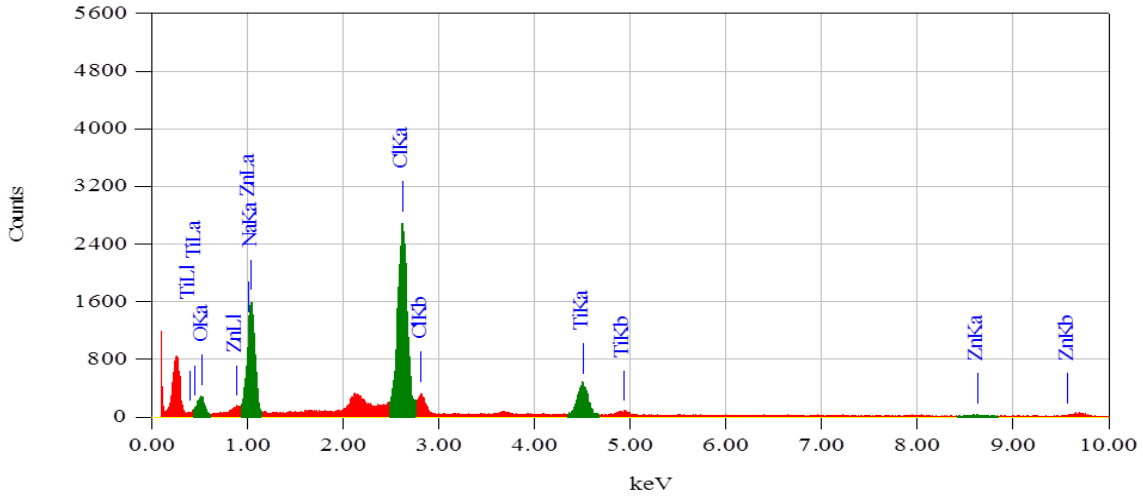

Figure 5.23 EDX results of co doped TiO_2 synthesized via Sol-Gel process

The EDX results indicate that there are no impurities, except chlorides and sodium in cases of Sol-Gel synthesized samples in trace amounts, which can be minimized by washing gel by distilled water but it influence the decrease in net yield of TiO_2 while the

hydrothermally synthesized samples shows that Titanium and Oxygen along with dopants are in appropriate ratios.

Table 5.1 Summary of the EDX results

Samples	EDX analysais (Atomic %)						
	Ti	O	Cl	Zn	Ag	Na	Process
Un-doped TiO_2	62.29	33.37	4.34	--	--	--	Sol-Gel
Un-doped TiO_2	13.52	86.48	--	--	--	--	Sol-Hyd.
Silver Doped TiO_2	6.41	92.13	--	--	1.46	--	Sol-Hyd.
Zinc Doped TiO_2	57.58	38.31	--	4.11	--	--	Sol-Hyd.
Co-doped TiO_2	32.28	66.0	--	1.19	0.53	--	Sol-Hyd.
Co-doped TiO_2	14.86	16.03	38.62	3.57	3.80	22.25	Sol-Hyd.

5.4 UV-Vis Spectrophotometer Results

The absorption of suspension is taken by BMS UV-2800 Spectrophotometer. Band gap is calculated by using Beer-Lambert law. Dilute suspension of the sample is prepared by mixing ethanol in ultrasonic bath and in UV spectrometer absorption with respect to wavelength is measured.

5.4.1 Undoped TiO_2 via Sol-Gel route

The plot shown in figure represents the band gap of undoped TiO_2 synthesized via Sol-Gel route shows the band gap of synthesized material is 3.42 eV.

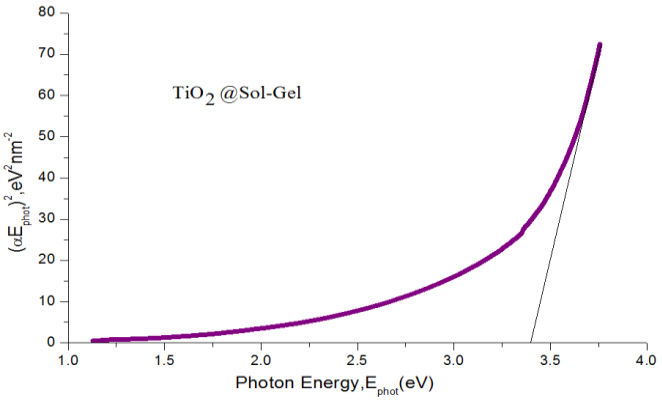

Figure 5.24 Band gap studies of undoped TiO_2 synthesized by Sol-gel process

5.4.2 Undoped TiO_2 via Sol-hydrothermal route

The plot shown in figure represents the band gap of undoped TiO_2 synthesized via Sol-hydrothermal route shows the band gap of synthesized material is 3.10 eV.

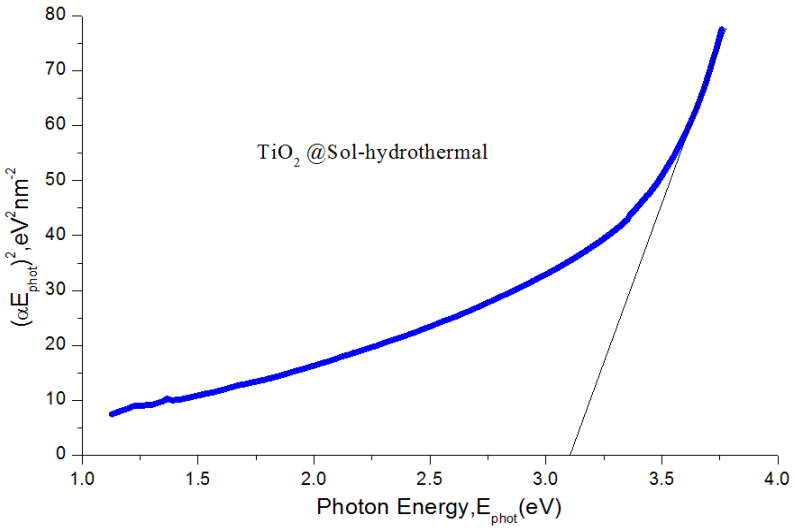

Figure 5.25 Band gap studies of undoped TiO_2 synthesized by Sol-hydrothermal process

5.4.3 Siler doped TiO_2 via Sol-hydrothermal route

The plot shown in figure represents the band gap of silver doped TiO_2 which shows the band gap of synthesized material is 3.24 eV

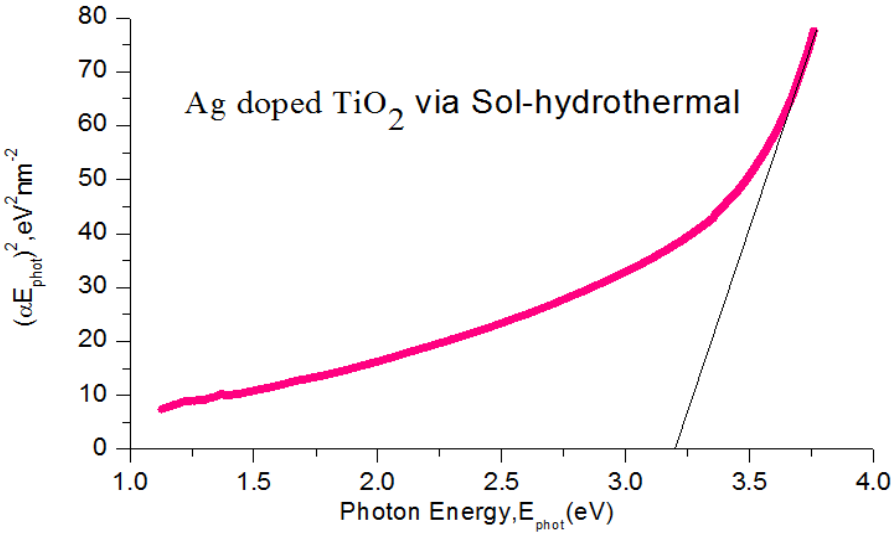

Figure 5.26 Band gap studies of silver doped TiO_2

5.4.4 Sol-Gel Synthesis of Zinc doped TiO_2

The band gap of zinc doped samples is measured with same process as discussed earlier.

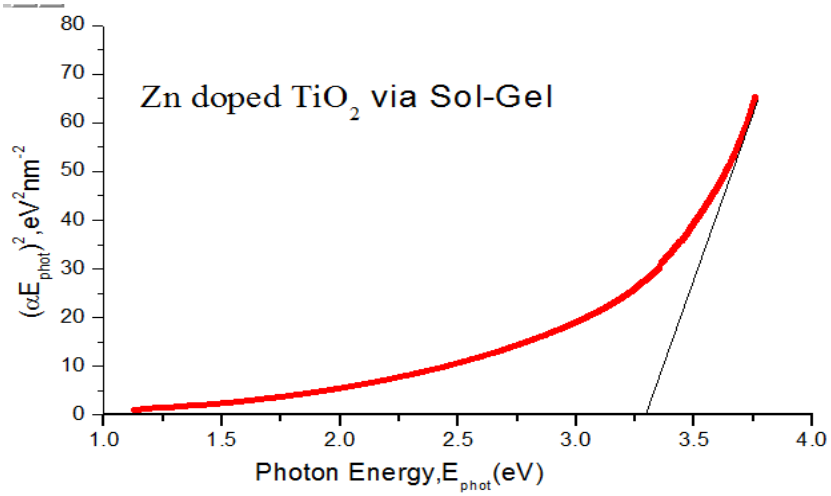

Figure 5.27 Band gap studies of Sol-Gel synthesized zinc doped TiO_2

The band gap of zinc doped TiO_2 is 3.15 eV as shown in figure (5.25) which is smaller than un-doped TiO_2.

5.4.5 Sol-Hydrothermal Synthesis of Zinc doped TiO_2

The band gap of hydrothermally synthesized zinc doped samples is measured with same process as discussed earlier. It is 3.09 eV as shown in figure (5.26).

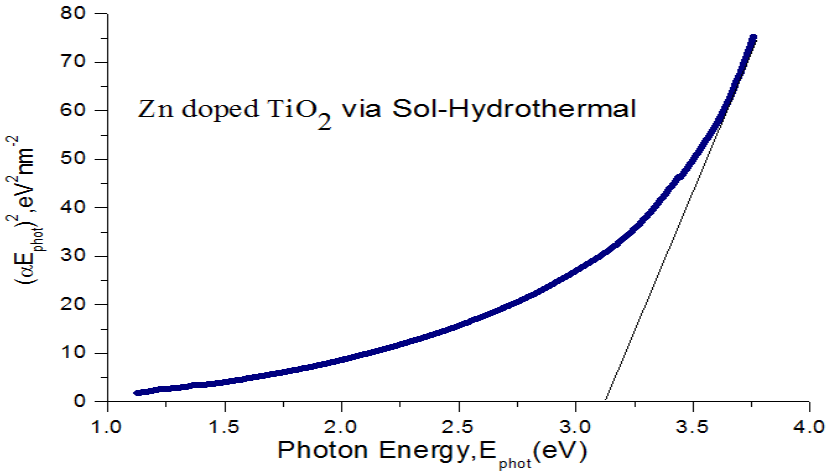

Figure 5.28 Band gap studies of zinc doped TiO_2 synthesized via sol-hydrothermal process

5.4.6 Sol-Gel Synthesis of co-doped TiO_2

The band gap of hydrothermally synthesized zinc doped samples is measured with same process as discussed earlier.

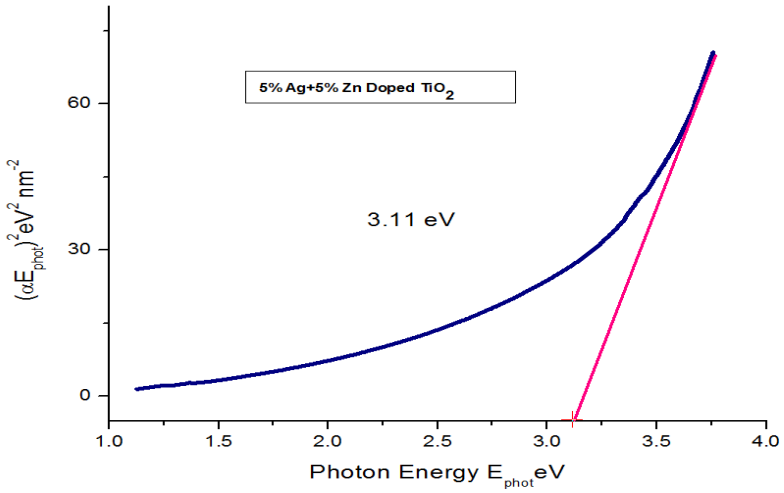

Figure 5.29 Band gap studies of zinc doped TiO_2 synthesized via sol-hydrothermal process

It is 3.11 eV as shown in figure (5.27) which is smaller than un-doped TiO_2.

CHAPTER 6

Discussion

The vibrant nature Sol-Gel& Sol-hydrothermal method is reported in the literature. These wet chemical routes provide control over the reaction parameters. The rates of hydrolysis and condensation play a key role in imparting crystallinity and specific morphology to obtained product. The rate of hydrolysis and condensations depend upon the pH of solution and temperature. The slow and more controlled hydrolysis leads to smaller particle sizes [34, 63, and 99]. By reducing particle size less than 100 nm the photo-catalytic performance of TiO_2 can be increased [120]. In our study Titanium tetra chloride is used as a precursor and metallic precursor zinc nitrate and silver nitrate are used for in situ doping with aim to enhance the absorption spectrum by decreasing band gap. In Some studies it is reported that mixed anatase and rutile phase shows better photo-catalytic activity like Li et al. hypothesized that solid-solid interface is key structural feature that act as a charge separator to prevent recombination and it also serve as an active site to initiate the catalytic activity [122-123] While anatase-TiO_2 has attracted more attention for its vital use as pigments [124], gas sensors [125], catalysts [17, 40] and photo catalysts [19, 126]. Anatase TiO_2 is more active photo catalyst than rutile [127]. By the comparison of reported literature it can be accomplished that crystalline anatase phase is more promising candidate for potential application as a photo-catalyst. In this study our prime objective was the synthesis of un-doped antase TiO_2 and doped antase TiO_2 with maximum crystallinity and surface area. We observed the effects of synthesis routes on phase stabilization, surface area and morphology of obtained samples and are discussed later in detail.

6.1 Effect of Synthesis routes on the formation of different phases and morphology of un-doped and doped TiO_2

6.1.1 XRD

The difference in the phases of sample synthesized via Sol-Gel and Sol-hydrothermal process is observed on characterization. Comparison of Sol-Gel and Sol hydrothermal

process for synthesis of pure TiO_2 as shown in figure (6.1) clearly indicates the difference. XRD results of hydrothermally synthesized samples show pure anatase phase without any impurity while in ordinary Sol-Gel process mixed phase's (Anatase and Rutile) are observed along with NaCl as an impurity. Crystallite size was also different as 12.9 nm hydrothermally synthesized and 25 nm for sol synthesized. The peaks indicate the presence of anatase phase, with (101) planes. The spectrums indicate that that all samples are crystalline no amorphous phase is observed. The formation of NaCl is due to use of NaOH in condensation process where the Na^+ ions react with Cl^- ions of Titania precursor and make NaCl as an impurity. 100% removal of NaCl from synthesized product was a complex job although it was significantly decreased by several time washing at lower temperature about 5^oC but it causes the decrease in yield of TiO_2. The problem of NaCl formation can be overcome by two ways,

- Sol hydrothermal synthesis process where several time washing can be done after hydrothermal treatment.
- Secondly by using ammonium hydroxide/ ammonia solution instead of sodium hydroxide in condensation process.

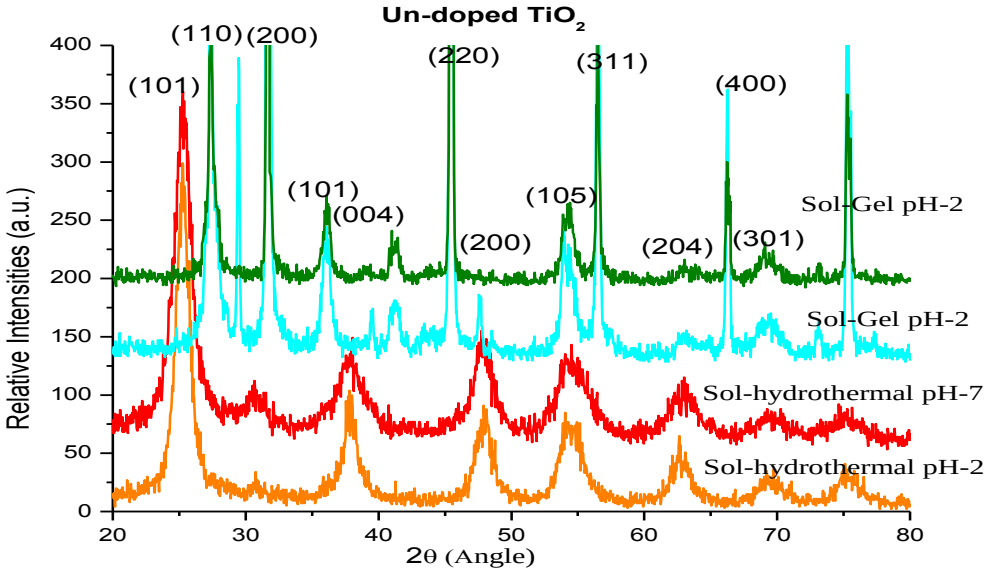

Figure 6.1 Comparison of un-doped Sol-Gel and sol-hydrothermally synthesized TiO_2

There is still a limitation noted during experiments that by using of ammonia solution we can get pH no more than 10 because of its week basic nature as compared to NaOH. In case of NaOH we can get samples up to pH 13.70.

XRD results of Sol-Gel and Sol hydrothermal synthesized zinc doped TiO_2 is shown in figure (6.2)

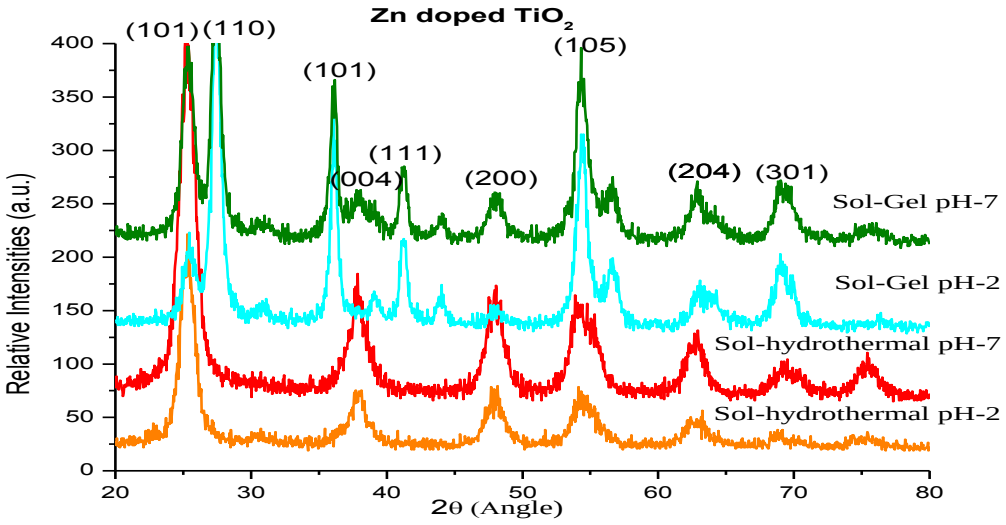

Figure 6.2 Comparison of zinc doped Sol-Gel and sol-hydrothermally synthesized TiO_2

Results of hydrothermally synthesized sample shows the anatase phase is stabilized along with dopants while in ordinary Sol-Gel process mixed phases (Anatase and Rutile) are observed. Average crystallite size in Sol hydrothermal process is 14.9 nm while 26 nm in Sol-Gel. But in both process spectrums indicate that that all samples are crystalline no amorphous phase is observed. Comparison of Sol-Gel and Sol hydrothermal co-doped TiO_2 is shown if figure 6.3. XRD results of hydrothermally synthesized samples show that anatase phase is stabilized along with dopants peaks while in ordinary Sol-Gel process mixed phases (anatase and rutile) are stabilized as shown in figure 6.3. Average crystallite size is 40 nm in Sol-Gel and 25.8 nm in hydrothermally synthesized samples. But in both processes spectrums indicate that that all samples are crystalline no amorphous phase is observed. Entire results of hydrothermally synthesized samples show the stabilization of antase phase while Sol-Gel synthesized show the mixed phases.

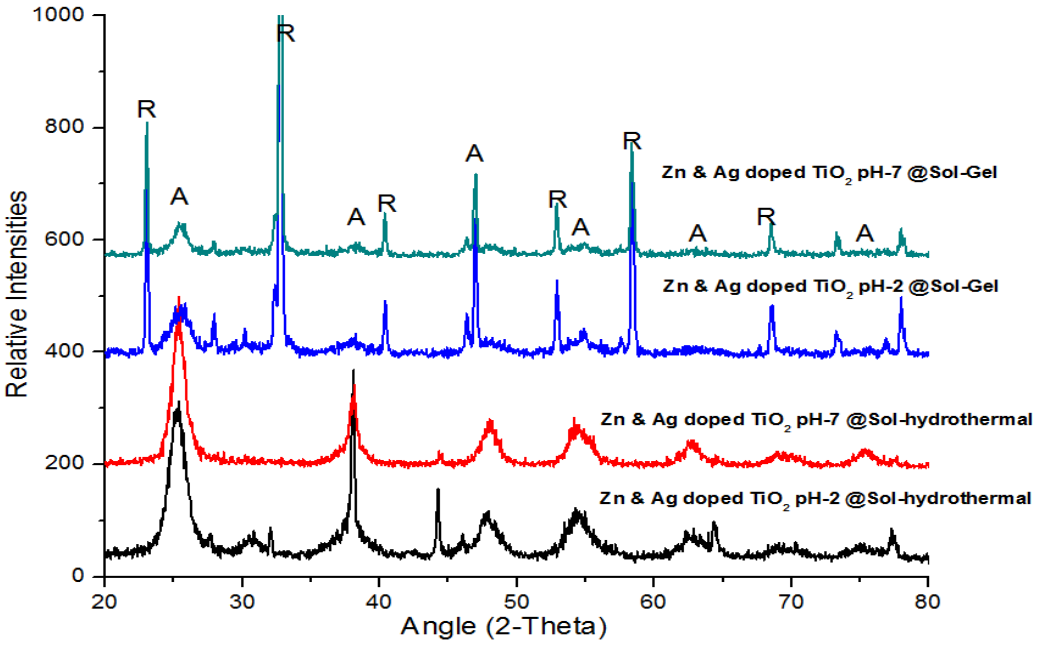

Figure 6.3 Comparison of zinc doped Sol-Gel and sol-hydrothermally synthesized TiO_2

6.1.2 SEM

SEM results of un-doped TiO_2 synthesized via hydrothermal technique as shown in figure (6.4).

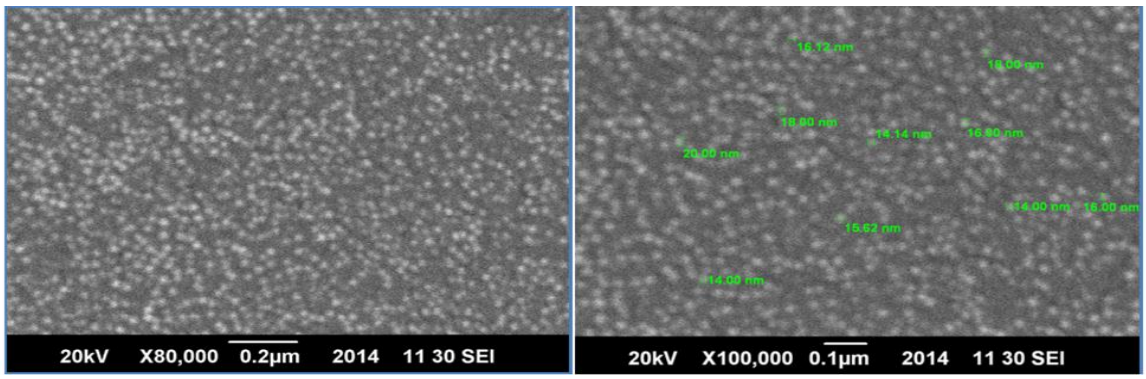

Figure 6.4 SEM result of un-doped TiO_2

It shows the well dispersed particles with spherical morphology. The particle sizeis 14 to 20 nm which shows much resemblance with the XRD calculated results by Scherer formula. SEM results of zinc doped Sol-hydrothermally synthesized samples shows the spherical morphology while Sol-Gel synthesized samples shows irregular morphology w-

ith higher particle size as shown in figure (6.5) and (6.6).

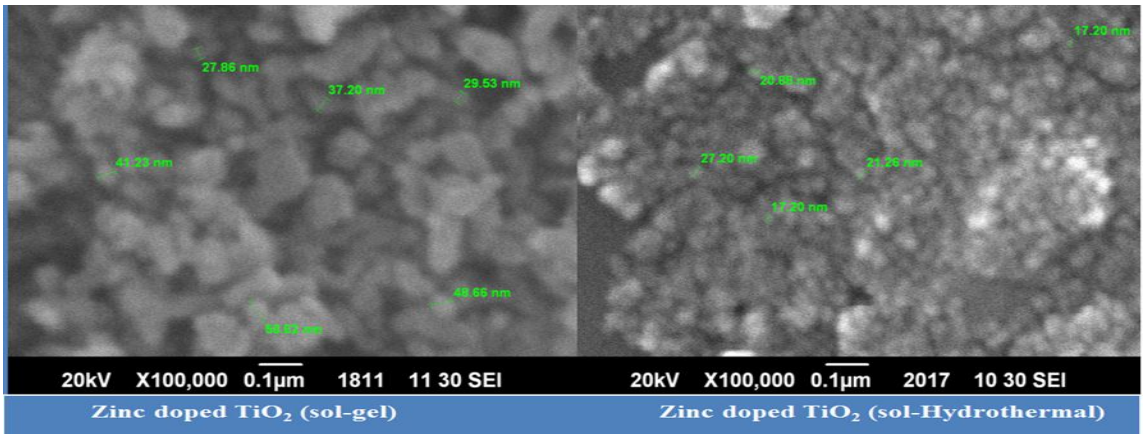

Figure 6.5 SEM results of zinc doped TiO_2

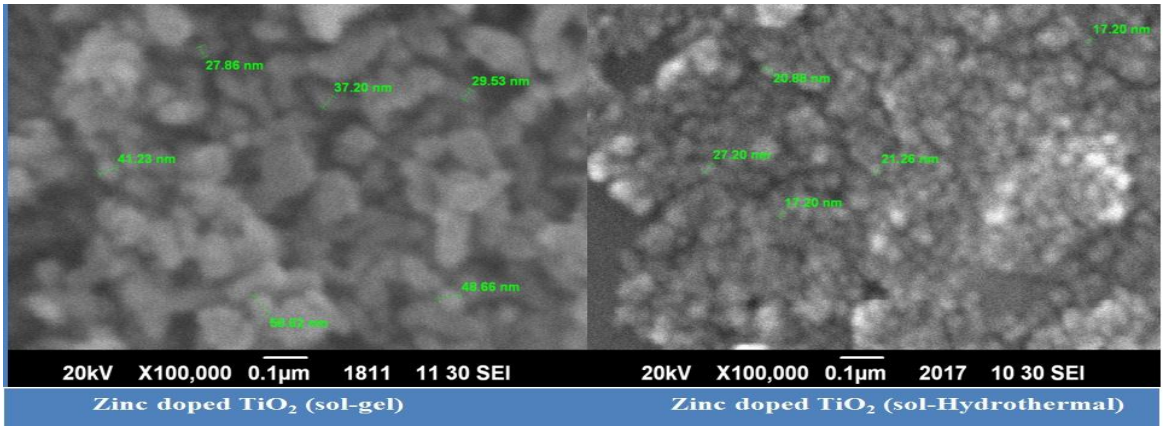

Figure 6.6 SEM results of zinc doped TiO_2 at higher magnification

The same morphology of zinc silver co-doped via Sol-Gel and sol-hydrothermal technique is observed as shown in figure (6.7).

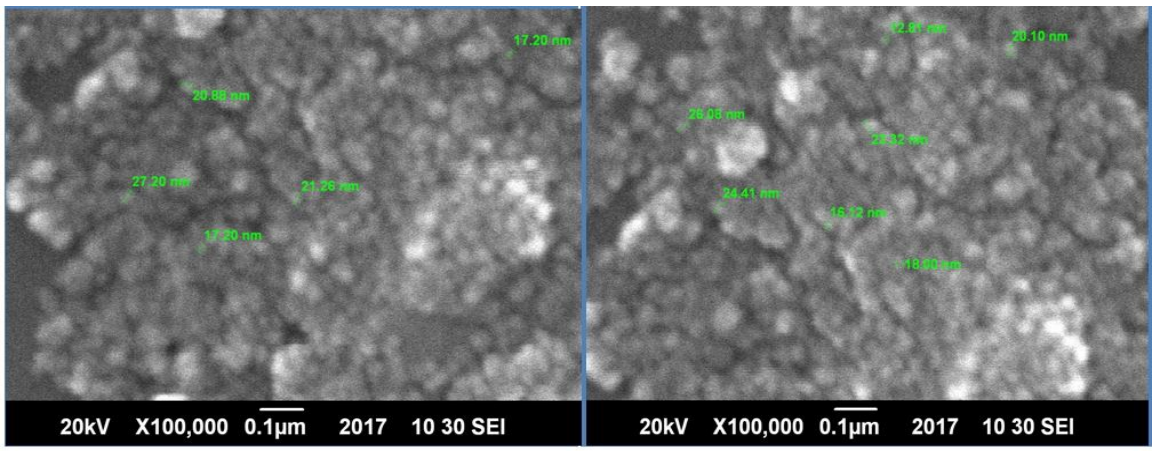

Figure 6.7 SEM result of silver and zinc doped TiO_2

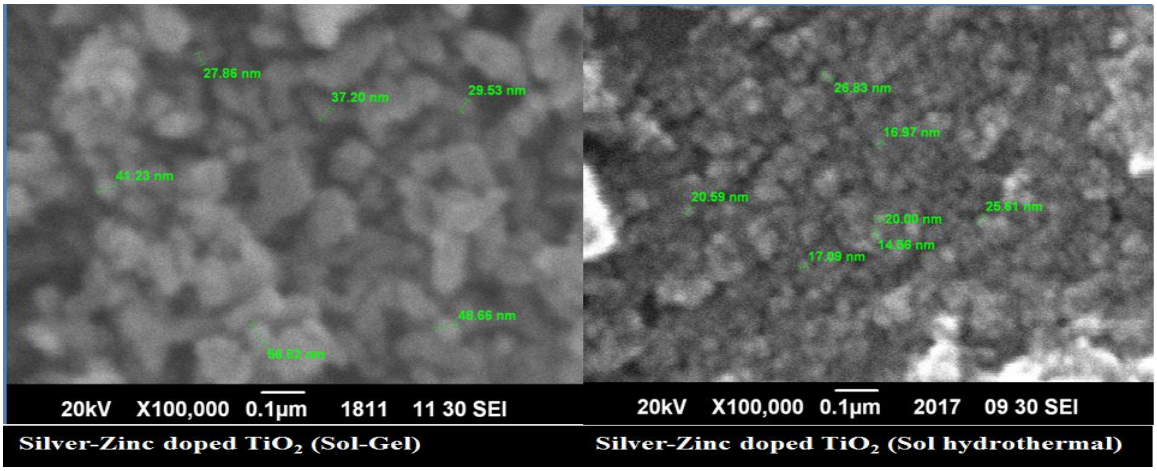

Figure 6.8 SEM result of silver and zinc doped TiO_2

The dispersion of powder is major problem for SEM analysis sample due to particle size of synthesize samples in nano domain. The dispersion of hydrothermally synthesized samples was done in water and ethanol followed by sonication of 20 minutes as shown in figure (6.9) and (6.10). The samples prepared in ethanol are well dispersed as compared to deionized water. The possible reason may be the use of ethanol during synthesis process but in case of doped samples the particles are not well dispersed.

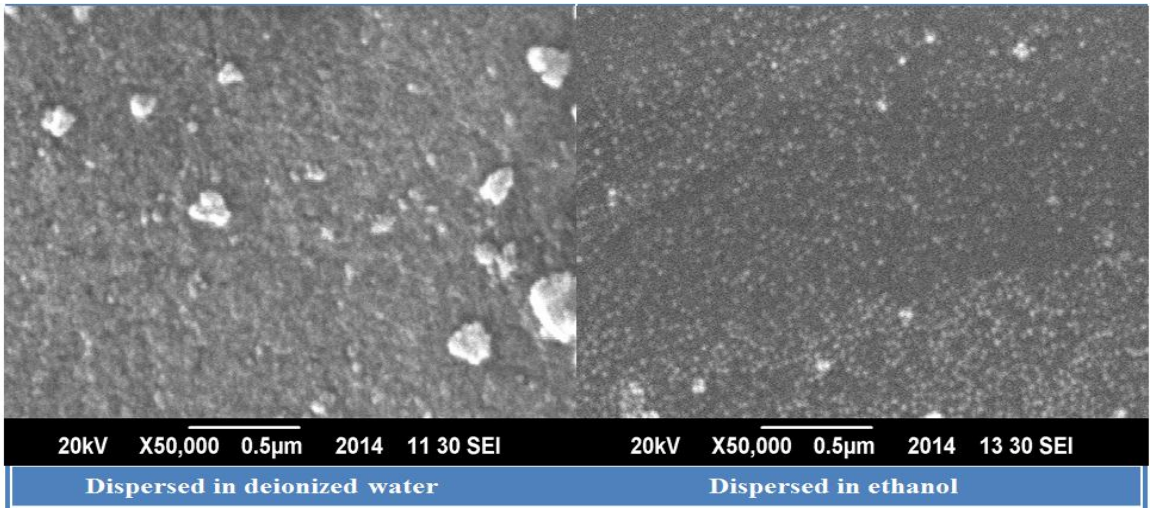

Figure 6.9 SEM results of dispersion in different solvents of un-doped TiO_2

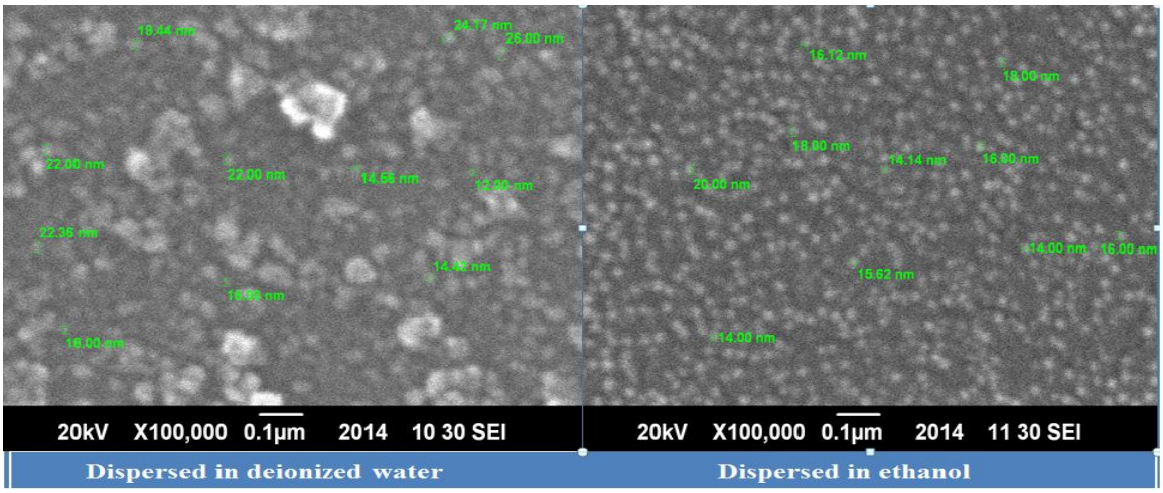

Figure 6.10 SEM results of dispersion in different solvents of un-doped TiO_2

Synthesized sample via sol-hydrothermal process shows the spherical morphology while in Sol-Gel process irregular morphology is observed as discussed earlier. We get control morphology and small particle size in Sol hydrothermal process. The EDX results indicate that there are no impurities, except chlorides and sodium in cases of Sol-Gel synthesized samples in trace amounts, which can be minimized by washing the TiO_2 gel by distilled water but it influence the decrease in net yield of TiO_2 while the hydrothermally synthesized samples shows that Titanium and Oxygen along with dopants are in appropriate ratios. The maximum obtained elemental composition of dopant obtained is 4.11 atomic % incase 5% zinc doped samples as mentioned in table (5.1).

6.1.3 UV- Vis Spectroscopy

Synthesis rout effect the band gap of the obtained samples. It can be differentiated easily by the comparison of Zn doped TiO_2 synthesized via sol gel and sol hydrothermal techniques. The band gaps of Sol-Gel synthesized zinc doped samples are 3.15 eV while sol-hydrothermally synthesized samples are 3.09 eV as shown in figure (6.11).

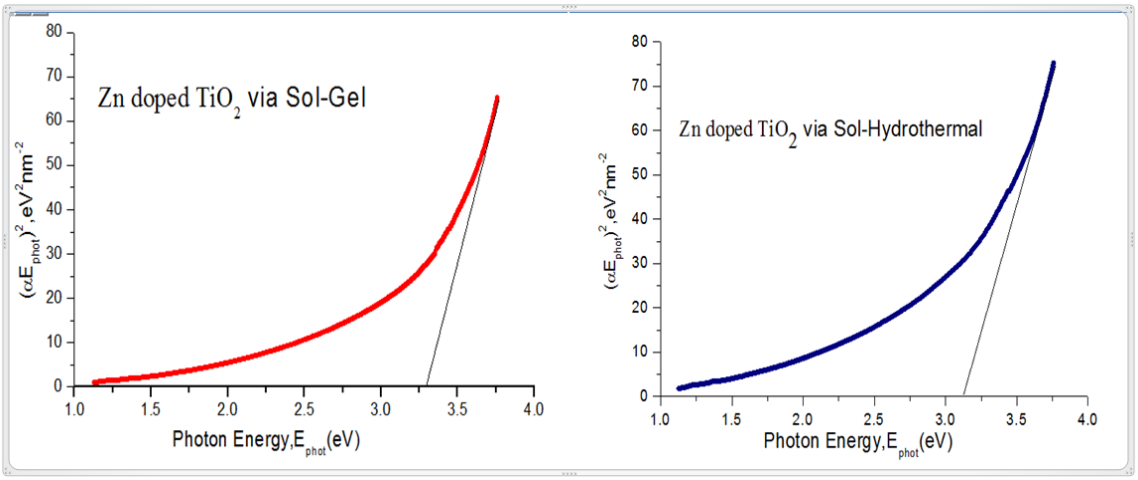

Figure 6.11 Effect of synthesis route on band gap

6.2 Effect of pH

The pH value of the Sol-Gel or sol hydrothermal process is a key factor for controlling the final particle size, surface area, morphology and phase. It is reported in the literature that the pure anatase phase can be synthesized at pH-3 [113,114]. While it is strongly reveal from the XRD results that un-dope and doped TiO_2 with anatase phase can be synthesized in strong acidic to strong basic range that is from pH-2 to pH-12 via Sol hydrothermal process but the size was increasing as pH value increased. Formation and stabilization of anatase phase is due to following reasons,

(i) The brookite phase is not formed because, it is stable only at very low temperatures (below 100^{o}C) [96, 129] while pure rutile phase is obtained at higher reaction temperatures than the anatase phase [128].

(ii) The chloride ions present inside sol accelerate the nucleation of anatase [63].

(iii) Surface free energy depends on the size. Anatase (101) is obtained, because (101) s plane of anatase is the most thermodynamically stable, having lowest energy, when particle size is below 15 nm [130].

The XRD results show that crystallite size of the samples synthesized at acidic pH ranges smaller than those synthesized in basic pH range. It shows that, crystallite size is increasing as pH value is increasing. Appearance of sharp peaks for all samples indicates that the nanoparticles are highly crystalline in both acidic and basic condition, no

amorphous phase is obtained. Average crystallite size of synthesized samples is 12.9 nm in sol-hydrothermal synthesis while it's up to 30 nm or higher in case of Sol-Gel process.

6.3 Effect of Crystallite size on the Surface Area

Surface area is playing a key role in photo-catalysis process because this process takes place at the surface of semiconducting material. Surface area is a function of particle size. If particle size decreases surface area increases and it is calculated by using crystallite size with following formula.

$$S = 6 \times 10^3 / \rho L$$

L is crystallite size and ρ is the density of TiO_2 that is 3.90 g/cm^3. Similarly it becomes clear that, with increase of crystallite size the surface area is decreasing while with decrease of crystallite size the surface area is increasing. The surface area of the samples synthesized in the acidic pH range is relatively smaller than Basic pH ranges. For zinc and silver doped samples the average crystallite size calculated from XRD results via Scherer formula is 12.9 nm and surface area calculated is 1.19 x 10^5 m^2/g which is much higher than the recent reported literature [131].

The surface calculated by above equation of synthesized samples is 48 to 170m^2/g. The surface area of co-doped TiO_2 is relatively smaller than silver doped and zinc doped TiO_2.

6.4 Effect of dopants on band gap

The band gap studies of zinc doped TiO_2 shows the decrease in band gap that is 3.08 eV while it is reported in literature that band gap of pure TiO_2 with anatase phase is 3.26 eV. The solutions of TiO_2 contain many hydroxyl groups that are used by both Zn and Ti. ZnO formed as the solution is heated above 80 ^{o}C. ZnO and TiO_2 took form that makes a combine structure with hydroxyl groups. The band gap of Zinc doped TiO_2 that's why changes [131,132].

Similarly the decrease in band gap of silver doped TiO_2 was also observed from UV-V is spectrum.

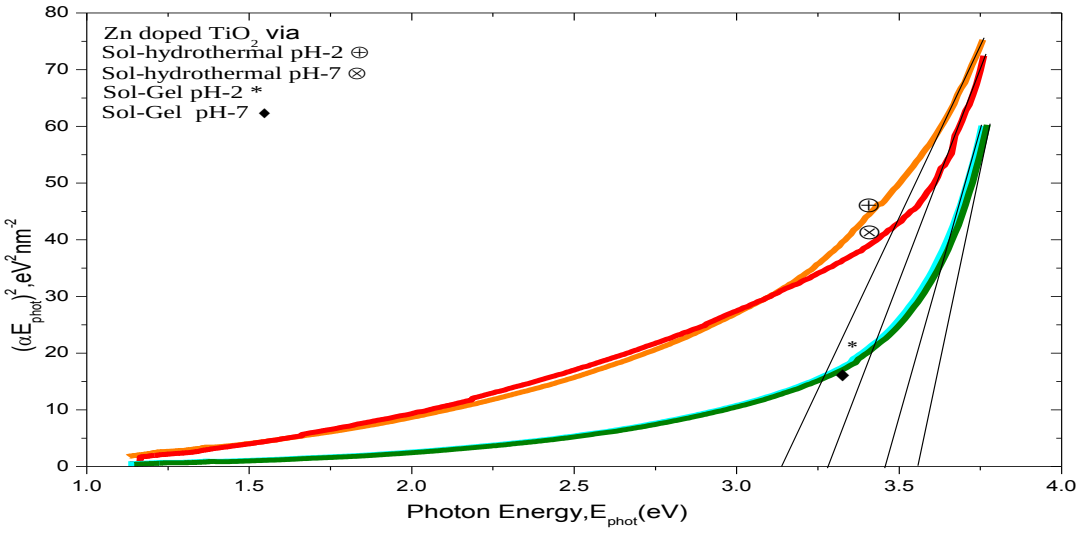

Figure 6.12 Comparison of zinc doped TiO_2 band gap studies

The entire samples shows there is some increase in band gap of all doped synthesized samples at nano scale while same philosophy is being reported in literature that due to Quantum confinement the band gap of TiO_2 nanoparticles increases form the original band gap [133]. The comparison of samples synthesized via Sol-Gel and Sol-hydrothermal routes shows that the decrease in band gap is higher in hydrothermally synthesized samples as compared to Sol-Gel synthesized samples as shown in Figure 6.12 & 6.13. So in our study it's concluded that the as the crystallite size decreases the band gap of un-doped and doped nanoparticles also decreased. This decrease in band gap is may be due to the following factors,

- Very high crsytallinity
- Un-doped and doped anatase phase
- Very high surface area as compared to reported literature
- Spherical morphology
- Crystallite size in nano-domain (12.9-26 nm)

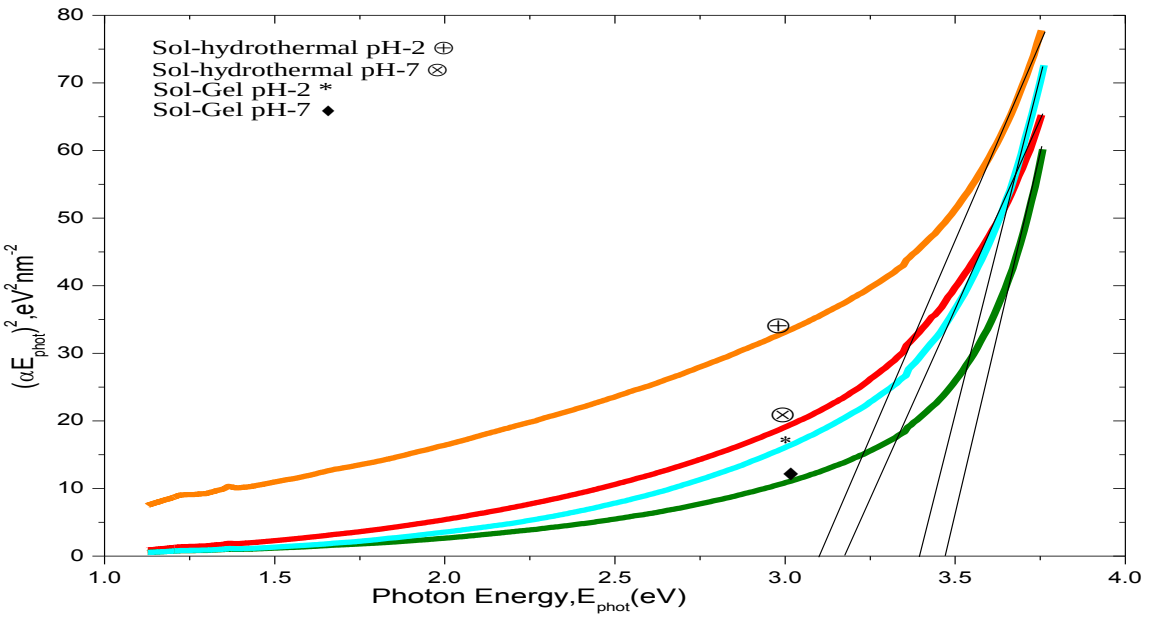

Figure 6.13 Comaprison of TiO_2 band gap studies

6.5 Effect of Calcination Temperature

The entire XRD results show very high crsytallinity, no amorphous phase is present because in Sol-Gel synthesized samples the calcination temperature was 500 ^{o}C for 5 hours and in hydrothermal synthesis the temperature was 150 ^{o}C for 5 hours.

Table 6.1 Comparison of sol-gel and sol-hydrothermal routes

Sample name	Impurities	Crystallite size (nm)	S (m^2/g)	Crystal structure	pH	Band gap (eV)	Dopant 5%wt	Synthesis Route
TiO_2	NaCl	25.6	60.1	Anatase+Rutile	2	3.34	X	Sol-Gel
TiO_2	X	32	48	Anatase+Rutile	7	3.39	X	Sol-Gel
TiO_2	X	9	170	Anatase	2	**3.13**	X	Sol-hydro.
TiO_2	X	11.5	134	Anatase	7	**3.26**	X	Sol-hydro.
Zn-TiO_2		25.9	59.4	Anatase+Rutile	2	3.51	4.11	Sol-Gel
Zn-TiO_2	X	32	48	Anatase+Rutile	7	3.56	4.01	Sol-Gel
Zn-TiO_2	X	12	128.21	Anatase	2	**3.19**	3.27	Sol-hydro.
Zn-TiO_2	X	17	90.50	Anatase	7	**3.29**	3.29	Sol-hydro.

Calcination temperature plays very important role in the surface area, crystallite size and photo-catalytic activity. From 300 to 600^{o}C the photo-catalytic activity increases while above 600^{o}C rapid decrease in the photo-catalytic activity is reported [134]. Entire Sol-Gel synthesized sample were calcinated at 500^{o}C in furnace while in hydrothermal synthesis all experiment were conducted at 150^{o}C temperature and normal pressure. No temperature variation effect was focused in this study.

CONCLUSION

In this study the samples were synthesized by Sol-Gel and Sol-hydrothermal routes, the effect of synthesis routes on formation of different phases, crystallize size and mainly the band gap study of un-doped and doped TiO_2 nanoparticles is discussed. Sol-Gel process yields TiO_2 nanoparticles by hydrolysis of $TiCl_4$ and condensation of the metal hydroxide complexes formed during hydrolysis. Synthesis routes paly very important role in phase stabilization of synthesized samples.

XRD results show that in Sol-Gel synthesized samples we get mixed phases while only anatase phase stabilized in hydrothermal process. The crystallite size is also very much dependent on synthesis route and pH of the obtained sample. Average crystallite size in case of hydrothermal synthesized samples is smaller than Sol-Gel and as the pH increases crystallite size increases. The surface area of hydrothermally synthesized sample is much higher than the surface area of Sol-Gel synthesized samples.

The decrease in band gap calculated by Lambert beer law is higher in case of hydrothermally synthesized samples as compared to sample synthesized via Sol-Gel process. There is no characteristic peak of Zn/Ag metal or ZnO/AgO which implies that zinc and silver ions are properly incorporated into the lattice of the anatase TiO_2. The decrease in band gap will increase the absorption of sun light and dopants will reduce the electron hole pair recombination.

Synthesized sample via Sol-hydrothermal route shows the spherical morphology while in Sol-Gel process irregular morphology is observed as discussed earlier. By Sol hydrothermal process we get control morphology, small particle, and higher surface area and stabilized anatase phase from pH-2 to pH-13.

REFERENCES

1. Orr, L., R. Bent, and R. Baker, *Energy: Science, policy, and the pursuit of sustainability*2002: Island Press.
2. Mao, S.S. and X. Chen, *Selected nanotechnologies for renewable energy applications.* International journal of energy research, 2007. **31**(6-7): p. 619-636.
3. Mor, G.K., et al., *A review on highly ordered, vertically oriented TiO_2 nanotube arrays: Fabrication, material properties, and solar energy applications.* Solar Energy Materials and Solar Cells, 2006. **90**(14): p. 2011-2075.
4. Kitano, M., et al., *Recent developments in titanium oxide-based photocatalysts.* Applied Catalysis A: General, 2007. **325**(1): p. 1-14.
5. http://www.canren.gc.ca/
6. Oelhafen, P. and A. Schüler, *Nanostructured materials for solar energy conversion.* Solar Energy, 2005. **79**(2): p. 110-121.
7. Lazarov, M., et al., *Optical constants and film density of TiN solar selective absorbers.* Journal of applied physics, 1995. **77**(5): p. 2133-2137.
8. Nalwa, H.S., *Handbook of nanostructured materials and nanotechnology*. Vol. 5. 2000: Academic Press.
9. Goetzberger, A. and V.U. Hoffmann, *Photovoltaic solar energy generation*. Vol. 112. 2005: Springer.
10. Goetzberger, A. and V.U. Hoffmann, *Photo-electrochemical cells*. Vol.414. 2001: Nature.
11. Fujishima, A., *Electrochemical photolysis of water at a semiconductor electrode.* nature, 1972. **238**: p. 37-38.
12. Grätzel, M., *Photovoltaic and photoelectrochemical conversion of solar energy.* Philosophical Transactions of the Royal Society A: Mathematical, Physical and Engineering Sciences, 2007. **365**(1853): p. 993-1005.
13. Matsuoka, M., et al., *Photocatalysis for new energy production: recent advances in photocatalytic water splitting reactions for hydrogen production.* Catalysis today, 2007. **122**(1): p. 51-61.
14. Joshi, K. and V. Shrivastava, *Photocatalytic degradation of Chromium (VI) from wastewater using nanomaterials like TiO 2, ZnO, and CdS.* Applied Nanoscience, 2011. **1**(3): p. 147-155.
15. Carp, O., C.L. Huisman, and A. Reller, *Photoinduced reactivity of titanium dioxide.* Progress in Solid State Chemistry, 2004. **32**(1–2): p. 33-177.
16. Chen, X. and S.S. Mao, *Titanium dioxide nanomaterials: synthesis, properties, modifications, and applications.* Chem Rev, 2007. **107**(7): p. 2891-959.
17. Asahi, R., et al., *Visible-light photocatalysis in nitrogen-doped titanium oxides.* Science, 2001. **293**(5528): p. 269-271.
18. Asahi, R. and T. Morikawa, *Nitrogen complex species and its chemical nature in TiO_2 for visible-light sensitized photocatalysis.* Chemical Physics, 2007. **339**(1): p. 57-63.
19. Baiju, K., et al., *Photocatalytic activity of sol-gel-derived nanocrystalline titania.* The Journal of Physical Chemistry C, 2007. **111**(21): p. 7612-7622.

20. Qiu, X. and C. Burda, *Chemically synthesized nitrogen-doped metal oxide nanoparticles.* Chemical Physics, 2007. **339**(1): p. 1-10.
21. Chen, C., et al., *Effect of transition metal ions on the TiO_2-assisted photodegradation of dyes under visible irradiation: a probe for the interfacial electron transfer process and reaction mechanism.* The Journal of Physical Chemistry B, 2002. **106**(2): p. 318-324.
22. Dürr, M., et al., *2006 Volume 110B Band-Gap Engineering of Metal Oxides for Dye-Sensitized Solar Cells.* The Journal of Physical Chemistry B, 2006. **110**(51): p. 26507-26507..
23. Janus, M. and A. Morawski, *New method of improving photocatalytic activity of commercial Degussa P25 for azo dyes decomposition.* Applied Catalysis B: Environmental, 2007. **75**(1): p. 118-123.
24. Madhusudan Reddy, K., et al., *S-, N-and C-doped titanium dioxide nanoparticles: synthesis, characterization and redox charge transfer study.* Journal of Solid State Chemistry, 2005. **178**(11): p. 3352-3358.
25. http://www.geocities.jp/ohba_lab_ob_page/structure6.html
26. Carp, O., C.L. Huisman, and A. Reller, *Photoinduced reactivity of titanium dioxide.* Progress in Solid State Chemistry, 2004. **32**(1–2): p. 33-177.
27. M. Schiavello, *Heterogeneous Photocatalysis*, Volume 3, First ed. Chiche: Wiley, 1997.
28. Carp, O., C.L. Huisman, and A. Reller, *Photoinduced reactivity of titanium dioxide.* Progress in Solid State Chemistry, 2004. **32**(1–2): p. 33-177.
30. Diebold, U., *The surface science of titanium dioxide.* Surface science reports, 2003. **48**(5): p. 53-229.
31. N. A. Serpone, Emeline, A.V. *Suggested terms and definitions in photocatalysis and radio-catalysis*, International Journal of Photoenergy, vol. 4: 2002.
32. Kutal, C. and N. Serpone, *Photosensitive metal-organic systems* 1993: ACS Publications.
33. Fernández-García, M. and J.A. Rodriguez, *Metal Oxide Nanoparticles.* Encyclopedia of Inorganic Chemistry, 2009.
34. Fujishima, A. and K. Honda, *Photolysis-decomposition of water at the surface of an irradiated semiconductor.* nature, 1972. **238**(5385): p. 37-38.
35. Philippe Rodriguez, Laurence Reinert. *Synthesis of structured titanium dioxide from carbonaceous templates Preparation of supported nano scaled Titania particles* Materials Chemistry and Physics 106 (2007) 102.
36. Shiraishi, Y. and T. Hirai, *Selective organic transformations on titanium oxide-based photocatalysts.* Journal of Photochemistry and Photobiology C: Photochemistry Reviews, 2008. **9**(4): p. 157-170.
37. Cozzoli, P.D., A. Kornowski, and H. Weller, *Low-temperature synthesis of soluble and processable organic-capped anatase TiO_2 nanorods.* Journal of the American Chemical Society, 2003. **125**(47): p. 14539-14548.
38. Sonawane, R., S. Hegde, and M. Dongare, *Preparation of titanium (IV) oxide thin film photocatalyst by sol–gel dip coating.* Materials chemistry and physics, 2003. **77**(3): p. 744-750.

39. Nagaveni, K., et al., *Synthesis and structure of nanocrystalline TiO_2 with lower band gap showing high photocatalytic activity.* Langmuir, 2004. **20**(7): p. 2900-2907.
40. Yu, J., et al., *Effects of calcination temperature on the microstructures and photocatalytic activity of titanate nanotubes.* Journal of Molecular Catalysis A: Chemical, 2006. **249**(1): p. 135-142.
41. Klabunde, K.J. and R. Richards, *Nanoscale materials in chemistry*2001: Wiley Online Library.
42. Fujishima, A. and X. Zhang, *Titanium dioxide photocatalysis: present situation and future approaches.* EM Comptes Rendus Chimie, 2005. **9**.
43. Wang, Z., et al., *The effects of different acids on the preparation of TiO_2 nanostructure in liquid media at low temperature.* Materials chemistry and physics, 2008. **111**(2): p. 313-316.
44. Guan, K. and Y. Yin, *Effect of rare earth addition on super-hydrophilic property of TiO_2/SiO_2 composite film.* Materials chemistry and physics, 2005. **92**(1): p. 10-15.
45. Ohtani, B., Y. Ogawa, and S. Nishimoto, *Photocatalytic activity of amorphous-anatase mixture of titanium (IV) oxide particles suspended in aqueous solutions.* The Journal of Physical Chemistry B, 1997. **101**(19): p. 3746-3752.
46. Grätzel, M., *Conversion of sunlight to electric power by nanocrystalline dye-sensitized solar cells.* Journal of Photochemistry and Photobiology A: Chemistry, 2004. **164**(1): p. 3-14.
47. Umebayashi, T., et al., *Analysis of electronic structures of 3d transition metal-doped TiO_2 based on band calculations.* Journal of Physics and Chemistry of Solids, 2002. **63**(10): p. 1909-1920
48. Liz Marzan, L.M. and P.V. Kamat, *Nanoscale materials* 2003: Springer.
49. A. K. Bandyopadhyay, Nano Materials, *New Age International (P) Limited Publishers*: New Delhi 2008.
50. A. K. Bandyopadhyay, Nano Materials, *New Age International (P) Limited Publishers*: New Delhi 2008.
51. Andreozzi, R,Caprio, V. Insola, A. Martota, R. Cat. Today, 1999, 53, 5 1-59
52. Jayant Dharma, niruddha Pisal., *Simple Method of Measuring the Band Gap Energy Value of TiO_2 in the Powder Form using a UV/Vis/ NIR Spectrometer PerkinElmer*, Inc. USA, 2009.
53. Pan, D., et al., *Facile synthesis and characterization of luminescent TiO_2 nanocrystals.* Advanced Materials, 2005. **17**(16): p. 1991-1995.
54. Hodes, G., *Chemical Solution Deposition of Semiconductor Films.* 2003.
55. Rama J. Pino, R. Meliorum *physical chemistry Technologies* 2002
56. Madhusudan Reddy, K., S.V. Manorama, and A. Ramachandra Reddy, *Bandgap studies on anatase titanium dioxide nanoparticles.* Materials chemistry and physics, 2003. **78**(1): p. 239-245.
57. Boehm, H., *Acidic and basic properties of hydroxylated metal oxide surfaces.* Discuss. Faraday Soc., 1971. **52**: p. 264-275.
58. Bell, G., *Modeling and characterization of supported catalytic centres*, 1994.

59. Kim, C.-S., et al., *Synthesis of nanocrystalline TiO_2 in toluene by a solvothermal route.* Journal of Crystal Growth, 2003. **254**(3-4): p. 405-410.

60. Yu, J., et al., *Preparation and characterization of super-hydrophilic porous TiO_2 coating films.* Materials chemistry and physics, 2001. **68**(1): p. 253-259.
61. Jang, H.D., *Effects of H2O on the particle size in the vapor-phase synthesis of TiO_2.* AIChE journal, 1997. **43**(S11): p. 2704-2709.
62. West, R.H., et al., *First-principles thermochemistry for the production of TiO_2 from TiCl4.* The Journal of Physical Chemistry A, 2007. **111**(18): p. 3560-3565.
63. http://www.wikipedia.com.
64. Ani K. John and G. D. Surender., *Experimental and Modeling Studies on Vapour Phase Synthesis of Titania Nanoparticles*. International Symposium of Research Students on Material Science and Engineering (ISRS) 2004.
65. Jaroenworaluck, A., et al., *Fabrication and characteristics of TiO_2 films by a microwave drying technique.* Surface and interface analysis, 2006. **38**(4): p. 765-768.
66. Han, S., et al., *Low-Temperature Synthesis of Highly Crystalline TiO_2 Nanocrystals and their Application to Photocatalysis.* Small, 2005. **1**(8-9): p. 812-816.
67. Ani, J.K., et al., *Characteristics of Titania Nanoparticles Synthesized Through Low Temperature Aerosol Process.* Aerosol and Air Quality Research, 2005. **5**(1).
68. Zeatoun, L. and D. Feke, *Characterization of TiO_2 Smoke Prepared Using Gas-Phase Hydrolysis of TiCl4.* Particle & Particle Systems Characterization, 2005. **22**(4): p. 276-281.
69. Zeatoun, L. and D. Feke, *Characterization of TiO_2 Smoke Prepared Using Gas-Phase Hydrolysis of TiCl4.* Particle & Particle Systems Characterization, 2005. **22**(4): p. 276-281.
70. Di Muzio, F., M. Masi, and S. Carrà, *Modeling of aerosol deposition of titania thin films.* Materials chemistry and physics, 2000. **66**(2): p. 286-293.
71. Kominami, H., et al., *Synthesis of titanium (IV) oxide of ultra-high photocatalytic activity: high-temperature hydrolysis of titanium alkoxides with water liberated homogeneously from solvent alcohols.* Journal of Molecular Catalysis A: Chemical, 1999. **144**(1): p. 165-171.
72. Park, H.K., D.K. Kim, and C.H. Kim, *Effect of solvent on titania particle formation and morphology in thermal hydrolysis of TiCl4.* Journal of the American Ceramic Society, 1997. **80**(3): p. 743-749.
73. Akurati, K.K., et al., *Flame synthesis of TiO_2 nanoparticles with high photocatalytic activity.* Solid state sciences, 2007. **9**(3): p. 247-257.
74. Trentler, T.J., et al., *Synthesis of TiO_2 nanocrystals by nonhydrolytic solution-based reactions.* Journal of the American Chemical Society, 1999. **121**(7): p. 1613-1614.
75. Madhusudan Reddy, K., S.V. Manorama, and A. Ramachandra Reddy, *Bandgap studies on anatase titanium dioxide nanoparticles.* Materials chemistry and physics, 2003. **78**(1): p. 239-245.

76. Li, Y.L. and T. Ishigaki, *Synthesis and structural characterization of titanium oxides and composites by thermal plasma oxidation of titanium carbide.* Thin Solid Films, 2002. **407**(1): p. 79-85.
77. Zhao, L. and J. Yu, *Controlled synthesis of highly dispersed TiO_2 nanoparticles using SBA-15 as hard template.* Journal of colloid and interface science, 2006. **304**(1): p. 84-91.
78. Komarneni, S., R.K. Rajha, and H. Katsuki, *Microwave-hydrothermal processing of titanium dioxide.* Materials chemistry and physics, 1999. **61**(1): p. 50-54.
79. Li, Y., et al., *High photoluminescence quantum yield of TiO_2 nanocrystals prepared using an alcohothermal method.* Luminescence, 2007. **22**(6): p. 540-545.
80. Yang, H.G., et al., *Solvothermal synthesis and photoreactivity of anatase TiO_2 nanosheets with dominant {001} facets.* Journal of the American Chemical Society, 2009. **131**(11): p. 4078-4083.
81. Kim, C.-S., et al., *Synthesis of nanocrystalline TiO_2 in toluene by a solvothermal route.* Journal of Crystal Growth, 2003. **254**(3-4): p. 405-410.
82. Seo, D.S., J.K. Lee, and H. Kim, *Synthesis of TiO_2 nanocrystalline powder by aging at low temperature.* Journal of Crystal Growth, 2001. **233**(1): p. 298-302.
83. Lu, J., et al., *Synthesis and characterization of TiO_2 nanopowders from peroxotitanium solutions.* Materials chemistry and physics, 2009. **115**(1): p. 142-146.
84. Xiao-Quan, C., L. Huan-Bin, and G. Guo-Bang, *Preparation of nanometer crystalline TiO_2 with high photo-catalytic activity by pyrolysis of titanyl organic compounds and photo-catalytic mechanism.* Materials chemistry and physics, 2005. **91**(2): p. 317-324.
85. Yin, S., et al., *Low temperature synthesis of nanosize rutile titania crystal in liquid media.* Materials chemistry and physics, 2002. **75**(1): p. 76-80.
86. Mongillo, J.F., *Nanotechnology 101*2007: Greenwood Publishing Group.
87. Anderson, C. and A.J. Bard, *An improved photocatalyst of TiO_2/SiO2 prepared by a sol-gel synthesis.* The Journal of Physical Chemistry, 1995. **99**(24): p. 9882-9885.
88. Kumar, S.A., P.H. Lo, and S.M. Chen, *Electrochemical synthesis and characterization of TiO_2 nanoparticles and their use as a platform for flavin adenine dinucleotide immobilization and efficient electrocatalysis.* Nanotechnology, 2008. **19**(25): p. 255501.
89. Qu, Y., et al., *Selective synthesis of TiO_2 nanopowders.* Glass Physics and Chemistry, 2008. **34**(5): p. 637-639.
90. Corriu, R. and N. Trong Anh, *Front Matter* 2009: Wiley Online Library.
91. Sigma-Aldrich USA Materials Matters, Vol.3, No.1, pp 14.
92. Lane, R., B. Craig, and W. Babcock, *the Coming Revolution: Science and Technology of Nanoscale Structures… 5.* AMPTIAC Newsletter, 2002. **6**(1).
93. Li, Y.L. and T. Ishigaki, *Synthesis and structural characterization of titanium oxides and composites by thermal plasma oxidation of titanium carbide.* Thin Solid Films, 2002. **407**(1): p. 79-85.
94. Wilson, M., et al., *Nanotechnology: basic science and emerging technologies*2002: Chapman & Hall/CRC.

95. Duncan, W.R. and O.V. Prezhdo, *Theoretical studies of photoinduced electron transfer in dye-sensitized TiO_2.* Annu. Rev. Phys. Chem., 2007. **58**: p. 143-184.
96. Saadoun, M., et al., *Polymer supported porous TiO_2: application to photo-catalysis.* physica status solidi (c), 2007. **4**(6): p. 2029-2033.
97. Kim, J.H., S. Fujita, and S. Shiratori, *Fabrication and characterization of TiO_2 thin film prepared by a layer-by-layer self-assembly method.* Thin Solid Films, 2006. **499**(1): p. 83-89.
98. Madhusudan Reddy, K., S.V. Manorama, and A. Ramachandra Reddy, *Bandgap studies on anatase titanium dioxide nanoparticles.* Materials chemistry and physics, 2003. **78**(1): p. 239-245.
99. Wilson, M., et al., *Nanotechnology: basic science and emerging technologies*2002: Chapman & Hall/CRC.
100. Liuxue, Z., L. Peng, and S. Zhixing, *Photocatalysis anatase thin film coated PAN fibers prepared at low temperature.* Materials chemistry and physics, 2006. **98**(1): p. 111-115.
101. Suciu, R., et al. *TiO_2 thin films prepared by sol–gel method*. in *Journal of Physics: Conference Series*. 2009. IOP Publishing.
102. Raja, K., et al., *Photo-electrochemical hydrogen generation using band-gap modified nanotubular titanium oxide in solar light.* Journal of power sources, 2006. **161**(2): p. 1450-1457.
103. Koch, C., *Bulk behavior of nanostructured materials.* Nanostructure Science and Technology, 1999: p. 93.
104. Michler, G.H., *Electron microscopy of polymers*2008: Springer.
105. Djerdj, I., et al., *Nonaqueous synthesis of metal oxide nanoparticles: short review and doped titanium dioxide as case study for the preparation of transition metal-doped oxide nanoparticles.* Journal of Solid State Chemistry, 2008. **181**(7): p. 1571-1581.
106. Zhao, Y., et al., *Surface characteristics and microstructure of dispersed TiO_2 nanoparticles prepared by diffusion flame combustion.* Materials chemistry and physics, 2008. **107**(2): p. 344-349.
107. Wang, Z., et al., *The effects of different acids on the preparation of TiO_2 nanostructure in liquid media at low temperature.* Materials chemistry and physics, 2008. **111**(2): p. 313-316.
108. Habibpanah, A.A., S. Pourhashem, and H. Sarpoolay, *Preparation and characterization of photocatalytic titania–alumina composite membranes by sol–gel methods.* Journal of the European Ceramic Society, 2011. **31**(15): p. 2867-2875.
109. Wang, Y., et al., *A general approach to porous crystalline TiO_2, SrTiO3, and BaTiO3 spheres.* The Journal of Physical Chemistry B, 2006. **110**(28): p. 13835-13840.
110. Nagaveni, K., et al., *Synthesis and structure of nanocrystalline TiO2 with lower band gap showing high photocatalytic activity.* Langmuir, 2004. **20**(7): p. 2900-2907.
111. Cozzoli, P.D., A. Kornowski, and H. Weller, *Low-temperature synthesis of soluble and processable organic-capped anatase TiO_2 nanorods.* Journal of the American Chemical Society, 2003. **125**(47): p. 14539-14548.

112. Barnard, A., et al., *Multi-scale modeling of titanium dioxide: controlling shape with surface chemistry.* Rev. Adv. Mater. Sci, 2005. **10**: p. 21-27.
113. Santana-Aranda, M., et al., *Physical properties of TiO_2 prepared by sol-gel under different pH conditions for photocatalysis,* 2005.
114. Qu, Y., et al., *Selective synthesis of TiO 2 nanopowders.* Glass Physics and Chemistry, 2008. **34**(5): p. 637-639.
115. Alekabi, H. Demayo, P. J. Phys. Chem.1986, 90,4075.
116. Carraway, E. R. Hoffman, A. J. and Hoffmann, M. R.Env. SciTech.1994, 28, 786.
117. Mahshid, S., et al., *Synthesis of TiO_2 nanoparticles by hydrolysis and peptization of titanium isopropoxide solution.* Semicond Phys Quantum Electron Optoelectron, 2006. **9**(2): p. 65-8
118. Qiu, S. and S.J. Kalita, *Synthesis, processing and characterization of nanocrystalline titanium dioxide.* Materials Science and Engineering: A, 2006. **435**: p. 327-332.
119. Habibpanah, A.A., S. Pourhashem, and H. Sarpoolay, *Preparation and characterization of photocatalytic titania–alumina composite membranes by sol–gel methods.* Journal of the European Ceramic Society, 2011. **31**(15): p. 2867-2875.
120. Kamat, P.V., *Photoinduced transformations in semiconductor-metal nanocomposite assemblies.* Pure and Applied Chemistry, 2002. **74**(9): p. 1693-1706.
121. Mongillo, J.F., *Nanotechnology 101*2007: Greenwood Publishing Group.
122. G. Li, S.M. Ciston, N. Dimitrijevic, T. Rajh, K.A. Gray *Photooxidation and Photoreduction using Mixed-phase Titanium Dioxide*, Journal of Catalysis, 2008, 253:105-110.
123. Li, G. and K.A. Gray, *The solid–solid interface: Explaining the high and unique photocatalytic reactivity of TiO_2 based nanocomposite materials.* Chemical Physics, 2007. **339**(1): p. 173-187.
124. Matsuoka, M., et al., *Photocatalysis for new energy production: recent advances in photocatalytic water splitting reactions for hydrogen production.* Catalysis today, 2007. **122**(1): p. 51-61.
125. http://www.titanpe.com/
126. Qiu, X. and C. Burda, *Chemically synthesized nitrogen-doped metal oxide nanoparticles.* Chemical Physics, 2007. **339**(1): p. 1-10.
127. Djaoued, Y., et al., *Low temperature sol-gel preparation of nanocrystalline TiO 2 thin films.* Journal of sol-gel Science and Technology, 2002. **24**(3): p. 247-254.
128. Zeatoun, L. and D. Feke, *Characterization of TiO_2 Smoke Prepared Using Gas-Phase Hydrolysis of TiCl4.* Particle & Particle Systems Characterization, 2005. **22**(4): p. 276-281.
129. Kaewgun, S., et al., *Influence of hydroxyl contents on photocatalytic activities of polymorphic titania nanoparticles.* Materials chemistry and physics, 2009. **114**(1): p. 439-445.
130. Alammar, T., et al., *Sonochemical preparation of TiO_2 nanoparticles in the ionic liquid 1-(3-hydroxypropyl)-3-methylimidazolium-bis (trifluoromethylsulfonyl) amide.* Materials chemistry and physics, 2010. **120**(1): p. 109-113.

131. Nguyen, T.B., M.J. Hwang, and K.S. Ryu, *Synthesis and High Photocatalytic Activity of Zn-doped TiO 2 Nanoparticles by Sol-gel and Ammonia-Evaporation Method.*
132. Sobczyński, A. and A. Dobosz, *Water purification by photocatalysis on semiconductors.* Polish Journal of Environmental Studies, 2001. **10**(4): p. 195-205.
133. Madhusudan Reddy, K., S.V. Manorama, and A. Ramachandra Reddy, *Bandgap studies on anatase titanium dioxide nanoparticles.* Materials chemistry and physics, 2003. **78**(1): p. 239-245.
134. Tanaka, Y. and M. Suganuma, *Effects of heat treatment on photocatalytic property of sol-gel derived polycrystalline TiO_2.* Journal of sol-gel Science and Technology, 2001. **22**(1): p. 83-89.